INFORMATION TO USERS

This manuscript has been reproduced from the microfilm master. UMI films the text directly from the original or copy submitted. Thus, some thesis and dissertation copies are in typewriter face, while others may be from any type of computer printer.

The quality of this reproduction is dependent upon the quality of the copy submitted. Broken or indistinct print, colored or poor quality illustrations and photographs, print bleedthrough, substandard margins, and improper alignment can adversely affect reproduction.

In the unlikely event that the author did not send UMI a complete manuscript and there are missing pages, these will be noted. Also, if unauthorized copyright material had to be removed, a note will indicate the deletion.

Oversize materials (e.g., maps, drawings, charts) are reproduced by sectioning the original, beginning at the upper left-hand corner and continuing from left to right in equal sections with small overlaps. Each original is also photographed in one exposure and is included in reduced form at the back of the book.

Photographs included in the original manuscript have been reproduced xerographically in this copy. Higher quality 6" x 9" black and white photographic prints are available for any photographs or illustrations appearing in this copy for an additional charge. Contact UMI directly to order.

UMI

A Bell & Howell Information Company
300 North Zeeb Road, Ann Arbor MI 48106-1346 USA
313/761-4700 800/521-0600

The Partitioning of Mercury Among the Solid Components of Sediments of the Saguenay Fjord, Québec

by

Andrew B. Bono

A thesis submitted to the
Faculty of Graduate Studies and Research
in partial fulfillment of the requirements for the
Degree of Master of Science

Earth and Planetary Sciences
McGill University
Montréal, Québec, Canada
May, 1997

National Library
of Canada

Acquisitions and
Bibliographic Services

395 Wellington Street
Ottawa ON K1A 0N4
Canada

Bibliothèque nationale
du Canada

Acquisitions et
services bibliographiques

395, rue Wellington
Ottawa ON K1A 0N4
Canada

Your file Votre référence

Our file Notre référence

0-612-29661-X

Canada

ACKNOWLEDGEMENTS

I am grateful to the following people who so generously aided and abetted the undertaking this thesis represents: C. Guignard for her patient assistance, problem solving, and magic touch with misbehaving instruments of all kinds; T. Arakaki for his good spirits and assistance with sulphur analyses; C. Gagnon for his assistance in the field and laboratory, as well as his patience bridging language gaps under cramped quarters; G. Keating and S. Lalli for technical assistance and as references for some of the finer points of practical trace metal analyses; and to D. Vaudrin and M. Boiridy for camaraderie and laboratory assistance. Dr. R. Raiswell assisted with analyses related to reactive iron, and G. Poirier provided generous assistance with microprobe analyses. Dr. G.W. Luther lent some of his considerable insight to some troublesome sulphur chemistry.

Dr. E. Pelletier provided cheerful organization and stewardship of the field work on the Saguenay and St. Lawrence. Additionally, thanks go to the captain and crew of the *Alcide C. Horth* who worked so hard helping us to meet our field objectives.

The Department of Earth and Planetary Sciences at McGill provided not only financial support in the form of scholarships and teaching assistantships, but also fostered an environment where science and scholarship flourish. Dr. J. Fein served as a voice of guidance and encouragement during the experimental work. A. Kosowski provided solutions to unforeseen administrative nightmares, several pitchers of Boréale, and supportive friendship.

To Dr. A. Mucci I wish to express my most sincere appreciation for his guidance and generosity, as well as his enthusiasm, persistence, patience, and friendship. His sense of discipline and dedication to rigourous scholarship were intrinsic to the completion of this thesis and my studies in geochemistry.

Thanks also go to T. Geraghty for unconditional support and faithful encouragement, P. Pike, who manned the enthusiasm department, as well as B. Casher, J. Kidman, and A. Zidle, who handled damage control and sanity maintenance during minor catastrophes along the way. Sensai D. Larendeau lent focus, drive, and confidence to this and other endeavours.

Finally, I wish to thank my family for their laymans common-sense approach to science while many in the laboratory sat perplexed -- my mom, who can apparently jury-rig anything, my dad, who always sees the possible, and my brothers, for asking the right questions. Their unwavering encouragement, support, and faith in me made this possible.

TABLE OF CONTENTS

LIST OF FIGURES

LIST OF TABLES

ABSTRACT

An estimated 60 tonnes of mercury, released from a chlor-alkali plant between 1947 and 1976, are buried in the sediments of the Saguenay Fjord. Despite rapid sedimentation rates, concentrations of Hg in surficial sediments remain well above pre-industrial levels. The partitioning of Hg among sedimentary solids was investigated to elucidate the fate of buried mercury and determine the source of contamination in surficial sediments.

Box cores from two stations along the axis of the Saguenay Fjord (SAG-6B, SAG-30B) and one from the Laurentian Trough (CL-1B) were collected in June, 1992. A sequential extraction protocol modified from existing techniques was tailored to evaluate the distribution of mercury among four operationally defined chemical fractions in Saguenay Fjord sediments: organic matter (C_{org}), iron and manganese (hydr)oxides, acid-volatile-sulphides (AVS), and pyrite.

Overall, the mass distribution of mercury among the various fractions followed:

$$C_{org} > \text{AVS} \approx \text{Fe/Mn (hydr)oxides} \geq \text{pyrite}.$$

The association of the majority of Hg with organic matter at most depths at each site, validates existing models which suggest that mercury is transported to surficial sediments following scavenging by particulate matter in the water column.

Normalization for the concentration and distribution of the solid substrates suggest that the comparative molar affinities of the respective solids for mercury may be represented as:

$$\text{AVS} \approx \text{pyrite} > C_{org} > \text{Fe/Mn (hydr)oxides}.$$

Pyrite and AVS, although present in comparatively minute quantities, have greater affinities for mercury, and can serve as the predominant reservoir for mercury in sulphidic sediments. Redistribution of Hg to Fe/Mn (hydr)oxides was only significant where total

mercury and Fe (hydr)oxide concentrations were high and no AVS had accumulated. Although pyrite has a high affinity for mercury, the paucity of pyrite in these sediments precluded significant incorporation of Hg by this phase.

The partitioning of mercury was markedly dependent on the concentration of total mercury. Where total Hg concentrations were low (< 1000 ng·g^{-1} dry sediment), partition coefficients remained relatively constant. In sediments with total mercury greater than 1000 ng·g^{-1}, characteristic non-linearities in the partition coefficients of each fraction were observed. A demonstrated increase in partitioning to sulphide fractions with increased total mercury, coincident with a decrease in Hg associated with C_{org}, indicates the enrichment of mercury in AVS and pyrite phases at the expense of organic matter.

Although significant redistribution of mercury from organic to inorganic phases occurs throughout most of the sediment strata, vertical remobilization appears to be inhibited by the rapid readsorption of dissolved mercury. Whereas diagenetic remobilization probably contributes some mercury to surficial sediments, the primary source appears to be resuspended particulate matter from contaminated upstream sediments.

This study provides new insight into the chemical pathways and fate of mercury within the Saguenay system, and contributes to a greater understanding of the geochemical behaviour of inorganic mercury in natural systems. Additionally, modifications made to the sequential extraction protocol may be applied and facilitate future studies of mercury partitioning in other systems.

RÉSUMÉ

De tout le mercure déversé par l'usine de chlor-alkali entre 1947 et 1976, on estime à 60 tonnes la quantité qui a été captée par la matière organique en suspension et enfouie dans les sédiments du Fjord du Saguenay. Malgré des taux de sédimentation élevés, la concentration de Hg dans les sédiments de surface du Fjord demeure supérieure aux niveaux pré-industriels. Le distribution du mercure entre certaines phases solides du sédiment a été étudiée afin d'élucider le devenir du mercure enfoui.

Deux carottes-boites ont été prélevées le long de l'axe du Fjord du Saguenay (SAG-6B et SAG-30B) alors qu'une troisième a été récoltée dans le chenal Laurentien (CL-1B) en juin, 1992. Une méthode d'extraction séquentielle, inspirée de techniques établies a été mise au point afin d'évaluer la distribution du mercure parmi quatre fractions opérationellement définies: matière organique (C_{org}), oxi(hydro)xides de fer et manganèse, monosulfures de fer, et la pyrite.

La distribution massique du mercure dans les sédiments du Fjord du Saguenay peut être représentée par:

C_{org} > monosulfures de fer ≈ oxi(hydr)xides de Fe/Mn ≥ pyrite.

L'association prédominante du Hg avec le C_{org} à presque toutes les profondeurs à chaque site d'echantillonage confirme les modèles courants qui suggèrent que le mercure fut transporté à l'interface eau-sédiment suite à sa capture par la matière organique particulaire.

La normalisation par la concentration et la distribution des substrats solides indiquent que les affinités molaires des solides sont respectivement:

Monosulfures de fer ≈ pyrite > C_{org} > oxi(hydro)xides de Fe/Mn.

Quoique la pyrite et les monosulfures de fer soient présents en concentrations relativement faibles, ils ont une plus forte affinité pour le mercure et peuvent dominer le

fractionnement du mercure dans les sédiments sulfidiques. Le partage du mercure avec les oxi(hydro)xides de Fe/Mn est notable seulement lorsque les concentrations de mercure total et oxi(hydro)xides de Fe sont élevées et que les monosulfures de fer sont absents. Malgré la forte affinité de la pyrite pour le mercure, la rareté cette dernière dans les sédiments du Fjord exclue une incorporation significative du mercure avec cette phase.

La distribution du mercure dépend grandement de la concentration du Hg total. Lorsque celle-ci est faible (<1000 ng·g^{-1} sédiments sec), les coefficients de partage sont relativement constants. Par contre, dans les sédiments contenant plus de 1000 ng·g^{-1} en Hg, les coefficients de partage varient pour chaque fraction et suggèrent un enrichissement du Hg dans les monosulfures de fer et la pyrite au détriment de la matière organique.

Malgré qu'une redistribution significative du mercure entre les phases organiques et inorganiques s'effectue dans la plupart des strates sédimentaires, la remobilisation verticale du mercure semble être limitée par une réadsorption rapide du mercure dissous. Quoique les processus de diagénèse précoce contribuent à maintenir les concentrations de mercure élevées dans les sédiments de surface, la source principale est probablement l'accumulation de matière particulaire provenant de la resuspension, en amont, de sédiments contaminés.

Cette étude apporte des nouveaux éléments de compréhension sur les modes de tranfert et le devenir du mercure dans le système du Saguenay, et contribue à une meilleure compréhension du comportement géochimique du mercure inorganique dans les systèmes naturel. De plus, les modifications apportées au protocol d'extractions séquentielles pourront s'appliquer et faciliter les études futures du fractionnement du mercure dans d'autres systèmes.

1. INTRODUCTION

1.1 Historical Setting

In the industrial and agricultural expansion that followed 1945, the use of new mercury-based compounds and manufacturing techniques resulted in widespread, large-scale dispersion of toxic organomercury compounds to natural environments. Common industrial uses for mercury prior to the discovery of the acute toxicity of alkylmercury derivatives included: the production of organomercurial pesticides (e.g. phenylmercury acetate, methylmercury dicyandiamide), antifungal agents, and paper pulp slimicides; the use of mercury as a catalyst in the synthesis of organic chemicals (e.g. acetic acid); in switches by the electronics industry; and as liquid cathodes in the production of Cl_2 and NaOH in chlor-alkali plants (NIPCC, 1970). Human consumption of foods contaminated with organomercury compounds resulted in the poisoning of whole communities, over ten-thousand cases of incurable neuropathy, and nearly a thousand fatalities have been reported: Minamata, Japan (1953-1960); Niigata, Japan (1965); Northern Iraq (1959); Pakistan, Guatemala, and Yugoslavia (1960's); Alamogordo, New Mexico (1970); and Muthana Province, Iraq (1972). (NIPCC, 1970; Bakir *et al.*, 1973; Takizawa, 1979). In each case, poisoning was the result of ingestion of organomercury compounds.

In Iraq, as well as in New Mexico, fatalities resulted from the ingestion of agricultural seeds were dressed with pesticides or antifungal agents. In Japan, although inorganic mercury was used in the catalytic synthesis of acetic acid, methylmercury was released as a by-product into two rivers discharging in areas which supported fishing villages (Takizawa, 1979). Since organic mercury compounds bioaccumulate throughout the food chain, humans who consumed contaminated fish absorbed crippling and fatal amounts of mercury.

Prior to the 1960's, release of inorganic mercury to the environment was thought to be of minor concern since it is much less toxic and non-reactive than its organic derivatives. In the late 1960's, however, it was discovered that microorganisms can methylate inorganic mercury (Jenson and Jernelöv, 1969). Beginning in 1970, Canadian industries releasing inorganic mercury wastes to the environment (e.g. the chlor-alkali industry) began to re-evaluate and alter their operating practices. The Canadian government implemented new regulations in 1972 drastically limiting the amount of mercury discharged in liquid effluents (Environment Canada, 1981).

The earliest research focused on human pathology and the determination of the source of unexplained neuropathy (Takizawa, 1979). Following this, levels of mercury in humans, wildlife, and fish worldwide were evaluated while global mercury sources and sinks were budgeted (Brosset, 1981; Smith and Loring, 1981; Nriagu and Pacyna, 1988). Geochemical cycles of mercury were elaborated which included a description of modes of mercury dispersion and vectors of transport in atmospheric, terrestrial, and aquatic systems (Wollast, *et al.*, 1975; Evans, 1986; Schroeder *et al.*, 1989; Xiao *et al.*, 1991; Krabbenhoft and Babiarz, 1992). A very active area of research remains the documentation of the biogeochemical behaviour of Hg in the biosphere and the identification of pathways of transfer to and accumulation within the food chain (St. Louis *et al.*, 1993; Dmytriw *et al.*, 1994; Mucci *et al.*, 1995; Gagnon *et al.*, 1996b; Tremblay *et al.*, 1996; Gagnon *et al.*, 1997).

1.2 Mercury Contamination of the Saguenay Fjord

In 1971, significantly elevated levels of mercury were detected in fish and shrimp of the Saguenay Fjord prompting the closure of commercial shrimp fisheries for fifteen years. The chlor-alkali plant at Arvida, which operated between 1947 and 1976, was identified as the point source of the contamination (Loring, 1978; Guay and Couillard, 1980). Cooperation with government guidelines in 1970 and implementation of government regulation in 1972 resulted in a decrease in the amount of mercury released to the fjord (Loring, 1978; Environment Canada, 1981); the plant was finally closed in 1976.

During its operation the plant released waste effluents containing between 136 and 200 metric tonnes of mercury (Loring and Bewers, 1978; Smith and Loring, 1981; Guay and Couillard, 1980). The mercury released to the water column was quickly scavenged by particulate organic matter which settled and accumulated at the sediment/water interface. Based on a mass balance calculation, Loring and Bewers (1978) estimated that approximately 53 tonnes of Hg reside in the sediments of the Saguenay River, while 60 tonnes are buried in the sediments of the Saguenay Fjord. Additionally, an estimated 12 tonnes of mercury were transported from the Fjord and deposited in the sediments of the St. Lawrence Estuary.

Sedimentation rates (ω) in the Saguenay Fjord are high: values average 4.0 $g{\cdot}cm^{-2}{\cdot}a^{-1}$ (7 $cm{\cdot}a^{-1}$) at the head of the fjord and between 0.31 and 0.07 $g{\cdot}cm^{-2}{\cdot}a^{-1}$ (0.5 to 0.1 $cm{\cdot}a^{-1}$) in the deep interior basin (Smith and Walton, 1980; Barbeau *et al.*, 1981a). Several sedimentation events (e.g., St. Jean-Vianney landslide - May, 1971) have also deposited thick layers of allochthonous material throughout the post-glacial period thus contributing to the sedimentary pile (Smith and Loring 1981). Despite burial, mercury concentrations in most surface sediments (i.e., top 2 cm) remain well above pre-industrial levels of ~ 0.15 $\mu g{\cdot}g^{-1}$ (Loring, 1975; Smith and Loring, 1981; Barbeau *et al.*, 1981b). In fact, researchers noted little variation in mercury levels in surface sediments between 1964 and 1978. Loring and Bewers (1978) reported surficial sediment Hg concentrations which ranged from 0.16 to 12 $\mu g{\cdot}g^{-1}$ for samples collected between 1964 and 1976, values similar to those published by Barbeau *et al.* (1981b) for sediments recovered between 1976 and 1978. In more recent studies, mercury concentrations in the 0-2 cm interval of surface sediments collected between 1978 and 1986 were reported to vary between 0.01 and 1.2 $\mu g \cdot g^{-1}$ (Pelletier, *et al.*, 1989a; Gobeil and Cossa, 1993).

Pelletier *et al.* (1989b) compared the vertical distribution of polyaromatic hydrocarbons (PAH) and mercury in the Saguenay Fjord sediments. PAH compounds, which are not subject to significant oxidation, biodegradation, or diagenetic remobilization, were released over roughly the same period as was mercury (Pelletier *et al.*, 1989b). They observed smooth PAH profiles with peak concentrations at depth and values which decreased near the sediment/water interface. In contrast, the mercury profile was more diffuse and showed peak concentrations at shallower depths than those of PAH, as well as comparatively high concentrations in surface sediments. These observations were interpreted as resulting from the diagenetic remobilization of mercury from deeper, contaminated sediments, thereby sustaining elevated Hg concentrations in surface sediments (Pelletier *et al.*, 1989a). Insufficient data, however, were available to rule out the possibility of continued anthropogenic input or re-suspension of contaminated upriver sediments (Pelletier *et al.*, 1989a), although resuspended Hg-contaminated sediments should also carry a high PAH signature.

Cossa and Desjardins (1984) published results of mercury levels measured in the edible portions of shrimp (*Pandalus borealis*) between 1970 and 1983. Values measured on samples recovered in 1983 were well above pre-industrial levels, but considerably reduced from 1970 contamination levels. The sustained mercury contamination was attributed to the persistence of mercury in the shrimp habitat (i.e surface sediments). Pelletier *et al.* (1989a) found mercury levels in *Pandalus borealis* to be insignificantly different from those found by Cossa and Desjardins (1984). Further, they found that mercury in the surface sediments were still one order of magnitude greater than pre-industrial levels and did not significantly differ from concentrations measured in sediments recovered from the same sites in 1978, 1982, and 1983. A more recent study (Desjardins, 1989) reports further attenuation of the biotic mercury load, with a ten-fold decrease in 1989 Hg concentrations from the 1970 levels. Each study found the highest concentrations of mercury to be present in biota which dwell on or near the sediment surface.

1.3 Diagenesis and Trace Metal Partitioning

1.3.1 Transport of Trace Metals to Sediments

Particulate matter comprising estuarine sediments is the product of several processes. Weathering and erosion of regional country rock result in the transport of silicates and terrigenous organic matter via river water to the estuary. The suspended matter which accompanies salt-water marine intrusions adds marine organic and inorganic particulate matter to estuarine sediments. Within the estuary itself, primary biological production in these nutrient-rich waters can serve as a major contribution to suspended particulate matter. Additionally, at the halocline, Fe, Al, Si, and organic colloids flocculate or coat existing particles prior to settling to the sediment/water interface.

Scavenging of trace metals in the water column by particulate and colloidal matter, most notably organic matter, is a recognized process by which trace metals are transported to sediments from the water column (Goldberg, 1954; Balistrieri *et al.*, 1981, Gagnon *et al.*, 1993). The affinity of particulate organic matter for mercury and other metals is well established (Lindberg and Harriss, 1974; Kerndorff and Schnitzer, 1980; Schnitzer and Kerndorff, 1981; Benes and Havlík, 1979). Loring (1975) estimated that over 70% of the mercury in the sediments of the Saguenay Fjord was transported to the sediment/water interface with organic matter. Accordingly, Gagnon *et al.* (1993) demonstrated a correlation between the distributions of sedimentary C_{org}, and of both Hg and Cu. Detrital and authigenic Fe and Mn oxyhydroxides or sesquioxides (M_2O_3) can also efficiently scavenge a number of metals (Cu, Co, Mn, Ni, Ti, Zn and Hg; Goldberg, 1954; Evans, 1989; Forbes *et al.*, 1974) from the water column as well as from porewaters.

1.3.2 Early Diagenetic Chemistry

Microbial oxidation of organic matter chiefly controls the redox conditions within sediments and soils. In organic-rich sediments, following oxygen depletion, a spectrum of electron acceptors are employed sequentially by microorganisms in the order of their metabolic efficiency. Following the consumption of oxygen, NO_3^-, Mn(III-IV) and Fe(III) phases (typically minerals and amorphous coatings of Mn, Fe oxides and oxyhydroxides), SO_4^{2-}, and finally CO_2 are reduced, respectively, to N_2, Fe(II) and Mn(II), HS^-, and CH_4 (Froelich *et al.*, 1979). In marine and estuarine sediments, the extent of NO_3^- reduction is limited by its availability. Manganese and iron reduction is dependent on the abundance and reactivity of Mn and Fe phases. The metals are released to porewaters where they may accumulate, diffuse along concentration gradients, or form authigenic phases. Diffusion into oxygenated sediments results in the re-precipitation of oxidized Fe and Mn solids (Sundby and Silverberg, 1985). In organic-rich, highly reducing marine sediments, the dominant oxidant following oxygen consumption is sulphate (Jorgensen, 1977, 1982; Edenborn *et al.*, 1987; Thode-Anderson and Jorgensen, 1989), a major constituent of seawater. As $S(VI)O_4^{2-}$ is reduced to $HS(-II)^-$, sulphide accumulates in the porewaters. Sulphide reacts rapidly with dissolved Fe^{2+} in porewaters to form FeS precipitates. Alternatively, HS^- may diffuse along concentration gradients into suboxic or oxic zones where reactions with Fe(III) phases or O_2 will partially oxidize the sulphide to S(0) and result in the formation of intermediate sulphur compounds, such as $S(0)_8$, $S_2O_4^{2-}$ (Chen and Morris, 1972; O'Brien and Birkner, 1977; Gagnon *et al.*, 1996a, 1995).

Where Fe^{2+} and HS^- precipitate, mineral phases including greigite (Fe_3S_4), mackinawite (FeS_{1-x}), or amorphous monosulphides (FeS) commonly form. Less reactive ferric minerals which survive exposure to suboxic conditions can be reduced in the presence of H_2S and precipitated as sulphides. In the presence of intermediate sulphur species (e.g. $S_2O_3^{2-}$, $S_4O_6^{2-}$, S_8) iron monosulphides are converted to pyrite (FeS_2)(Berner, 1970; Luther, 1991). The direct precipitation of pyrite has been reported in salt-marsh sediments (Howarth, 1978) and *in vitro* (Rickard and Luther, 1996; Rickard, 1996), but only at pH conditions markedly lower than those which occur in estuarine and marine systems. Pyzik and Sommer (1981) found that the presence of an iron monosulphide precursor phase and dissolved S^0 species (e.g. $S_2O_3^{2-}$, $S_nO_6^{2-}$) is necessary for pyrite formation under pH and redox conditions encountered in most estuarine and marine environments. Pyrite is less reactive than the iron monosulphide phases and serves as a more stable sink for reduced sulphur, iron, and co-precipitated trace metals.

1.3.3 Diagenetic Remobilization of Trace Metals

Diagenetic remobilization is the process by which materials, following deposition and burial at the sediment/water interface, are released to porewaters as the carrier phase is degraded or altered due to physico-chemical changes and biological activity. The diagenetic behaviour of several trace metals in marine sediments is well documented (Sawlan and Murray, 1983; Shaw *et al.*, 1990; Macdonald *et al.*, 1991; Klinkhammer and Palmer, 1991; Fernex *et al.*, 1992; Thomson *et al.*, 1993; Lapp and Balzer, 1993).

Several researchers have noted that metals commonly associated with organic matter (e.g., Cd, Cr, Cu, Ni, Pb, U, V, Zn) in the water column and sediments are released to the porewaters near the sediment/water interface as a result of the rapid degradation of organic matter under aerobic conditions (Sawlan and Murray, 1983; Gobeil *et al.*, 1987; Shaw *et al.*, 1990; Fernex *et al.*, 1992, Klinkhammer and Palmer, 1991; Lapp and Balzer, 1993). In addition, Gagnon *et al.* (1997) also report release of mercury to sediment porewaters following the degradation of organic matter.

As a result of burial and the onset of suboxic conditions, metals associated with detrital or authigenic iron and manganese oxides and oxyhydroxides are released to porewaters. Accordingly, Gobeil and Cossa (1993) observed a correlation between iron and mercury concentrations in porewaters of Laurentian Trough sediments. They interpreted this observation as the simultaneous release of the two metals beneath the zone of oxygen penetration following reductive dissolution of Fe hydroxides and sesquioxides and the associated mercury. Other metals (e.g. Co, Cu, Mo, Ni, and V) have been reported to display a similar behaviour and this process is now well documented (Shaw *et al.*, 1990; Huerta Diaz and Morse, 1992).

Iron sulphide minerals show a pronounced ability to adsorb and incorporate metals from surrounding porewaters. Arakaki and Morse (1993) examined the incorporation of Mn into mackinawite, whereas Dyrssen and Kremling (1989) determined the scavenging capacity of iron monosulphides for Cd, Co, Cu, Mn, and Ni in anoxic bottom waters of the Baltic Sea. Pankow and Morgan (1979) suggested that metals which form insoluble metal sulphides (i.e., Ag, Hg, Pb, and Zn, in addition to those listed above) may be expected to associate with authigenic iron monosulphides. Laboratory studies have since established that mercury is strongly and specifically adsorbed to the surface of iron and lead monosulphides (Jean and Bancroft, 1986; Hyland *et al.*, 1990). Pyritization of trace metals such as As, Cd, Co, Cu, Mn, Mo, Ni, Pb, Zn, and Hg during diagenesis in anoxic sediments has also been reported by several researchers (Raiswell and Plant, 1980; Luther *et al.*, 1980; Belzile and Lebel, 1986; Skei *et al.*, 1988; Huerta Diaz and Morse, 1990, 1992).

Authigenic iron monosulphide minerals which form under anoxic conditions become unstable when exposed to a number of oxidants (e.g., O_2, NO_2, Mn(II), Fe(III)). The sulphides become exposed to the oxidants as a result of bioirrigation, resuspension of sediments, or seasonal migration of the redoxcline. Pankow and Morgan (1980) demonstrated that under oxidizing conditions mackinawite, which is less reactive than amorphous FeS, is oxidized and dissolves within minutes. Pyrite is, however, both less soluble (Emerson *et al.*, 1983) and more resistant to oxidation (Cornwell and Morse, 1987) than the iron monosulphides. Upon exposure to oxygenated environments, iron sulphides (particularly monosulphides) are therefore expected to decompose and release their trace metal load to porewaters.

1.4 Objectives of this Study

Several sequential extraction techniques have been devised to characterize the partitioning of trace metals into various operationally defined sediment and soil compartments (Tessier *et al.*, 1979; Lord, 1982; Robinson, 1984; Huerta-Diaz and Morse, 1990; Huerta-Diaz *et al.*, 1993; Dmytriw *et al.*, 1994). Each extraction protocol was designed to suit the geochemistry of the geological materials studied. Although sequential extraction techniques have been severely criticized (see **Section 4.3**), these procedures remain useful in examining the association of trace metals to the various solid components of soils and sediments. In many cases, the protocols were designed to characterize trace metal association with one or two specific phases (i.e., carbonates, pyrite, iron monosulphides; Huerta-Diaz and Morse, 1990; Span and Gaillard, 1986; Huerta Diaz *et al.*, 1993). Whereas the horizontal and vertical distribution of ΣHg in the Saguenay Fjord sediments has been reported, few attempts have been made to identify the nature and extent of Hg association with various components of the sediments. Likewise, although the distribution of mercury in HCl-, NaOH-extractable and residual compartments of a soil profile has been established (Dmytriw *et al.*, 1994), few studies have applied published procedures intended to separate the solid components of a sediment (Tessier *et al.*, 1979; Mahan *et al.*, 1988; Jordao and Nickless, 1989; Clevenger, 1990) to determine mercury partitioning. Attempts to do so (Eganhouse et al., 1978; Giordano et al., 1992; Huerta-Diaz and Morse, 1992; Gobeil and Cossa, 1993; Dmytriw, *et al.*, 1994; Gagnon *et al.*, 1997; Matty and Long, 1995) have shed little light into the nature, extent, and processes of mercury partitioning in sediments because the authors failed to modify existing techniques to suit either the specific chemistry of the sediments under investigation, or the particularities of mercury extraction.

The objectives of this study were to:

1. Devise and apply a sequential extraction protocol to determine the partitioning of mercury between various trace metals reservoirs in oxic and anoxic sediments of the Saguenay Fjord: metals associated with organic matter, reactive Fe and Mn minerals, clays, and pyrite.

and in so doing:

2. Document and model the diagenetic behaviour of Hg (i.e., the association to other phases) following the degradation of organic matter in sediments in order to evaluate the temporary and long-term sinks of the metal in the Saguenay Fjord.

This research project complements work carried out by C. Gagnon (Gagnon, 1994) regarding mercury distribution and speciation in porewaters. A common goal of both studies was to identify the source of the anomalously high Hg concentrations in the surface sediments. More specifically, we sought to determine whether diagenetic remobilization or re-suspension of contaminated upriver sediments was responsible for maintaining high Hg concentrations in surficial sediments long after the point source had been eliminated and contaminated sediments had been buried.

2. LITERATURE REVIEW

2.1 Speciation of mercury in natural systems

Within the stability field of water, mercury may exist in three oxidation states: Hg(0), (I), or (II). Elemental mercury, a liquid at room temperature and atmospheric pressure, is sparingly soluble (56 ng/g at 25°C; Schuster, 1991) and volatile ($1.22 \cdot 10^{-3}$ mm at 20°C; Schuster, 1991). Most dissolved mercury is found in the Hg(II) form. The mercurous or Hg(I) ion is most commonly present as Hg_2^{2+}, which is unstable under natural aqueous conditions and dismutates to Hg(0) and Hg(II).

Mercury is classified as a IIB transition metal. As a Pearson "Class B" metal, it has a large, easily polarized electron field, and consequently forms stable complexes with similar ligands such as thiols, HS^-, and CN^- (Pearson, 1963). Oxyanions (CO_3^{2-}, SO_4^{2-}, PO_4^{3-}) and F^- do not form stable complexes with IIB metals as their electron fields are tightly held and are not easily distorted (Pearson, 1963). The stability constants of mercury complexes with several ligands have been experimentally determined (Smith and Martell, 1976) or calculated (Dyrssen and Wedborg, 1991). The stability of mercury complexes with the following ligands appears as:

$$RS^- \text{ (thiols)} > HS^- > CN^- \gg I^- > OH^- > Br^- > Cl^- > NH_3 \gg F^-, NO_3^{2-}, SO_4^{2-}$$

Hg(II) is a d^{10} transition metal and typically exhibits octahedral geometry, although mercury forms complexes with two *trans* bonds much shorter than the other four. As a result, HgL_2 (where L=ligand) exhibits linear geometry (Forbes *et al.*, 1974; Greenwood and Earnshaw, 1984). Less commonly, Hg(II) has also been shown to exhibit planar

(HgI_3^-, trigonal bipyramidal ($HgCl_3^-$), and tetrahedral ($HgCl_4^{2-}$) geometries (Greenwood and Earnshaw, 1984; Porterfield, 1984).

On the basis of thermodynamic considerations, Hg solubility at 25°C, in contact with the atmosphere, in the presence of 10^{-3} M Cl^- and S, is determined by the stability of the HgS, $Hg(OH)_2$, $HgCl_2$, Hg(OH)Cl, and Hg° solid phases (see **Figure 2.1**). The solubility of mercury under mildly oxidizing to strongly reducing conditions is quite low (60 $\mu g \cdot L^{-1}$; Schuster, 1991), as it is determined by metallic mercury, or by the considerably more insoluble $HgS_{(s)}$ (2 $pg \cdot g^{-1}$; Schuster, 1991). The solubility of Hg under strongly reducing conditions may be increased at high pH by the formation of HgS_2^{2-} complexes.

In well oxygenated natural systems, the uncomplexed Hg^{2+} ion exists only under very acidic (pH<3) and low chlorinity conditions (see **Figure 2.2**). Over the majority of pCl^- and pH conditions encountered in natural waters, the uncharged linear complexes $Hg(OH)_2^0$ and $HgCl_2^0$ are the dominant dissolved species of mercury. Hg(OH)Cl is only sparingly soluble and not a predominant species under any natural conditions. At very high chlorinity, such as in sea water ($Cl^- \sim 0.55M$ or $pCl^- \sim 0.25$), $HgCl_4^{2-}$, a tetrahedral complex, predominates at pH < 9. Thermodynamic considerations preclude the existence of predominance fields for the complexes $HgOH^+$ and $HgCl_3^-$ (Smith and Martell, 1976; Dyrssen and Wedborg, 1991).

While providing a useful means of examining trends in behaviour, Eh-pH diagrams are severely oversimplified and insufficient to completely describe mercury speciation in both natural waters and sediments. Organic matter plays a prominent role in the speciation of mercury by adsorption of Hg and the formation of Hg-organic complexes. Furthermore, in sediments, the co-precipitation of mercury with oxides, hydroxides, and sulphides likely controls Hg speciation beyond the fields addressed by the predominance

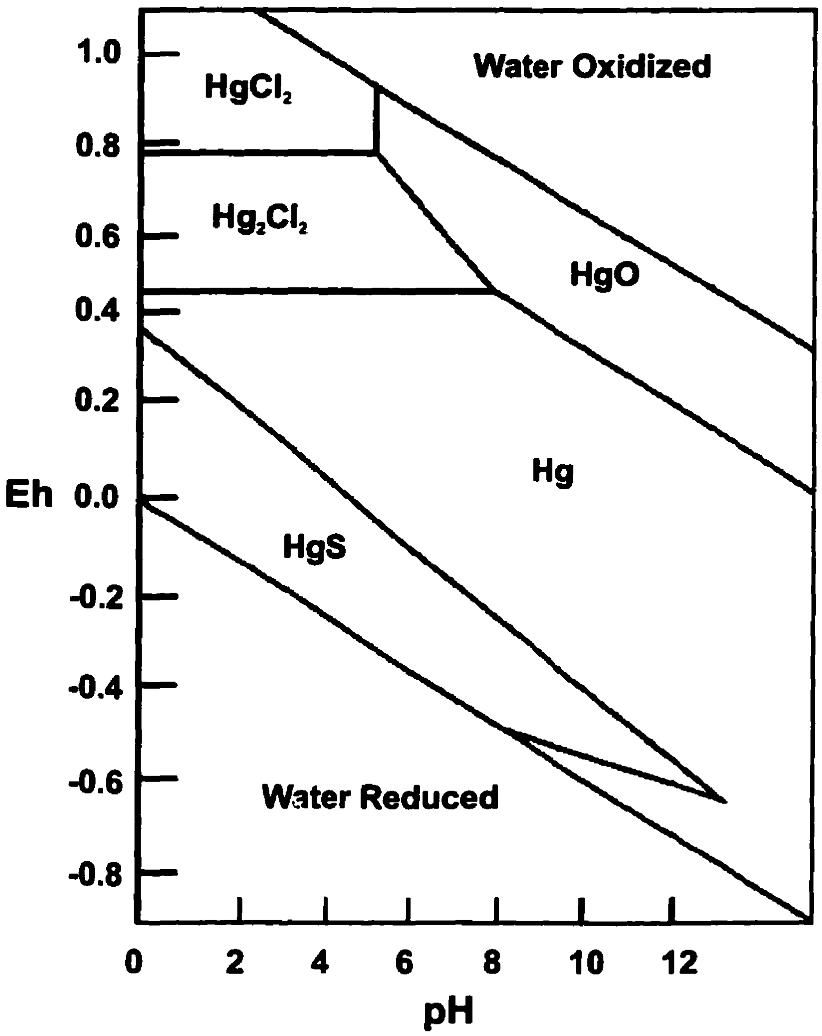

Figure 2.1 Fields of stability of insoluble mercury phases as a function of Eh and pH

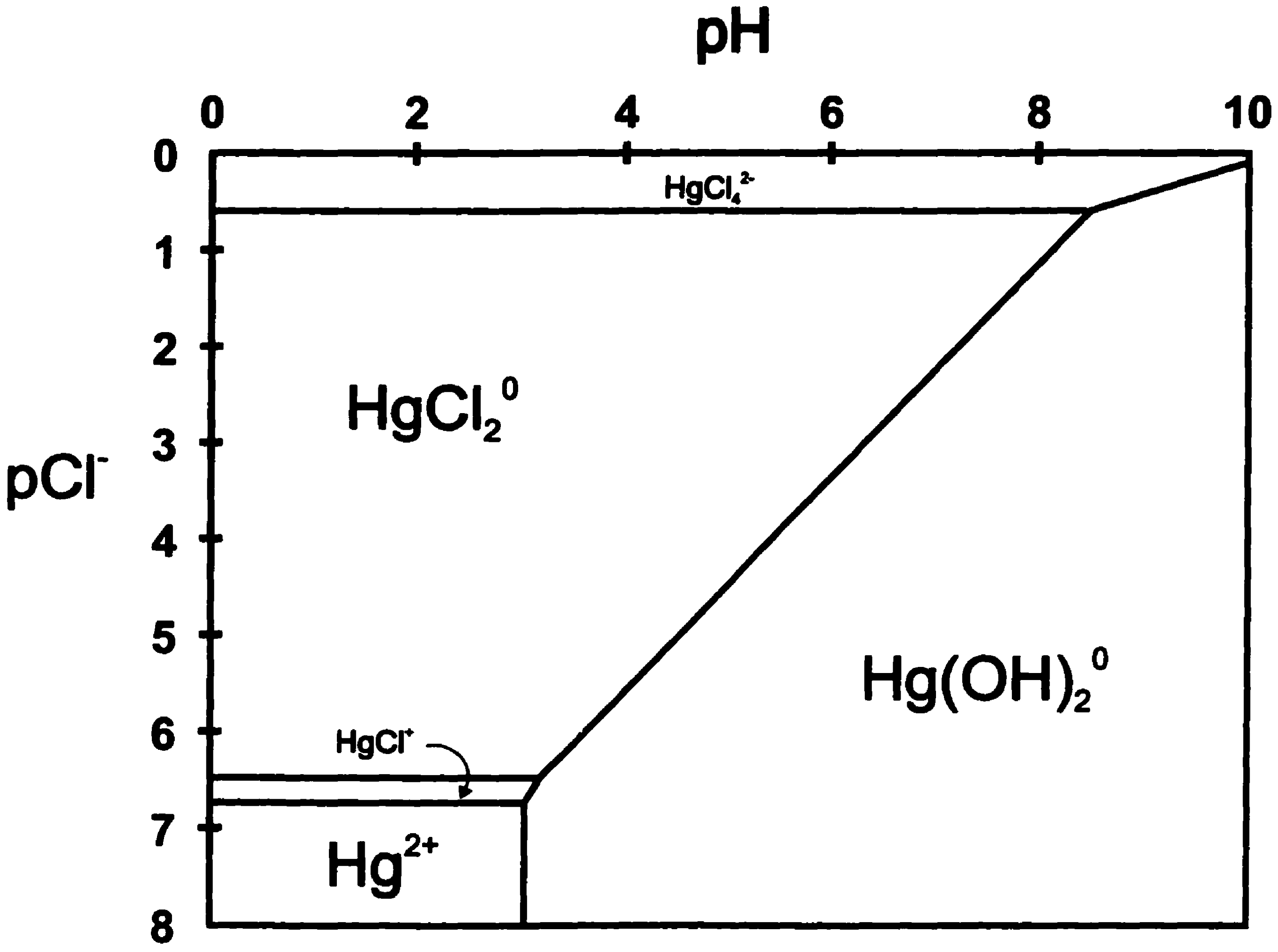

Figure 2.2 Fields of predominance of dissolved inorganic mercury species as a function of pCl^- and pH

diagram in **Figure 2.2**. Closer examination of adsorption and co-precipitation of mercury with various solid sedimentary components provides a more complete representation of its behaviour in natural systems.

2.2 Association of Hg to Organic Matter

Organic matter is the most important particulate adsorbent of mercury in the natural environment (Loring, 1975; Dmytriw *et al.*, 1994). It is important to emphasize that organic matter cannot be considered as simply a single phase with consistent behaviour, but varies with origin, transport, and deposition. Clearly, the role of organic matter in sediments and its relationship to mercury merits review.

Organic matter in estuarine sediments is generally a mixture of both terrigenous and marine materials in proportions determined by the source functions, the circulation, and the morphology of the system. Whereas humic matter makes up the majority of the organic matter in estuarine sediments (as high as ~70% C_{org}; Mayer, 1985), the rest is comprised of identifiable organic compounds (lignin, carbohydrates, proteins, lipids, and others).

2.2.1 Geochemistry of Estuarine Organic Matter

2.2.1.1 Identifiable Organic Matter

Lignin is a highly refractory biopolymer found exclusively as the xylem of land plants. The structure of lignin is mostly aromatic, of high molecular weight, and includes many phenolic functional groups (Killops and Killops, 1993). Lignin is oxidized and dissolved in strong acids or hot concentrated NaOH in the presence of Cu(II)O (Flaig *et al.*, 1975). Since it undergoes very slow microbial degradation during diagenesis, lignin is often a chief precursor of humic compounds.

Cellulose comprises 50-70% of the dry weight of terrestrial plants. Although it bears hydroxyl functional groups, cellulose is soluble only in strong acid. Degradation of cellulose in sediments generally occurs only through microbial enzyme pathways (Greenland and Oades, 1975). Hemicellulose and starch compounds are also major components of both marine and terrestrial organic matter. Since they bear many hydroxyl, carboxylic, and carbonyl functional groups, hemicellulose and starches are more hydrophilic, are soluble in dilute base, and decompose quickly (Greenland and Oades, 1975; Solomons, 1988).

Proteins are the chief constituent of identifiable marine organic carbon. Rich in amino, hydroxyl, carboxyl, and carbonyl functional groups, proteins are also the principal source of nitrogen. As well, proteins which contain cysteine and methionine serve as the major source of primary organic sulphur (thiols, thioesters, and disulphides) to sediments. Proteins are hydrophilic and degrade rapidly in the water column and after reaching the sediment water interface. Proteins may, however, also react with other organic compounds, undergo condensation reactions, and become incorporated into humic substances (Rashid, 1985).

Lipids are hydrophobic, aromatic compounds which are highly resistant to degradation, but which form only a small proportion of terrestrial and marine organic carbon (Rashid, 1985).

2.2.1.2 Humification

The alteration of primary organic matter begins with chemical and biological degradation in the water column and continues at and below the sediment/water interface. Under aerobic conditions, benthic fauna contributes to the catabolic breakdown of this material, whereas microorganisms (bacteria and fungi) enzymatically degrade the compounds. Because benthic fauna require oxygen to metabolize nutrients, degradation of organic matter under anoxic conditions occurs solely via microbial metabolic pathways. Proteins and carbohydrates are degraded first, followed by lignin and other refractory plant residues. Organic matter is initially broken down to simpler compounds, while abiotic reactions result in condensation and polymerization reactions between partially degraded organic molecules. The rate of degradation is controlled by several factors: increased temperature, reactivity of organic matter, and the availability of labile oxidants result in an increased rate of biotic attack of organic matter in sediments (Rashid, 1985). Lignin and cellulose comprise a significant portion of humified material, since both compounds are resistant to degradation and therefore decay slowly. With humification, oxidation of functional groups occurs: hydroxyl sites decrease in number, while carboxylic groups increase; phenolic functional groups are converted to quinones. This results in a corresponding increase in the cation exchange capacity. In addition to the products of lignin and cellulose decay, microorganisms produce phenolic compounds as metabolic by-products from aliphatic acids and acetals. Polysaccharides and proteins, as well as their component sugars and peptides may chemically precipitate with ligneous compounds, particularly via ketone and quinone condensation with amine groups. Finally, there is the polymerization through microbial and non-microbial intermediaries of decomposition products into higher molecular weight humic materials (Flaig *et al.*, 1975)

2.2.1.3 Humic Compounds

Humus is a general term used to define organic matter altered by bacterial processes in soils and sediments (Brady, 1974). It has no fixed composition or structure, but is comprised principally of carbon, hydrogen, oxygen and minor quantities of sulphur, nitrogen, and phosphorus. Humic substances are generally considered to be depleted in easily metabolized nutrients, which precludes further biotic attack and causes them to be stable and lasting components of sediments (Flaig *et al.*, 1975).

Humic substances are separated and operationally defined by solubility, in order to group components by size and functional groups. Although there is no common size, structure, or set of functional groups for any class of humic material, researchers have attempted to describe them using operational definitions (see **Figure 2.3**)

Fulvic acids (FA) have a lower molecular weight than humic acids and a significantly higher O/C ratio, which result from a high concentration of oxygen bearing functional groups. Models of fulvic acids (Schnitzer and Khan, from Stevenson (1985)) suggest near saturation of substitutable sites with carboxylic acid and phenolic or alcoholic functional groups (see **Figure 2.4**). Sulphur bearing functional groups are usually as much as twice as plentiful in fulvic acids relative to humic acids (Kerndorff and Schnitzer, 1980). Fulvic acids are soluble in both acids and bases because the ratio of structural carbon to amphoteric functional groups is large.

Humic acid structural type models have been developed from humic acid functional groups and elemental analysis (Stevenson, 1985). The solubility of humic acid in base is principally due to abstraction of acidic protons. The O/C ratio is lower than for fulvic acids, and much of the oxygen contributes to backbone structures rather than functional groups. Fewer reactive acidic and hydroxyl groups are present, and despite the presence of amide and amine groups, there is usually, but not always, a decrease in nitrogen with increased degree of humification (Kerndorff and Schnitzer, 1980; Schnizter and Kerndorff, 1980; Rashid, 1985). Terrigenous humic acids bear a stronger lignin signature than fulvic acids, with a more aromatic skeleton and a larger number of phenolic and quinone sites (Swift, 1985). **Figure 2.5** shows the type structure for humic acid according to Stevenson (1985).

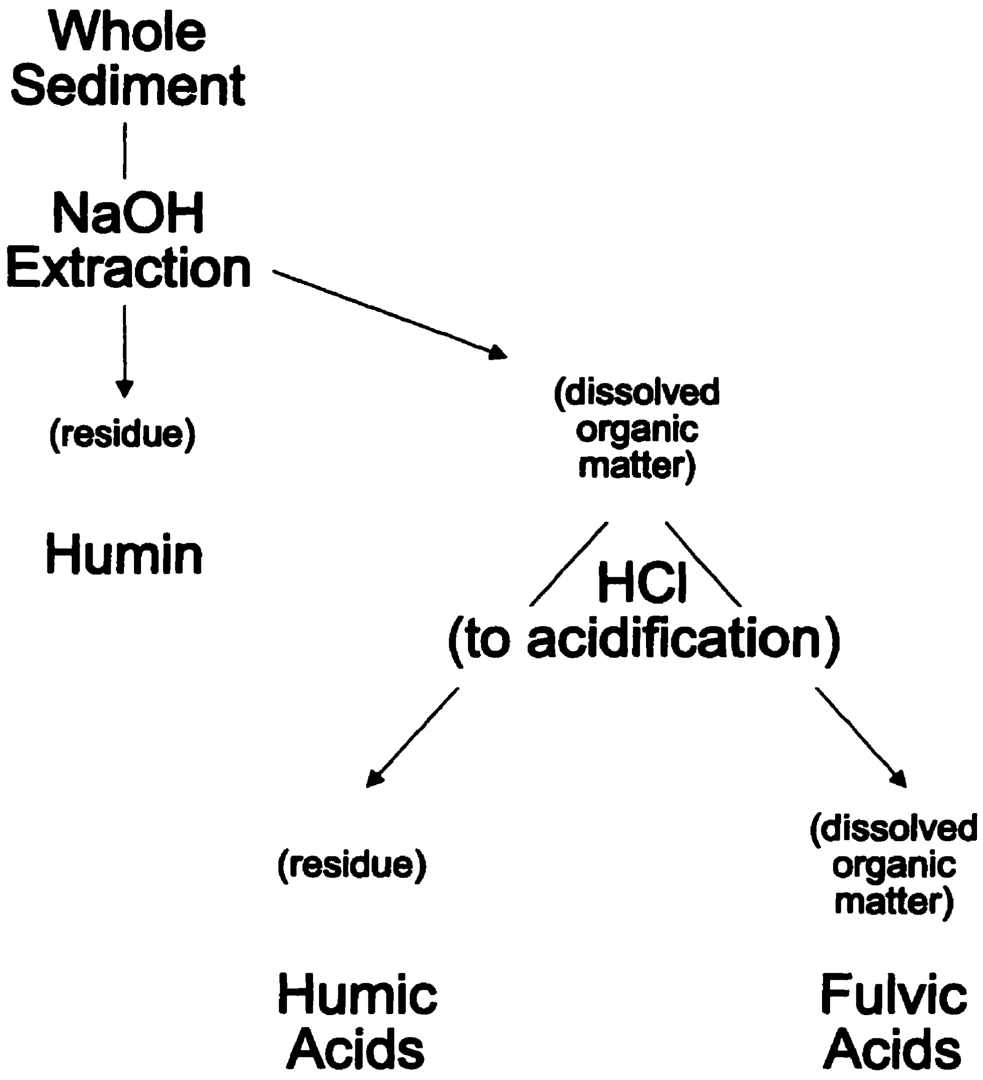

Figure 2.3 **Fractionation and classification scheme of humic substances (from Flaig *et al.*, 1975).**

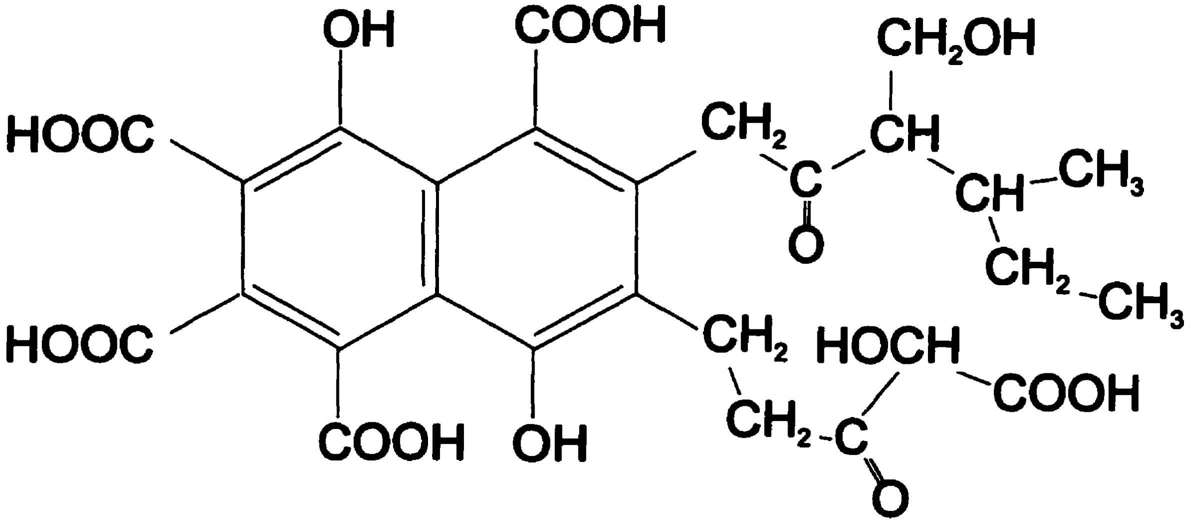

Figure 2.4: Type structure of fulvic acid proposed by Buffle, 1977 (from Stevenson, 1985)

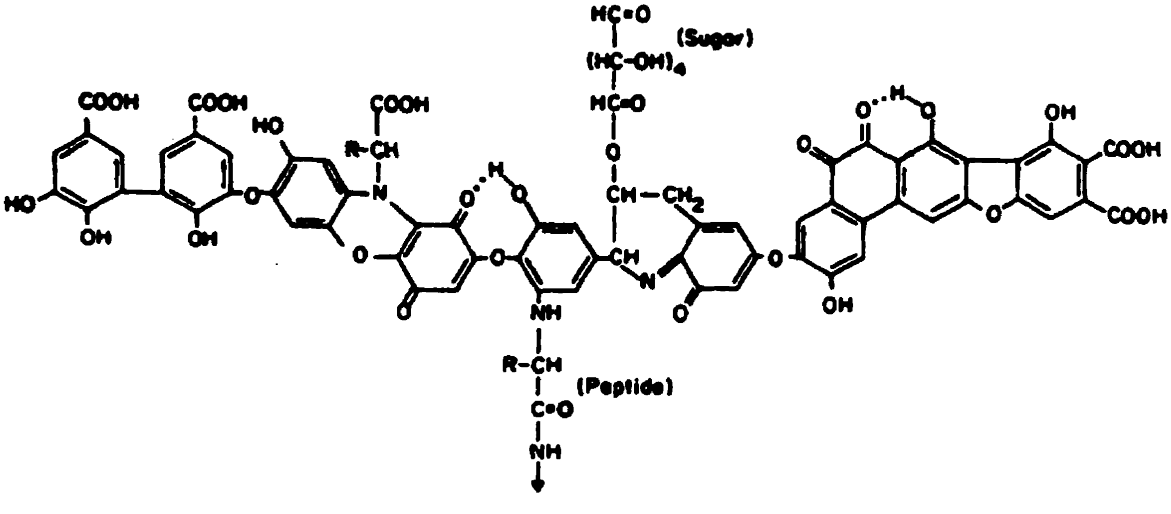

Figure 2.5: Type structure of humic acid (from Stevenson, 1985)

Humins have comparatively few functional groups and are insoluble in acid or base. Of humic compounds, they have the largest molecular weight, lowest O/C ratio, fewest acidic functional groups, and lowest nitrogen content. Humic compounds from terrestrial sources bear a strong lignin signature. Because of the similarity of functional groups and elemental composition between humins and humic acid, the distinctness of a humin phase has been questioned (Hatcher, *et al.*, 1985). It was found that when treated with HF, a significant fraction of "humin" became soluble in NaOH (Stevenson, 1994). It was concluded that because of the humate classification scheme, **clay-organic complexes** (see **Section 2.2.3**) are mistakenly classified with humins.

2.2.1.4 Characteristics of Estuarine Organic Matter

The terrestrial origin of most of the organic matter in estuaries is reflected in both the identifiable organic and humic matter reaching the sediment/water interface (Mayer, 1985). Whereas marine organic compounds are rich in proteins (as much as 60% of primary C_{org}) and carbohydrates, terrigenous matter is composed mostly of lignin, cellulose, and starch as well as their degradation products (Rashid, 1985). As a result, estuarine sedimentary organic matter is more aromatic in structure with a characteristically high C/N ratio (marine: 5-15; terrigenous: 10- >100; Rashid, 1985). Although marine sediments may contain S_{org} concentrations 10 times higher than in soils and may constitute 10% of S_{tot} (Rashid, 1985), it is unclear whether this results from the elevated protein content in marine particulates, or the uptake of diagenetically reduced sulphur by humic compounds (Rashid, 1985). Estuarine sediments are likely to share aspects of both terrestrial and marine organic matter and will likely vary from site to site. The Saguenay Fjord in particular exhibits a more terrestrial character, with low S_{org} values (Louchouarn, 1996).

2.2.2 Organic - Inorganic Interactions

Organic matter, particularly humates bind to metals and hydroxide surfaces at a variety of reactive sites and, accordingly, employ different bond types. Reactions between negatively charged or acidic functional groups and positively charged surface sites or cations result in a weak **electrostatic association**. The reversible reaction may typically be represented as: $R\text{-}COOH + M^{n+} \rightleftharpoons R\text{-}COOM^{(n-1)+} + H^+$. Although humates comprise only a few percent of sediment mass, their specific surface areas are much greater than other, more prevalent solid phases such as clays (See **Table 2.1**). This results in the exposure of more cation-exchange sites per gram, so that the cation exchange capacity (CEC) values attributable to organic carbon in sediments are often comparable or greater than those of other solid phases (Rashid, 1985).

Table 2.1 Specific surface areas and ion exchange capacities of some solid surfaces.

Material	Specific Surface Area ($m^2 \cdot g^{-1}$)	Ion Exchange Capacity ($meq \cdot 100\ g^{-1}$)
Kaolinite	10-50	3-15
Illite	30-80	10-40
Chlorite		20-50
Montmorillonite	50-150	80-120
Amorphous FeOOH	300	10-25
Humic Acids	1900	170-590

The formation of **coordination bonds** between organic compounds and metals is by far the most important type of inorganic-organic association. Coordination bonds form when ligands donate electrons to a central metal atom. Where ligands have two or more binding sites, they are referred to as **chelates**, and the resulting complex is particularly stable. Individual reactive sites (see **Figure 2.6**) may serve as bidentate ligands if the complex forms a localized ring. As well, humates exist as large, complex organic molecules with a large number of reactive sites, so that more distant functional groups may also serve as chelating ligands. The resulting complexes adopt a more stable conformation and often result in the irreversible binding and sequestration of metals to the organic phase. At low pH or high ionic strengths, the electrical double layer is thin and organic ligands may penetrate the inorganic hydroxide layer and form coordination bonds with surface metal atoms.

van der Waals forces are interparticulate associations arising from dipole interactions rather than the sharing of electrons or attraction between charged particles. Dipole-dipole interactions occur between two dipoles of opposite polarity. Dipoles bear no charge, and arise when two covalently bonded atoms have significantly different electronegativities, causing asymmetry in the electron density. **Hydrogen bonds** occur between the positive dipole of an X-H bond (where X is an electronegative atom such as O, N, or S), and a negative dipole (typically heteronuclear functional groups). Although the electrostatic attraction between the positive -H dipole and negative dipole in another molecule is weak, plentiful carboxyl, carbonyl, amine, and mercapto sites allow H-bonding to serve as a major bonding mechanism between humates and M-OH groups. **Induced dipole** interactions occur when an existing dipole deforms the electron density of a neighboring bond. Over large adjacent surface areas, the cumulative effect of induced dipole interactions can be significant. Another form of van der Waals bond, **water bridges**

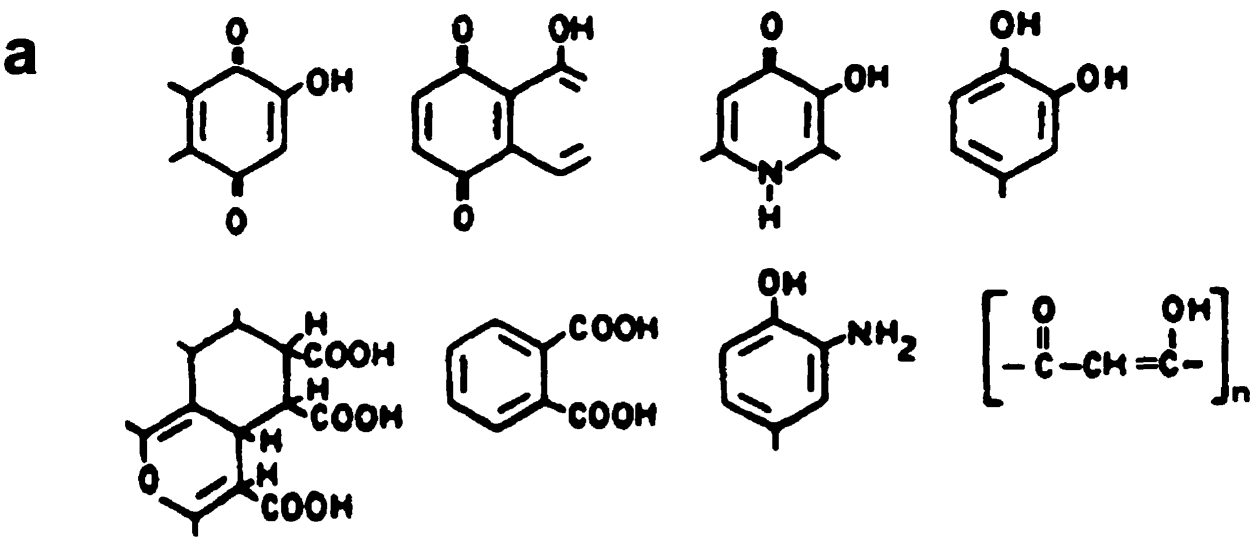

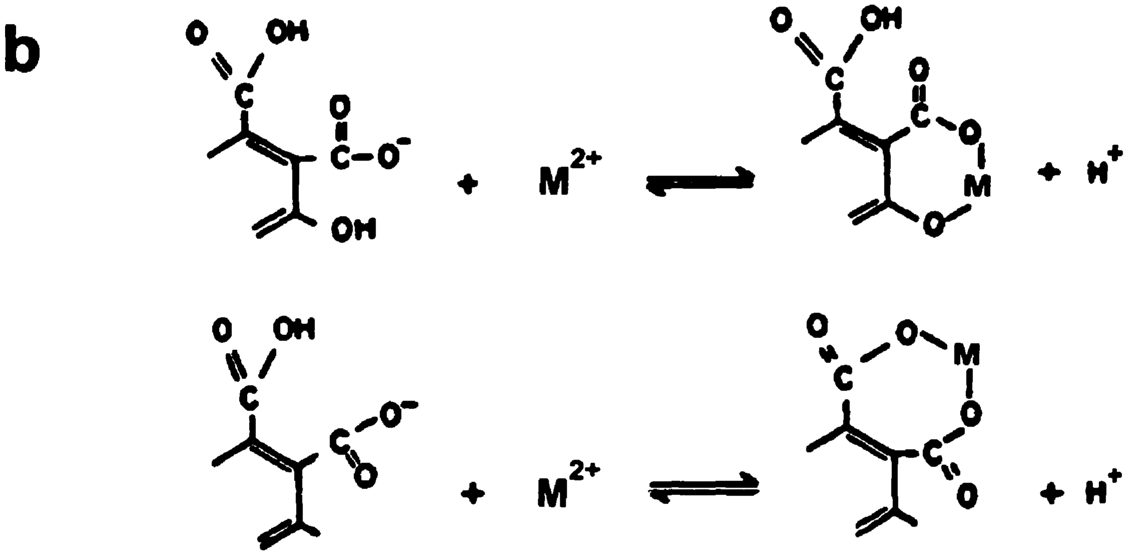

Figure 2.6a Chelates common in natural settings (Stevenson, 1985)

Figure 2.6b Organometallic complex formation with bidentate organic ligands. Abstraction of a proton produces a second negatively charged site; the localized ring greatly enhances complex stability (from Stevenson, 1985).

form when water molecules are trapped between the dipole (or even charged sites) on two opposing surface sites too distant to interact with each other directly.

2.2.3 Coatings

The tendency of organic matter and Fe/Mn hydroxides to form coatings on clay and hydroxide surfaces is well documented (Stumm and Morgan, 1972; Rashid, 1985; Gagnon *et al.*, 1992; Mayer, 1994). The formation of an organic coating can completely alter the surface electrostatic and chemical characteristics of the particulate substrate and may serve to dramatically alter the cation exchange capacity and specific surface area of the particle (Tipping, 1981; Petrovic, *et al.*, 1994). When large organic molecules bind to clay surfaces, the numerous binding sites between the two phases cumulatively effect a very stable association or "surface complex". The accumulation of coatings may create clay-metal-organic complexes by incorporating polyvalent metal cations which are bound at humate chelation sites, covalently bound to the clay surface, or found at cation exchange sites (Tipping, 1981; Stevenson, 1985). The formation of clay-metal-organic complexes serves to further bind the two phases as well as sequester metals to an organo-clay phase (see **Figure 2.7**). Consequently, clay-metal-organic complexes may play an important role in trace metal partitioning in natural aquatic and sedimentary systems (Lion *et al.*, 1982; Gagnon *et al.*, 1992).

Clay-organic complexes persist over geological time-scales, since adsorption of organic matter to clay pores < 8 nm in size affords protection of clay-organic complexes even against hydrolytic enzymes (Mayer, 1994). In addition, association to clays has been shown to lend humates (fulvic and humic acids) resistance to treatments normally designed to extract and solubilize organic matter (Stevenson, 1994; Lion *et al.*, 1982).

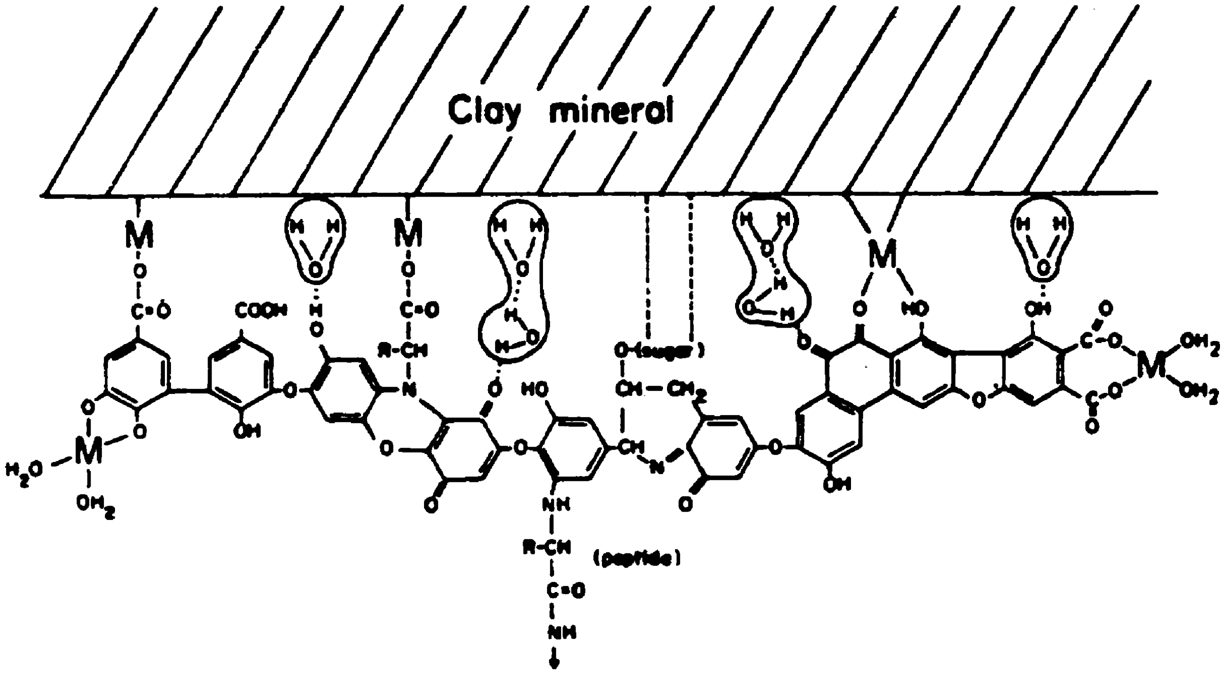

Figure 2.7 Proposed structure of a clay-metal-organic complex (from Stevenson, 1985).

As a result, on the basis of any extraction procedure (i.e. humate classification or sequential extraction schemes), materials sequestered to clay-metal-organic complexes will appear more refractory than their individual components.

2.2.4 Mercury - Organic Association

The association of mercury to organic matter in sediments has been studied extensively, both in the laboratory and in natural systems. Much evidence exists to suggest that organic matter is by far the most important Hg sequestering phase in sediments. Numerous studies have focussed on the accumulation of mercury in peats, organic-rich sediments, and soil horizons (Reimers *et al.*, 1974; Lindberg and Harriss, 1974; Loring, 1975; Fang, 1979; Andersson, 1979; Xu and Allard, 1991; Dmytriw *et al.*, 1994). Laboratory experiments indicate greater than 90% uptake of Hg from a 40 $\mu g{\cdot}mL^{-1}$ solution by organic soils (Andersson, 1979). Furthermore, the same study noted variable adsorption by clays and oxides (0% to ~90%) with a strong pH dependence, whereas organic adsorption curves showed no response to pH. Similarly, it was reported by Xu and Allard (1991) that even in the presence of minute quantities of fulvic acid (1 mg/L), nearly all mercury ($\Sigma Hg=5.6\ \mu g{\cdot}mL^{-1}$) is chelated to organic sites.

The high stability of organo-mercury complexes is well documented. Organo-mercury bonding is strongly covalent in character, rather than electrostatic (Reimers *et al.*, 1974; Randle and Hartmann, 1987; Dyrssen and Wedborg, 1991). The affinity of humic acids for mercury is among the highest of any metal (Kerdorff and Schnitzer, 1980). According to Reimers *et al.* (1974), desorption of mercury is negligible following adsorption to sedimentary organic matter. Furthermore, mercury cannot be removed from organic matter either via displacement by other metals, nor stripped from organic sites by competing ligands (Reimers *et al.*, 1974; Kerndorff and Schnitzer, 1980; Randle and Hartmann, 1987).

As pointed out by many researchers, Hg in the presence of organic compounds behaves quite differently than do other metals (Randle and Hartmann, 1987; Kerndorff and Schnitzer, 1980; Xu and Allard, 1991). Most metals are thought to bind to the carboxyl and hydroxyl sites in various amphoteric functional groups (Rashid, 1985). In addition, most transition metals adsorb to these sites best while in the form of hydrolyzed complexes (Kerndorff and Schnitzer, 1980). Consequently, metals such as Fe(III),Pb, Cu, Al, Ni, Cr(III), Cd, Zn, Co, and Mn demonstrate a humate adsorption curve markedly dependent on pH, while Hg does not (Kerndorff and Schnitzer, 1980; Schnizter and Kerndorff, 1980).

Organo-mercury complex stabilities appear to follow the order of affinity presented in **Section 2.1** with respect to functional group chemistry. Reimers *et al.* (1974) used C_{10} homologues to determine the following sequence of the mercury complexing capacities for organic functional groups:

mercaptans >> amines > carboxyls.

Similarly, Morel *et al.* (1973) reported the Hg-organic speciation in an aqueous solution containing four organic ligands. Under oxygenated conditions, in the presence of citrate, glycine, nitrilotriacetate (NTA), and cysteine, all of the mercury appears to be associated with cysteine. With naturally occurring humic and fulvic acids from a variety of lakes and rivers, thio- sites appear to play a predominant role in organic chelation of mercury (Frimmel *et al.*, 1984). The adsorption of Hg to thio- and amino sites may, in part, explain the pH independence of humate-mercury adsorption curves, as the effect of pH on these functional groups has been shown to be minimal (Reimers *et al.*, 1974).

An elaboration of mercury-thiochelate speciation (see **Figure 2.8**) reveals that the stability of the complexes depends on both the affinity of mercury for other electron donor sites in the chelate, and the bond strain within the chelate required to accommodate the Hg coordination sphere structure. The formation of the two foreshortened, highly covalent bonds oriented 180° to each other may also force distorted or strained configurations, even though tetrahedral and distorted octahedral geometries, among others, are possible (Greenwood and Earnshaw, 1984; Frimmel *et al.*, 1984). Additionally, because N has a greater capacity to form covalent bonds with mercury than O, nitrogen bearing secondary functional groups will form stronger complexes than the oxygen bearing analogs. Furthermore, the chelate must be sufficiently flexible (preferably through the formation of a 5 or 6 member ring) to accommodate the structure of Hg complexes. Finally, because the short, highly covalent bonds are positioned *trans* to each other, additional constraints are placed on the structures of stable complexes (Forbes *et al.*, 1974; Frimmel *et al.*, 1984).

Since organic matter, most notably humates, serve as a major adsorbate for Hg and the association between them is long and lasting, the solubility (and therefore mobility) of Hg should be largely dependent on the behaviour of the organic phase in a sediment or soil. In the porewaters of Mobile Bay sediments, the supersaturation of Hg relative to HgS is thought, in part, to result from the stability of soluble organic-Hg complexes (Randle and Hartmann, 1987). According to Reimers *et al.* (1974), changes in Hg solubility with pH are due to changes in organic matter solubility rather than to release of Hg to solution. In other words, as the solubility of organic matter increases with increasing pH, more Hg is solubilized as humate complexes.

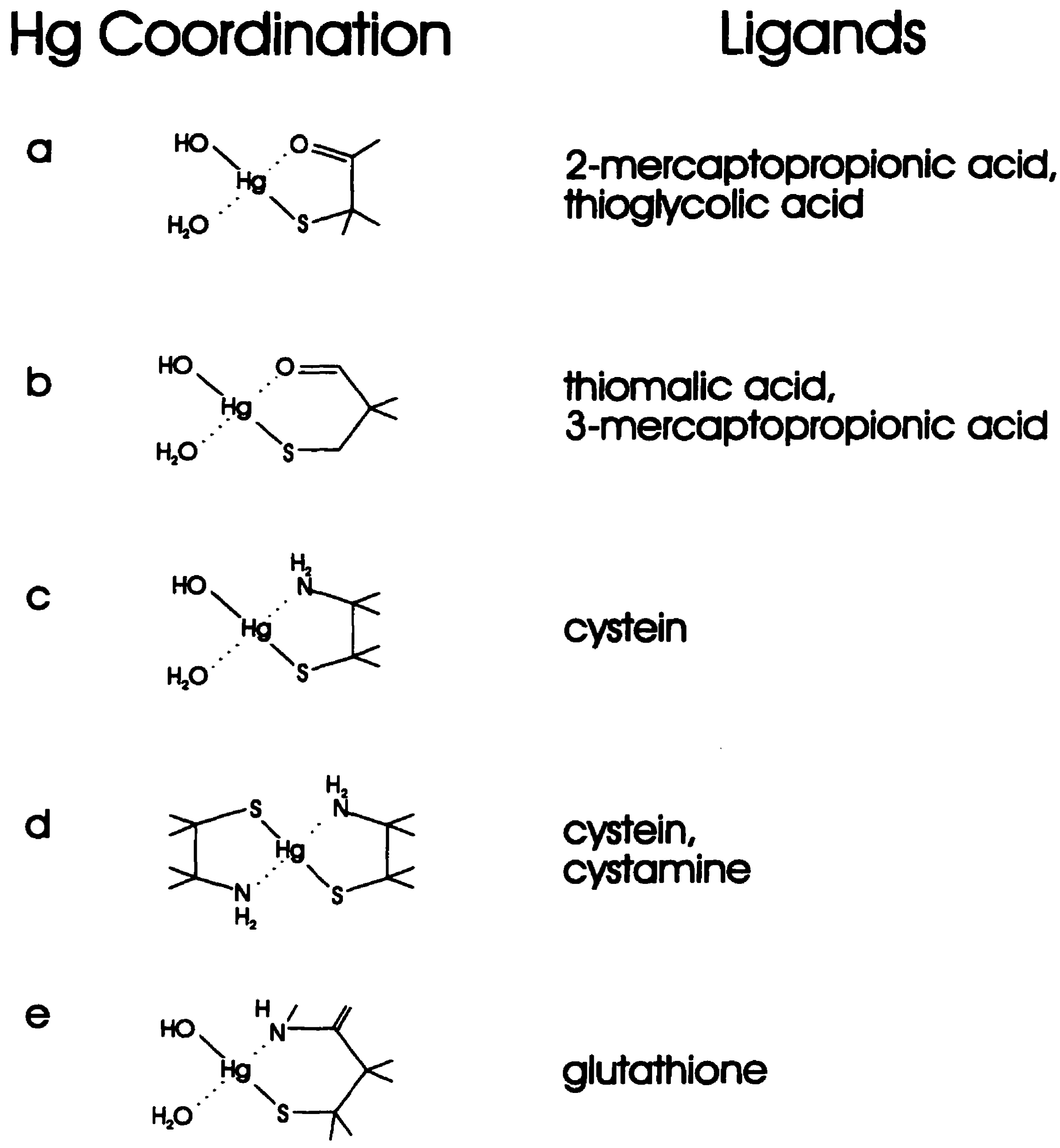

Figure 2.8 Representative thiochelate-mercury structures (after Frimmel *et al.*, 1984). The order of complex stability is a < b < c < d < e and reflects the importance of functional groups (S, N >>> O) and bond strain within the ligand structure.

In brief, organic matter, which comprises only a very small fraction of most estuarine sediments (~1-3%), determines to a large extent the early diagenetic chemistry of mercury. The magnitude of the organic input to sediments influences the amount of mercury transferred to sediments. More precisely, the concentration of high-affinity chelation sites within humic compounds controls the amount of mercury associated with the organic fraction and the strength of this association. In addition, humic matter may form coatings on clays and other inorganic particulates and effectively sequester mercury in highly refractory clay-metal-organic complexes.

2.3 Adsorption of Hg by Hydrated Inorganic Solids

The solids which include clays, tectosilicates, as well as iron and manganese (hydr)oxides are grouped together since each group presents surface hydroxyl groups as the principal sites of specific adsorption. Unsatisfied hydroxyl groups on the surface of these materials may carry a variable charge, as a result of their amphoteric nature. The polarity and overall magnitude of the charge of hydrated surfaces is dependent on the pH of the surrounding system. The pH at which the net surface charge of hydroxyl-bearing surfaces is zero is called the iso-electric point (IEP) or pH_{znc} (pH of zero net charge) and is dependent on the acidity of the exposed oxygens, which is related to the internal structure of the solid. Where pH < IEP, the majority of surface hydroxyl groups are protonated and positively charged ($-OH_2^+$). In contrast, where pH > IEP, deprotonation occurs and sites exist principally as negatively charged $-O^-$ groups (Stumm and Morgan, 1972).

Due to the amphoteric behaviour of the hydroxyl groups, these surfaces become less-positive, or negatively charged, with increasing pH. At the same time, under acidic conditions, most dissolved metals exist as the free metal ion but hydrolyze to form hydroxyl complexes under more neutral pH conditions. As a result, the charge of dissolved metal ions also becomes less positive with increasing pH. Dissolved metals are specifically adsorbed to oxide surfaces via coordination bonding through shared hydroxyl ligands (Fields and Claridge, 1975; Evans, 1989). A sample reaction appears as:

$$\equiv S\text{-}O^{-} + M\text{-}OH^{y+} \rightarrow \equiv S\text{-}O\text{-}M\text{-}OH^{(y-1)+} \quad (2.1)$$

(Evans, 1989). The adsorption of most metals to (hydr)oxide surfaces increases with pH, appearing as a sigmoidal curve, since electrostatic repulsion between dissolved metals and the Fe/Mn oxide surface decreases (Forbes, *et al.*, 1974; Evans, 1975; Barrow and Cox, 1992). For metals which precipitate as insoluble hydroxides, such adsorption may serve as a precursor to the formation of a discrete metal hydroxide phase under very alkaline conditions (Evans, 1975).

2.3.1 Silicates

2.3.1.1 Clays

Second only to tectosilicates in abundance in Saguenay Fjord sediments (see **Section 3.2**), clays are hydrous aluminosilicates with laminar structures, which classify them as phyllosilicates. They commonly form as a result of the chemical weathering of tectosilicates. Structurally, clays are comprised of various combinations of layers of silica tetrahedra and metal hydroxide octahedra (generally populated by Al^{3+}, Mg^{2+}, Ca^{2+}, and $Fe^{3+,2+}$). Clay minerals are classified structurally by the relationship of octahedral and tetrahedral layers bound covalently into repeating units. Described in **Figure 2.9**, kaolinite serves as a common example of the "T-O" structure, whereas the "T-O-T" structure could be represented by talc. Chlorite resembles the "T-O-T" structure followed by a discrete octahedral layer. These structures are dependent on interlayer Van der Waals forces and tend to have low specific surface areas, low CEC values, and have no interlayer cations or water. In other clays, an internal, permanent, usually negative

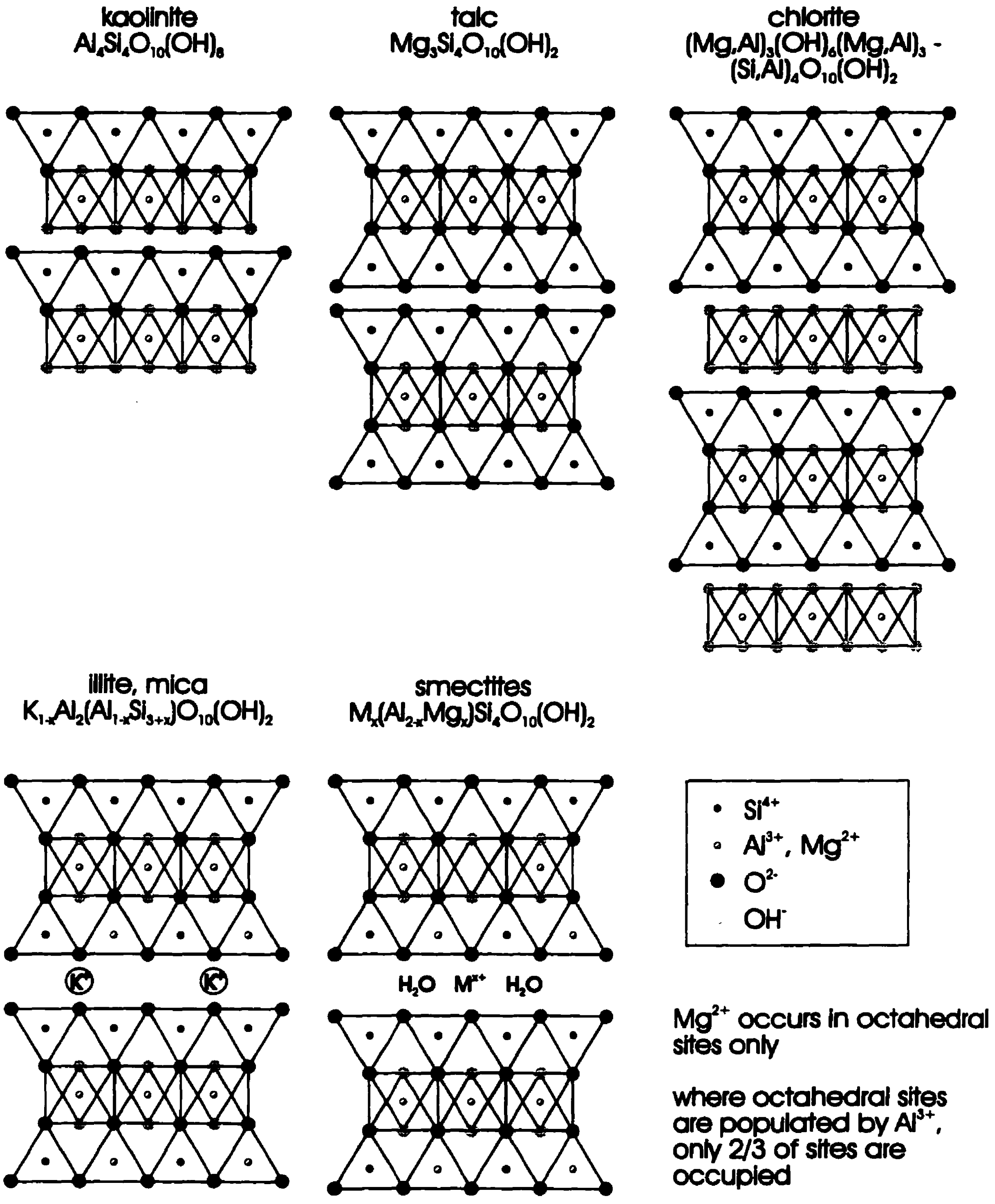

Mg^{2+} occurs in octahedral sites only

where octahedral sites are populated by Al^{3+}, only 2/3 of sites are occupied

Figure 2.9: Clay mineral structures (after Klein and Hurlbut, 1985).

fixed charge arises from the isomorphous substitution of Al^{3+} for Si^{4+}, or a divalent metal for Al^{3+}. Among clays of this type, micas counter the fixed charge with ordered sites of tightly bound interlayer counterions (generally K^{-}). Alternatively, smectites have lower interlayer charges and take on water and very weakly bound hydrated cations between their layers. As a result, smectites (e.g. montmorillonite) have significantly greater CEC values compared to micas (e.g. illite) (Yong, 1988). In addition to the fixed charge of clay surfaces, all clays have variable charge sites (as discussed above) where broken edges or external layers present unsatisfied hydroxy groups. Whereas the negative fixed charge is important for the weak coulombic physisorption at cation exchange sites, the variably charged sites are much more important with respect to the specific adsorption of metals to the clay surface.

The adsorption of mercury to **clays (kaolinite, illite, montmorillonite)** was also found to be differ markedly from that of other transition metals (Farrah and Pickering, 1978). In brief, Hg adsorption to kaolinite and illite remains constant with pH and adsorption to montmorillonite exhibits a dramatic decrease with increased pH. Farrah and Pickering (1978) suggest that this indicates a partial ability by sites on illite and kaolinite to cause the dissociation of one of the Hg-OH bonds, while montmorillonite sites appear incapable of adsorbing $Hg(OH)_2$ to any measure. This may be partly due to the increase in active adsorption sites on kaolinite and illite surfaces with increasing pH, as opposed to the relatively constant population of reactive sites on montmorillonite (Farrah and Pickering, 1977). As a result, over most pH conditions, the affinity of the clays for Hg appears as illite > montmorillonite > kaolinite. That this trend does not reflect the respective ion exchange capacities of the clays is attributable to the predominance of the neutral $Hg(OH)_2^0$ species at low pCl^- above pH = 4 (Farrah and Pickering, 1978). Thus, in the case of mercury complexation on clay surfaces, specific adsorption is far more important than electrostatic interactions.

In the presence of chloride, kaolinite, illite, and montmorillonite were found to adsorb only minute amounts of $HgCl_2$ (Farrah and Pickering, 1978). All clays, however, demonstrated an Hg adsorption maximum where concentrations of $HgOHCl^0$ were highest. As discussed previously, although $Hg(OH)_2^0$ and $HgCl_2^0$ are both stable dissolved complexes, $HgOHCl^0$ is only sparingly soluble. Farrah and Pickering (1978) proposed that $HgOHCl^0$ may be more easily dissociated by surface sites than $Hg(OH)_2^0$. They also reported that clays are unable to adsorb the negatively charged mercury species present at higher chloride concentrations (i.e. $HgCl_3^-$, $HgCl_4^{2-}$).

2.3.1.2 Tectosilicates

Tectosilicates, such as feldspars and quartz, are the most abundant geological materials in the earth's crust and are the principal solids found in Saguenay Fjord sediments. Essentially, tectosilicates are silicoalumino(hydr)oxides. Structurally, they consist of silica tetrahedra linked through a shared oxygen atom in three dimensions. The result is a strong structure, resistant to both physical and chemical weathering. There are few reactive sites accessible to dissolved species, while surface reactive sites consist of variably-charged, exposed hydroxyl sites. Isomorphic substitution of Al^{3+} for Si^{4+} may lead to the incorporation of charge balancing metals (e.g. K^+) or may result in localized fixed charge sites. Nevertheless, the reactive surface area of tectosilicates is much less than that of clays and Fe/Mn (hydr)oxide solids (Stumm and Morgan, 1972).

Like most transition metals (e.g. Cu^{2+}, Cd^{2+}), mercury exhibits a sharp increase in degree of adsorption to SiO_2 as it hydrolyses (Stumm and Morgan, 1972; MacNaughton and James, 1974). Hg adsorption to silica differs markedly from typical metal behaviour as it *decreases* with increasing pH. MacNaughton and James (1974) suggest that the increase in adsorption prior to hydrolysis of Hg(II) occurs as the electrostatic repulsion between the positively charged silica surfaces and the Hg^{2+} ions decreases.

Simultaneously, the concentration of $HgOH^+$ also increases, and the adsorption maximum appears to correlate with the peak concentrations of $HgOH^+$. Because the adsorption of $Hg(OH)_2$ to the SiO_2 surface requires the dissociation of one of the Hg-OH bonds, which are unusually covalent for a divalent metal, adsorption of mercury decreases with increasing pH as a result of the decreasing $HgOH^+$ concentration (MacNaughton and James, 1974). The presence of chloride ions also prevents the adsorption of Hg(II) because of the formation of either the neutral $HgCl_2^0$ complex or of the negatively charged polychloride complexes $HgCl_3^-$ and $HgCl_4^{2-}$.

Given the inability of silicates to physisorb anionic Hg complexes and the poor adsorption qualities of chloro compounds, both studies concluded that negligible quantities of inorganic Hg(II) should be found adsorbed *directly* to silicate surfaces in marine sediments. It must be restated and emphasized, however, that in natural systems clay surfaces do not usually behave as the pure phases examined in the above studies. The accumulation of both organic and inorganic coatings dramatically alters the surface chemistry of clay particles (**Section 2.2.3**). In addition, the interaction of separate phases results in the formation of distinct chemical environments at phase interfaces (e.g. clay-metal-organic complexes) which may exert significant control on the speciation and partitioning of trace metals.

2.3.2 Fe/Mn (Hydr)Oxides

Like organic matter, iron and manganese oxides, hydroxides, and oxyhydroxides comprise a small portion of estuarine sediments, but significantly affect the early diagenetic behaviour of trace metals. Like clays, the surfaces of Fe/Mn (hydr)oxides are populated by unsatisfied hydroxyl groups. Hydroxide and oxide minerals are noted as effective scavengers of organic matter and trace metals (Forbes *et al.*, 1974; Sholkovitz, 1976; Moore *et al.*, 1979; Laxen, 1979; Canfield, 1989; Shaw *et al.*, 1990; Gobeil and Cossa, 1993; Burdidge, 1993). Iron and manganese (hydr)oxides also serve as one of the most reactive solid components of sediments after organic matter. Diagenetic cycling results from burial below the redoxcline, followed by dissolution of reducible phases, diffusion to oxic sediments, and finally, oxidation and re-precipitation above the redoxcline (Presley *et al.*, 1972; Sundby and Silverberg, 1985; Shaw *et al.*, 1990; Mucci and Edenborn, 1992). Because associated trace metals are strongly influenced by the early diagenetic behaviour of Fe and Mn, their possible role in the transport and partitioning of mercury is discussed here.

2.3.2.1 Origins and chemistry

Estuaries are the site of significant flux of iron from river water to sediments (Boyle *et al.*, 1974; Sholkovitz, 1976). Iron-oxyhydroxide colloids, which are stable in fresh water, become de-stabilized upon exposure to sea water because increasing ionic strength decreases interparticulate electrostatic repulsion (Sholkovitz, 1976). Consequently, iron oxide, hydroxide, and oxyhydroxide flocs and coatings on other particulates are transported to the sediment/water interface. Additionally, iron (hydr)oxide minerals, (e.g. magnetite) may originate as detrital material and be transported to sediments as particulate matter settles through the water column.

The behaviour of dissolved manganese, on the other hand, is predominantly conservative during estuarine mixing and Mn is not believed present in colloidal form (Holliday and Liss, 1976; Moore, *et al.*, 1979). Mn dissolved in natural waters is believed to dominantly exist as "free" metal ion Mn^{2+}, with the remainder (as much as 30%) in the form of organically complexed Mn(II) and Mn(III) (Moore *et al.*, 1979; Burdidge, 1993). Although dissolved Mn behaves conservatively, significant concentrations of Mn oxides

Table 2.2 Fe and Mn oxide, hydroxide, and oxyhydroxide minerals common to estuarine sediments.

	Fe
Goethite	α-FeOOH
Ferrihydrite	$5\ Fe_2O_3 \cdot 9\ H_2O$
Akageneite	ß-FeOOH
Lepidocrocite	γ-FeOOH
Magnetite	Fe_3O_4
	Mn
Todokorite	$(Ca,Na,K)(Mg,Mn^{2+})Mn_5O_{12} \cdot x\ H_2O$
Vernadite (δ-MnO_2)	$MnO_2 \cdot n\ H_2O \cdot m\ (R^{z+}{}_{2/z}O)$ where R=Na,Ca,Co,Fe,Mn
Birnessite	$(Na,Ca,K)(Mg,Mn^{2+})Mn_6O_{14} \cdot 5\ H_2O$
Hausmannite	Mn_3O_4
Feitknechtite	β-MnOOH

and hydroxides coat suspended particulate matter, which consequently serves as a manganese input to sediments upon deposition (Sundby and Loring, 1977; Moore *et al.*, 1979).

Both Mn and Fe (hydr)oxide solids, excluding detrital particulates, tend to exhibit poor crystallinity and a characteristic lack of long-range order, making identification of specific oxide minerals difficult (Burdidge, 1993). The common Fe and Mn oxide minerals and solids found in sediments appear in **Table 2.2.**

Following reduction to Fe(II) and Mn (II) below the redoxcline, both Fe(II) and Mn(II) diffuse up along their concentration gradients until they are oxidized and re-precipitated in the presence of oxygen. Consequently, solid-phase peaks of both oxidized Fe and Mn appear near the redoxcline in sediment profiles under steady-state conditions. Despite apparent similarities in behaviour, considerable differences often exist in the diagenetic cycles of iron and manganese (Burdidge, 1993). Because the oxidation of iron proceeds much more rapidly than that of Mn, the easily reducible Fe peak usually appears below that of Mn, since Mn(II) may penetrate further within the O_2 penetration zone before being oxidized and precipitated. In addition, Fe oxides are commonly found below the redoxcline, depending on their reactivity or the ease by which they are reduced and solubilized (Canfield, 1989; Canfield *et al.*, 1992; Raiswell *et al.*, 1994; Postma and Jakobsen, 1996). Other iron solids may form, since Fe^{2+} may also precipitate as monosulphides, siderite ($FeCO_3$), or vivianite ($Fe_3(PO_4)2{\cdot}8(H_2O)$). In modern sediments, iron monosulphides are common, vivianite is rare, and siderite only forms when CO_3^{2-} concentrations increase due to fermentation following depletion of SO_4^{2-}.

2.3.2.2 Adsorption of Mercury

The chemisorption of mercury to (hydr)oxides surfaces is distinctly different from the adsorption of other metals (Forbes *et al.*, 1974; Barrow and Cox, 1992). Most metals exhibit the characteristic sigmoidal adsorption curve around pH = pK_1 (first hydrolysis constant). With increasing pH, near complete adsorption of the metal occurs rapidly. Mercury does not follow this pattern, even as the surface charge on goethite changes polarity at pH 7.6 (Forbes *et al.*, 1974). The degree of adsorption of mercury at pH = pK_1 (3.75) is considerably less compared to other metals (Forbes *et al.*, 1974; Barrow and Cox, 1992). As well, the slight increase in Hg adsorption around pK_1 is followed but a slight *decrease* or no change at all with increasing pH (Forbes *et al.*, 1974; Lockwood and Chen, 1974; Barrow and Cox, 1992). In contrast, Gunneriusson *et al.* (1995) reported a slight increase in Hg adsorption with increasing pH, but their study suffered from serious difficulties in accounting for unrecovered Hg and large uncertainties in the measurement of adsorbent specific surface area.

The presence of Cl^- ions severely inhibits the adsorption of mercury to goethite surfaces (Lockwood and Chen, 1974; Forbes *et al.*, 1974; Barrow and Cox, 1992). Lockwood and Chen (1974) reported that no significant mercury was sorbed at pH ~ 7 and $pCl^- = 0.22$ despite the fact that the surface charge of goethite is positive and $HgCl_4^{2-}$ is the predominant mercury species. Forbes *et al.* (1974) also found that the uncharged $HgCl_2^0$ was not adsorbed to goethite surfaces under acidic and mildly alkaline conditions. The consensus of these researchers is that adsorption of mercury occurs via surface complexation of hydroxy ligands, while no specific adsorption sites exist for chloro complexes.

There is no consensus about the structure of the mercury surface complex with iron hydroxides. It is likely a combination of adsorption of $Hg(OH)_2^0$ and $Hg(OH)^+$ (Forbes *et al.*, 1974; Barrow and Cox, 1992). The adsorption maximum of mercury to goethite coincides with the field of predominance of $HgOH^+$ (Barrow and Cox, 1992). As pH increases, deprotonation of surface sites reduces positive charge repulsion while the population of $HgOH^+$ increases. At higher pH, the net surface charge on goethite becomes negative, which further favours $HgOH^+$ adsorption, but the population of $HgOH^+$ simultaneously decreases. If adsorption could be ascribed to $Hg(OH)^+$ alone, there would be a sharp decrease in adsorption with increasing pH as $Hg(OH)^+$ is converted to $Hg(OH)_2^0$. Despite the covalent character of the Hg-OH bond, the contribution of $Hg(OH)_2^0$ to overall Hg adsorption is significant (Forbes, *et al.*, 1974). The linear molecule $Hg(OH)_2$ should be positioned either parallel to the surface, as a distorted ("banana-shaped") doubly bound surface complex, or else perpendicular to the hydroxide surface via one hydroxy bridge **(See Figure 2.10)**. Other metals, such as Cu(II), Co(II),

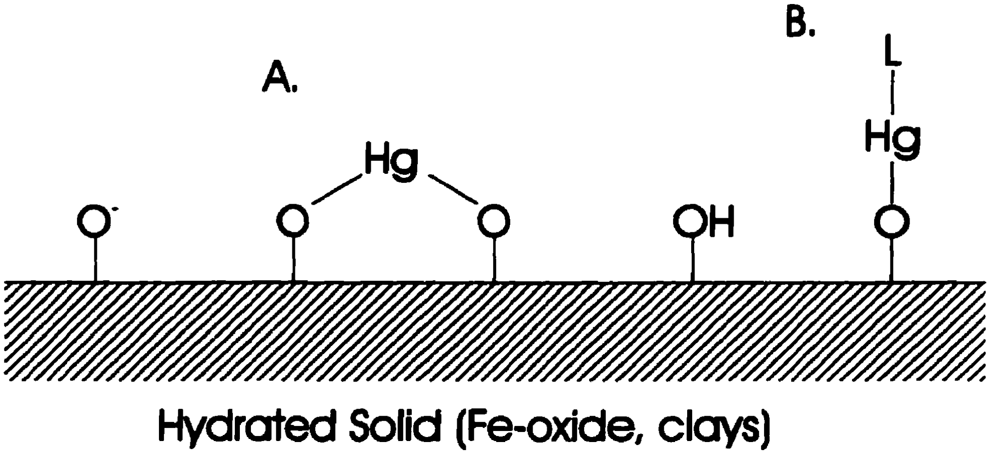

A Distorted Linear ("banana-shaped") surface complex
B. Linear singly-bound mercury surface complex (L=Ligand)

Figure 2.10 Mercury complexes on the surfaces of hydrated solids

or Zn(II), which form octahedral or tetragonal hydroxy complexes do not suffer from the conformational strain of the linear molecule and bind stably at two sites (Forbes *et al.*, 1974).

Although generally present in smaller quantities in natural systems, manganese oxides and hydroxides are considerably more effective at Hg adsorption than their iron counterparts (Lockwood and Chen, 1974; Thanabalasingam and Pickering, 1985). Like Fe-hydroxides, the Hg is sorbed to a considerably lesser degree than other metals (Lockwood and Chen, 1974; Thanabalasingam and Pickering, 1985). Also, mercury is adsorbed without the release of cations, suggesting that association with MnO_2 also occurs via chemisorption. The amount of mercury adsorbed increases with pH, then levels off, and the creation of new negatively charged sites via proton abstraction does not appear to affect Hg adsorption (Thanabalasingam and Pickering, 1985). Adsorption of mercury to manganese oxides, however, shows some significant differences in behaviour from iron minerals. In the presence of Cl^- ($pCl^- = 2.0$), adsorption at low pH is greatly reduced compared to the chloride-free system and *decreases* with increasing pH to a minimum around pH = 4.5. Above pH = 4.5, the amount of Hg adsorbed increases gradually to levels similar to a chloride-free system by pH 10. Based on these observations, Thanabalasingam and Pickering (1985) conclude that, unlike Fe-(hydr)oxides, a mechanism exists for the uptake of both the $Hg(OH)_2^0$ and $HgCl_2^0$ species of mercury on MnO_2, and for the exclusion of the $HgCl^+$ and $HgOH^+$ species.

Thanabalasingam and Pickering (1985) suggest that both the increased uptake relative to goethite and the adsorption of $HgCl_2^0$ may partly be due to the presence of tunnels, pores, and pits in Mn oxide and hydroxide minerals. Mn minerals with structures bearing more pits and tunnels exhibited a greater ability to adsorb mercury (hydrous Mn oxide > α-MnO_2 > γ-MnO_2). Tunnels, pores, and pits could create an environment for ligand exchange (replacing OH^- for Cl^-) as well as permit the formation of a discrete hydrous mercury solid phase. Furthermore, they suggest that the reduced uptake of mercury relative to smaller metal ions could in part be attributed to the steric constraints created by the radii of the various structural openings.

Despite the observations that there is greater uptake of mercury by Mn rather than Fe oxides and hydroxides, the surface complexes formed between manganese oxide surfaces and Hg are weak. Although unaffected by $Na_4P_2O_7$, Na_3cit and NH_3COONH_4, mercury was effectively stripped from Mn oxides by more aggressive reagents, such as EDTA, DTPA and 0.5 M HCl (Thanabalasingam and Pickering, 1985).

2.3.2.3 Hg and Fe/Mn (Hydr)Oxides in Natural Systems

The relationship between Hg and oxide minerals in natural systems has been documented by several researchers (Giordano *et al.*, 1992; Huerta-Diaz and Morse, 1992; Gobeil and Cossa, 1993; Dmytriw *et al.*, 1994; Gagnon *et al.*, 1997) but remains unclear. Gobeil and Cossa (1993) reported the simultaneous release of Hg and Fe(II) to porewaters at and below the redoxcline in St. Lawrence estuary sediments. In addition, they noted that hydroxylamine-extractable mercury, manganese, and iron each exhibit maxima in the upper 2 cm of the sediment profile. They interpreted these results as an indication of significant uptake of mercury by iron hydroxide and possibly manganese oxide solids. Gobeil and Cossa (1993), however, neglect to consider the effect of organic carbon on mercury distribution within the profile, and did not explore whether hydroxylamine is capable of extracting organic matter.

Other researchers have investigated the relationship between Hg and Fe/Mn hydroxide/oxide minerals via sequential extraction techniques, but with mixed results. Gagnon *et al.* (1997), Huerta-Diaz and Morse (1992), and Giordano *et al.* (1992) found considerable or negligible amounts of mercury associated to Fe/Mn (hydr)oxides depending upon the methodology used (**Section 4.3.2.3**).

Based on the discussion presented in the previous section (**4.3.2.2**), the behaviour of mercury at the surfaces of Fe/Mn (hydr)oxides results from both structural and chemical characteristics of mercury complexes. Because the Hg-O bond is more covalent than that of other metals, the first hydrolysis constant of mercury is considerably lower. Furthermore, the covalent character causes hydroxy-mercury complexes to form weaker associations with the oxide surfaces compared to other metals. Since $Hg(OH)_2^0$ predominates over most pH conditions, the characteristic sigmoidal adsorption curve with increasing pH, which is typical of most metals, is comparatively muted. Finally, $Hg(OH)_2^0$ is linear, inhibiting the formation of multiple stable coordination bonds with the (hydr)oxide surface. As is consistent with adsorption of mercury by most substrates, the effect of dissolved chloride is to considerably lessen the ability of (hydr)oxide solids to take up mercury. In natural systems, iron and manganese (hydr)oxides serve as effective adsorbents, but have much lower affinities for mercury than do other substrates. In a natural system where other phases, particularly organic matter, are present in significant concentrations, Fe/Mn (hydr)oxide solids will play only a secondary role in the adsorption of mercury.

2.4 Adsorption and Co-Precipitation of Hg with Iron Sulphides

Iron sulphides serve as a significant class of marine and estuarine sedimentary solids and seriously impact the geochemical cycles of many trace metals. Generally, iron sulphide solid phases are separated into two categories. On the basis of reactivity (via chemical separation), pyrite is distinguished from iron monosulphides. Iron monosulphides include amorphous FeS, mackinawite, greigite, and sometimes pyrrhotite, and are also termed acid-volatile sulphides (AVS) (Rickard *et al.*, 1995). Pyrite (FeS_2) is highly resistant to oxidation and is metastable in oxic sediments. As the diagenetic end product of iron in the presence of reduced and elementary sulphur, pyrite is the dominant iron sulphide in most sediments (Cornwell and Morse, 1987). Conversely, monosulphide phases are highly reactive metastable solids which oxidize within minutes upon exposure to oxygen and are soluble in HCl. Pyrrhotite ($Fe_{1-x}S$) rarely forms authigenically in sediments (Cornwell and Morse, 1987), but is often used in laboratory experiments because it is metastable under atmospheric conditions (Brown *et al.*, 1979; Jean and Bancroft, 1986; Hyland *et al.*, 1990).

Iron sulphide minerals act as effective scavengers of several metals, including Hg, both via co-precipitation and adsorption on solid surfaces (Raiswell and Plant, 1980; Luther *et al.*, 1980; Jean and Bancroft, 1986; Belzile and Lebel, 1986; Skei *et al.*, 1988; Dyrssen and Kremling, 1989; Huerta Diaz and Morse, 1990; Hyland *et al.*, 1990; Huerta Diaz and Morse, 1992; Arakaki and Morse, 1993; Morse and Arakaki, 1993). As a stable reservoir of trace metals, pyrite could represent an important permanent sink of mercury in sediments. Conversely, mercury associated with monosulphides would represent a significant environmental hazard as disturbance of reduced sediments and re-oxidation of AVS solids could result in the release of associated trace metals. Iron sulphide forms, mechanisms of formation, and nature of association with Hg are discussed here.

2.4.1 Formation of Iron Sulphides

Following the consumption of other electron acceptors (O_2, NO_3^-, and reactive Mn and Fe (hydr)oxides), sulphate is reduced to sulphide by the metabolic action of microorganisms. Reaction of sulphide with dissolved ferrous ions or reducible ferric minerals will lead to the formation of AVS (**Table 2.3**)

Table 2.3 Rate constants and half-lives of sedimentary iron minerals with respect to their sulphidization (from Canfield *et al.*, 1992).

Iron mineral	Rate constant (yr^{-1})	Half-life
Ferrihydrite	2,200	2.8 hours
Lepidocrocite	> 85	< 3 days
Goethite	22	11.5 days
Hematite	12	31 days
Magnetite (uncoated)	$6.6 \cdot 10^{-3}$	105 years
"Reactive" silicates	$3 \cdot 10^{-3}$	230 years
Phyllosilicates	$8.2 \cdot 10^{-6}$	84,000 years
Ilmenite, garnet, augite, amphibole	$<< 8.2 \cdot 10^{-6}$	>> 84,000 years

Laboratory experiments by Schoonen and Barnes (1991) suggest that the incremental formation of each monosulphide phase represents the formation of increasingly thermodynamically stable minerals via the progressive sulphidization in the presence of intermediate sulphur compounds (**Figure 2.11**)

The unnamed cubic form of FeS discussed by Schoonen and Barnes (1991) was isolated *in vitro*, but has not been reported in natural systems, since it is unstable and reacts quickly. The formation of mackinawite results from the removal of iron (rather than the addition of sulphur) from FeS_{amorph} to form a more thermodynamically stable solid (Schoonen and Barnes, 1991). Greigite results from the reaction of mackinawite with either solid elemental sulphur or dissolved intermediate sulphur compounds (e.g. $S_2O_3^{2-}$). Similarly, the formation of pyrite from precursor phases requires reaction with intermediate or elemental sulphur phases (Berner, 1970; Luther, 1991; Pyzik and Sommer, 1981; Schoonen and Barnes, 1991).

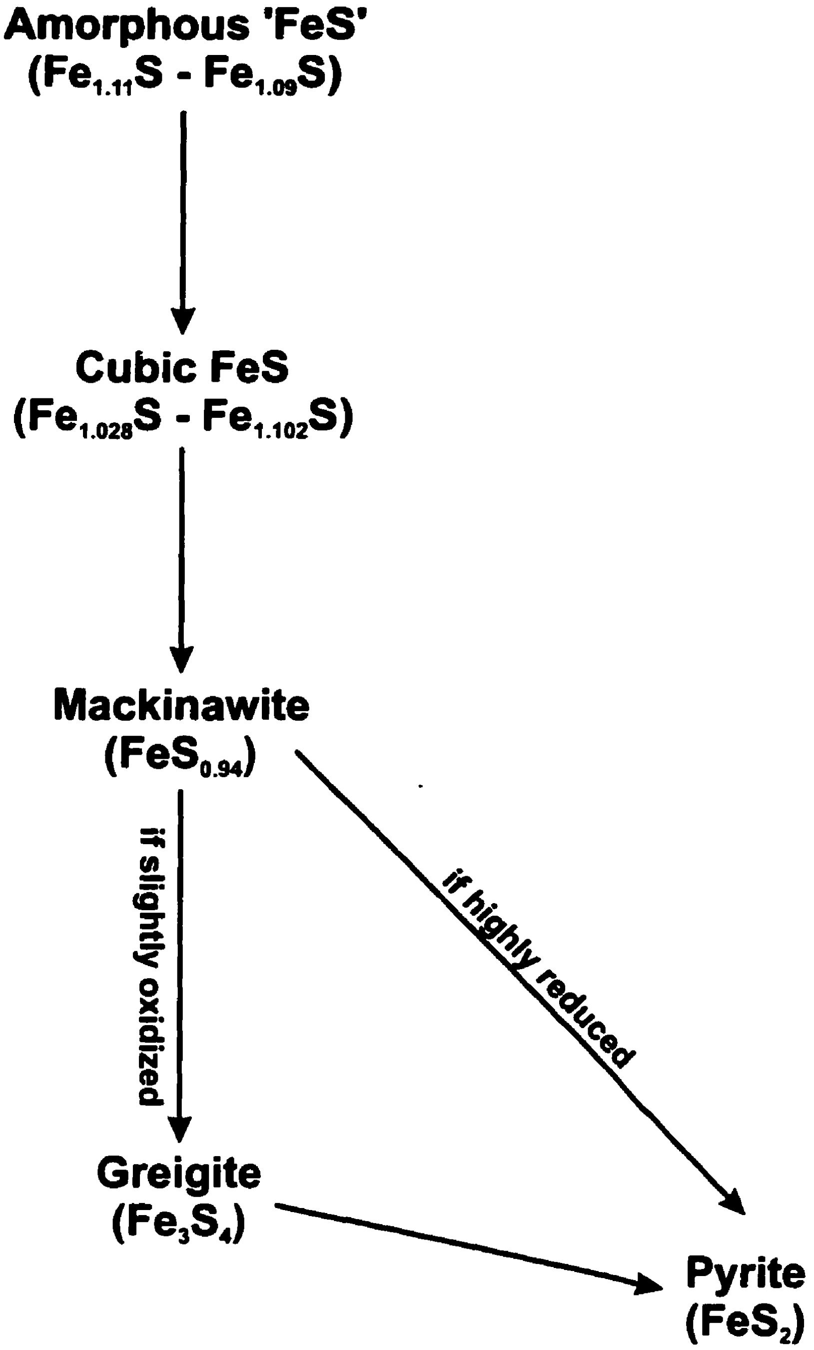

Figure 2.11 Proposed sequence of sulphidization of AVS solids at pH > 6 (from Schoonen and Barnes, 1991).

According to Schoonen and Barnes (1991), greigite serves as an intermediate between mackinawite and the end-product pyrite under slightly oxidizing conditions. The formation of pyrite directly from mackinawite requires highly reducing conditions and is much slower. As a result, the rate and extent of monosulphide conversion to pyrite may be controlled by both the availability of intermediate sulphur compounds and the intensity of sedimentary redox conditions.

2.4.2 Hg Association with iron sulphides

The partitioning between "free" mercury and mercury-sulphur complexes represents one the largest partitioning coefficients of any metal in the presence of dissolved sulphide (Smith and Martell, 1976). Consequently, mercury sulphides are among the most insoluble of any metal (Smith and Martell, 1976; Schuster, 1991). This has led some researchers to explore the role of sulphur in the sequestration of mercury in natural waters (Lindberg and Harriss, 1974; Dyrssen and Wedborg, 1991). Although mercury-polysulphide complexes have been identified as a source of mercury supersaturation in sulphur-rich porewaters (Lindberg and Harriss, 1974), no researchers have reported the *authigenic* formation of discrete HgS solids in sediments (Benes and Havlik, 1979; Schuster, 1991), other than single layer coatings (Hyland *et al.*, 1990). Most likely, this arises from the tendency of Hg to adsorb to every available surface (Benes and Havlik, 1979), thus lowering the activity of dissolved mercury in solution. Also, Hg appears to be rapidly co-precipitated and assimilated into other sulphide minerals, particularly iron monosulphides, which typically incorporate many chalcophilic trace metals (Brown *et al.*, 1979; Arakaki and Morse, 1993; Morse and Arakaki, 1993; Morse, 1993; Huerta Diaz *et al.*, 1993, 1996).

The association of several trace metals, including Hg to iron sulphide minerals, via both co-precipitation and adsorption were investigated by a number of researchers (Brown *et al.*, 1979; Belzile and Lebel, 1986; Jean and Bancroft, 1986; Hyland *et al.*, 1990; Huerta-Diaz and Morse, 1992; Morse and Arakaki, 1993; Huerta-Diaz *et al.*, 1993; Morse, 1994; Huerta-Diaz *et al.*, 1996).

2.4.2.1 Pyrite

Adsorption and desorption studies have been carried out to investigate the ability of pyrite to adsorb or incorporate Hg. Employing Auger electron spectroscopy (AES), Hyland *et al.* (1990) reported that Hg both adsorbs and precipitates on pyrite surfaces. However, they found Hg to be only weakly bound to pyrite surfaces and easily stripped by a thiosulphate solution. This may, in part, be explained by the apparent formation of a mercury monolayer on pyrite in which Cl remains attached to the Hg (Hyland *et al.*, 1990). Likewise, Brown *et al.* (1979) also reported the adsorption of $HgCl_2$ complexes to pyrite surfaces. As discussed above, the covalent character of the Hg-Cl bond often limits the strength of complexes bound to solid surfaces. Hyland *et al.* (1990) also point out that the kinetic stability of pyrite with respect to adsorbed mercury prevents the disruption of surface Fe-S bonds.

Huerta-Diaz and Morse (1992) reported strong pyritization of mercury in sediments of the Gulf of Mexico. Using a sequential extraction procedure (Huerta-Diaz and Morse, 1990), they isolated pyrite and determined the degree of trace metal pyritization (DTMP) values (DTHgP in the case of mercury):

$$(2.2) \qquad DTMP = DTHgP = \frac{Pyrite\text{-}Hg}{Pyrite\text{-}Hg + Reactive\text{-}Hg}$$

where the reactive mercury is that associated to HCl (1M) soluble phases (generally hydroxides, monosulphides, carbonates, and hydrous aluminosilicates). Similarly, the degree of iron pyritization (DOP) was determined as an indicator of the partitioning of iron between "reactive" solids and pyrite (Berner 1970), where

$$DOP = \frac{Pyrite\text{-}Fe}{Pyrite\text{-}Fe + Reactive\text{-}Fe} \tag{2.3}$$

They found increasing DTMP values for Hg, As, and Mo with increasing DOP values, with DTMP(Hg) values often reaching 100%. Conversely, Cr, Pb, Zn, and Cd showed negligible uptake and Co, Cu, Mn, and Ni showed only moderate uptake. Huerta-Diaz and Morse (1992) concluded that this represented the rapid and often complete incorporation of Hg into pyrite grains during early diagenesis. Similarly, Morse (1994), also using the separation technique of Huerta-Diaz (1989), determined the DTHgP in surface sediments of Galveston Bay as well as from a dredge spoil site. He reported that between 50 and nearly 100% of the Hg was pyritized. A caveat to these observations comes from Huerta-Diaz *et al.* (1993) who point out that the method of Huerta-Diaz and Morse (1990) can severely overestimate the degree of pyritization due to the inability to completely remove organic matter from the pyrite fraction. Although the behaviour of Hg in the presence of sulphur, particularly when compared to other metals, supports the likelihood of the high pyritization of mercury, the extreme (~ 100%) extent of pyritization must be viewed with caution.

2.4.2.2 Monosulphides

Iron monosulphide *surfaces* appear significantly more reactive to mercury than their pyrite counterparts. Pyrrhotite appears to have a significantly greater capacity for Hg adsorption than does pyrite (Hyland *et al.*, 1990; Brown *et al.*, 1979). Hyland *et al.*

(1990) reported that several forms of mercury appeared sorbed to the surface of pyrrhotite. A weakly held form was stripped by Cl^- and SO_3^{2-}, a more strongly held form stripped by $S_2O_3^{2-}$, and a tightly held Hg surface complex stripped only by CN^-. Although Hyland *et al.* (1990) were unable to determine the exact nature of surface complexes on pyrrhotite, the study included an X-ray photoelectron spectroscopy (XPS) and AES investigation of Hg sorbed onto PbS which suggests that the three complexes may form: a surface HgS layer overlain by a less strongly held $Hg_3S_2Cl_2$ complex, which underlies a weakly held $HgCl_x$ layer. These findings agree with the XPS study of Jean and Bancroft (1986) in which they report the presence of a surface monolayer of HgS on pyrrhotite and an overlying weakly (physisorbed) layer of $HgCl_x$. Experiments performed by Morse and Arakaki (1993) examined the co-precipitation in addition to the adsorption of various trace metals to mackinawite. They found that metals with decreasing sulphide solubilities were increasingly incorporated into the mackinawite structure and also exhibited greater adsorption to mackinawite surfaces.

In summary, incorporation via co-precipitation of *available* mercury into both pyrite and AVS solids is expected to serve as a major sink of sedimentary mercury. This includes mercury released to porewaters (such as that from decaying organic matter), as well as Hg associated to the iron (hydr)oxide solids which dissolve under reducing conditions. Despite strong incorporation into its structure, little Hg is expected to be adsorbed to the surface of pyrite since Hg is easily stripped away by competing ligands in sediment porewaters. In contrast, while metastable and only a short-term sink, AVS surfaces have a strong affinity for Hg and mercury complexes are strongly bound.

3. ENVIRONMENTAL SETTING

3.1 Geographic and Morphological Setting

The Saguenay Fjord is a narrow (1-6 km wide), partially submerged glacial valley of the Canadian Shield (see **Figure 3.1**). It extends 93 km east-southeast from the mouth of the Saguenay River at Chicoutimi to Tadoussac where it joins the St. Lawrence Estuary. A relatively shallow arm, the Baie des Ha!Ha!, protrudes west from the upper half of the fjord toward the village of La Baie. The Saguenay Fjord is comprised of two elongated basins (200-274 m deep), separated by a sill (70 m). A shallower sill (20 m) separates the seaward basin from the St. Lawrence Estuary.

A thin fresh water (S ~ 1-5) lens extends to about 20 m depth (Drainville, 1968) and shallows along the axis of the fjord to the estuary. Below a strong pycnocline lies well- mixed, oxygenated marine waters (S ~ 28 to 31) which are subject to semidiurnal saline intrusions from the St. Lawrence Estuary (Sundby and Loring, 1978; LeClerc *et al.*, 1986). Whereas the temperature of the surface layer is variable (0 - 12°C), the lower layer remains between -1 and 1°C (Sundby and Loring, 1978). Detailed hydrographic descriptions of the Saguenay Fjord can be found in the literature (Schafer et al., 1983).

3.2 Physical and Chemical Characteristics

Suspended particulate matter (SPM) concentrations in the waters of the Saguenay Fjord vary from 0.5 to 10 $mg \cdot l^{-1}$, showing an inverse relationship to salinity and a strong decrease in concentration below the halocline (Sundby and Loring, 1978). Marine and periglacial clays of the Mer de LaFlamme, an extension of the Champlain Sea, deposited during the glacial retreat of the late Wisconsinian (8,000 - 11,000 yrs) were elevated ~ 70 m above sea level as a result of post-glacial isostatic rebound. Erosion of these clays supplies much of the particulate matter to the Saguenay Fjord (Locat and Leroueil, 1988).

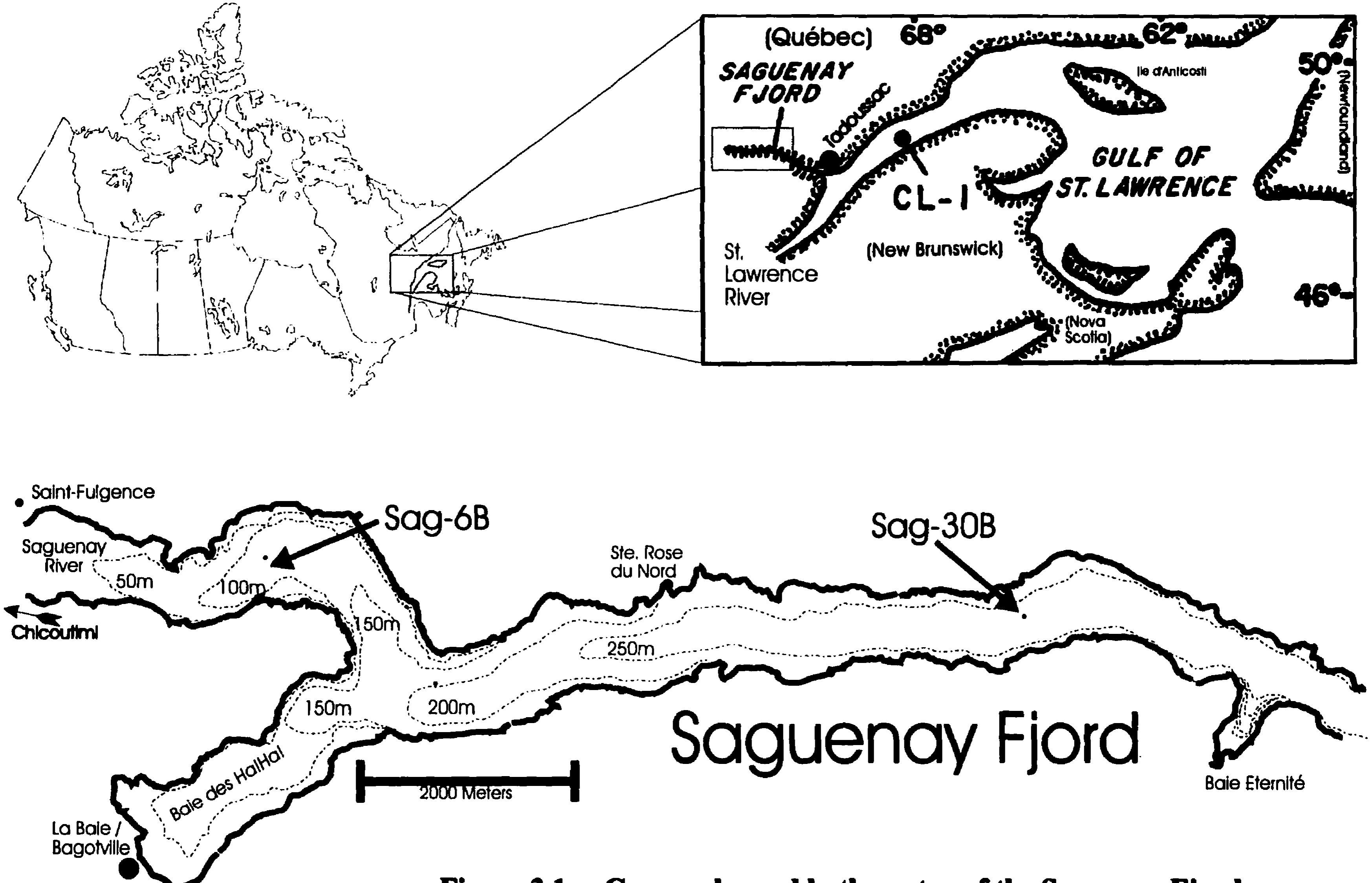

Figure 3.1 Geography and bathymetry of the Saguenay Fjord

Saguenay Fjord SPM is predominantly rock flour (29-44% feldspar, 10-30% quartz, 2-4% amphibole, and some illite and chlorite) with significant quantities (1.5 to 3.7 % wt) of organic matter (Sundby and Loring, 1978; Gagnon *et al.*, 1995). The organic material is mostly anthropogenic and terrigenous, resulting from discharge of lignin-rich effluents from pulp and paper mills (Pocklington and Leonard, 1979; Schafer *et al.*, 1983; Louchouarn, *et al.*, 1995). Leclerc et al. (1986) reported grain-size distribution data which suggested that the majority of the suspended load is supplied to the sediments by the Saguenay River. Since coarser particles accumulate near the head of the fjord and finer particles are carried further downstream, the importance of compaction increases seaward.

Sedimentation rates (ω) are relatively high and generally decrease seaward (Smith and Walton, 1980; Barbeau *et al.*, 1981b). During the 1960's and 1970's ω was evaluated by vertical distribution of Pb^{210} (Smith and Walton, 1980) and Cs^{137} (Barbeau *et al.*, 1981b). Sediments accumulate at an ambient rate of ~4.0 $g \cdot cm^{-2} \cdot a^{-1}$ (7 $cm \cdot a^{-1}$) at the head of the fjord to between 0.31 and 0.07 $g \cdot cm^{-2} \cdot a^{-1}$ (0.5 to 0.1 $cm \cdot a^{-1}$) in the deep interior basin. Estimations of ambient ω in the Saguenay Fjord are generally constant over the past century, but exclude frequent pulsed inputs of landslide-derived material, which significantly add to the total rate of sedimentation (Smith and Walton, 1980; Smith and Loring, 1981).

High concentrations of iron are found (as high as 90 $mg \cdot g^{-1}$ dry weight) in the suspended particulate matter within the fjord. Iron colloids from fresh waters flocculate and coat particles which accumulate at the halocline as surface charge barriers are overcome due to increases in ionic strength (Sholkovitz, 1976; Boyle *et al.*, 1977; Sholkovitz *et al.*, 1978; Sundby and Loring, 1978; Moore *et al.*, 1979; Mayer, 1982; Heimenz, 1986; Hunter and Leonard, 1988). Vertical mixing carries Fe-rich SPM to deep waters of the inner and outer basins. The flow of deep water in the Saguenay Fjord is considerably slower than that at the surface. As a result, the residence time of particulate matter is much longer in the waters of the deep basins (Sundby and Loring, 1978). The increased residence time in deeper waters permits continued colloid aggregation (Sundby and Loring, 1978). As a result, concentrations of reactive iron within Saguenay Fjord sediments are high, with Fe_{HCl} between 20-40 $mg \cdot g^{-1}$ dry sediment (Gagnon *et al.*, 1995).

The sediments of the Saguenay Fjord have been divided into three distinct lithotopes (Smith and Walton, 1980). The **upper fjord lithotope** occurs at the beginning of the fjord (depth ≤ 75 m) and is distinguished by alternating layers of clayey muds and sandy muds with high Corg concentrations. The **transitional lithotope** is found in the upper branches of the fjord (Saguenay River and Baie des Ha!Ha!) between depths of about 75 m to 175 m. Sediments here grade from black anoxic sandy (5-10%) muds with Corg of 0.5 - 3% into the dark greenish-grey muds of the **deep fjord lithotope**, which is predominant in the deep basin of the fjord. Covering the shallow basin adjacent to the St. Lawrence Estuary is a coarsely grained sand/gravel mixture. The upper fjord and transitional lithotope sediments show distinct light gray clay layers with comparatively low Corg values (≤1.1%). These layers represent occasional reworking via slumping and fluvial high-discharge events of Mer de LaFlamme clays, such as the one which delivered an estimated $5.5 \cdot 10^6$ m^3 of clay to the Saguenay River following the 1971 St. Jean-Vianney landslide (La Rochelle, 1973; Schafer, *et al.*, 1980; Smith *et al.*, 1983). Because transitional lithotope sediments rest on a steeply sloping bed, more frequent slumping events complicate the interpretation of the stratigraphy in samples from these sites.

In response to the rapid input of organic material to surface sediments, microbial degradation leads to the depletion of oxygen within the first two centimeters of sediment throughout the fjord. At the head of the fjord, sulphate reduction begins within millimeters of the sediment/water interface (Mucci and Edenborn, 1992; Gagnon *et al.*, 1995), despite bioirrigation and sediment mixing by benthic organisms in the top 10 cm (Edenborn *et al.*, 1987). As a result, the normal sequence of electron acceptors (O_2, NO_3^{2-}, Fe/Mn oxides, SO_4^{2-}) utilization is compressed to millimeters, well beyond the resolution of the sampling techniques utilized in this study (Edenborn, *et al.*, 1987; Mucci and Edenborn, 1992; Gagnon *et al.*, 1995).

The sulphate reduction rates (SRR) in the Saguenay Fjord sediments are significantly higher than those found in the deep ocean, but much lower than those measured in comparable coastal waters. Edenborn *et al.* (1987) attribute this to relatively low bottom temperatures, sedimentation rates, as well as to the nature and concentration of Corg. Partial to complete depletion of porewater sulphate within our sampling interval (35-40 cm) only occurs at the head of the fjord where C_{org} and sedimentation rates are highest (Gagnon *et al.*, 1995).

Unusually high concentration of acid volatile sulphide (AVS) solids and low pyrite content are characteristic of the Saguenay Fjord sediments (Gagnon *et al.*, 1995). The availability of reactive iron in these sediments limits the accumulation of porewater sulphide via precipitation of AVS solids. In the absence of a strong concentration gradient, little sulphide can diffuse to the suboxic and oxic zones. Without the partial oxidation of sulphide to intermediate sulphur compounds by oxygen or Fe/Mn (hydr)oxides, the formation of pyrite is severely inhibited. Consequently, $AVS:S_{pyrite}$ values as high as 14 (1.6 on average) have been reported in these sediments and the formation of pyrite is slow relative to other coastal sediments (Gagnon *et al.*, 1995).

4. EXPERIMENTAL PROCEDURES

4.1 Sediment Sampling

Sediment samples were collected in June, 1992 at three stations in the Saguenay Fjord (**Figure 3.1**): in the transitional lithotope (Sag-6B-1992, 122m; Sag-15B-1992; 175m), and in the deep fjord lithotope (Sag-30B-1992; 274m). Ambient sedimentation rates measured near these sites are 0.29, 0.17, and 0.14 $g \cdot cm^{-2} \cdot a^{-1}$, (0.48, 0.28, and 0.25 $cm \cdot a^{-1}$ respectively (Smith and Walton, 1980). Because of complexities regarding stratigraphic reworking, analyses of sediments from SAG-15B are not detailed in this study. For comparison, a fourth site in the Laurentian Trough (St. Lawrence Estuary), 250 km downstream from the mouth of the Saguenay Fjord (CL-1B, 1992; 312m), was also sampled. Sedimentation rates at the Laurentian Trough station have been reported as 0.075 $g \cdot cm^{-2} \cdot a^{-1}$, or 0.1 $cm \cdot a^{-1}$ (Silverberg *et al.*, 1986; Edenborn *et al.*, 1987).

Sediments were collected using an Ocean Instruments Mark II box corer (Hessler type). The core was transferred to a custom designed N_2 glove box (Edenborn *et al.*, 1986). After purging the box several times with N_2, the front plate of the box core was lowered, sequentially exposing the sediment. The sediment was sampled at various depth intervals (see **Appendix 1**) whereas that in direct contact with the corer frame or front plate was discarded. Eh measurements were carried out at each interval with platinum-calomel electrodes (Radiometer P1312-K4112). Electrodes were calibrated using a ferri/ferro cyanide buffer solution (+196 ± 10 mV relative to standard calomel electrode at 25°C). The quantitative interpretation of Eh measurements in natural systems is limited due to thermodynamic and electrochemical disequilibrium as well as physical heterogeneities (Hostettler, 1984). Nevertheless, vertical profiles of Eh provide an approximate and relative description of redox gradients with depth.

Sediment samples were transferred to pre-weighed plastic scintillation vials for the determination of water content and solid phase composition. Sediments in these vials were freeze-dried, ground, and homogenized in an agate mortar (see Discussion, **Section 4.3.1.2**). Minicorers constructed of truncated screw-cap test tubes (8 cm^3) and 10 mL syringe pistons were used to sample each depth interval and maintain the redox integrity of the sediments. The minicores were sealed and frozen (-20°C) until on-shore sulphide determinations were performed. Porewaters were extracted using modified Reeburgh-type sediment squeezers (Reeburgh, 1967). Fresh sediment samples were loaded into squeezer chambers, covered with a latex sheet, and sealed with the chamber top. The squeezers were then transferred out of the glove box to a specially designed vise where pressurized N_2 was used to force the latex film against the sediments, squeezing interstitial waters through a Millipore™ 45 μm cellulose filter into a syringe with minimal exposure to O_2. Porewaters were analyzed for SO_4^{2-}, chlorinity, Ca^{2+}, alkalinity, Fe, Mn, total mercury, methylmercury and dissolved reduced sulphur species. A more detailed discussion of both protocols and results of porewater analyses appears in Gagnon (1994).

4.2 Instrumental Analyses

It should be noted that for all samples analyzed by the author, or submitted by the author for independent analysis, background analyte concentrations were ascertained with the use of methodological blanks which contained reagents only and were treated identically to the sediment samples. Rigourous care was taken to apply the methological blanks with each batch of samples in order to guard against reagent contamination.

4.2.1 Carbon and Nitrogen

Total carbon (ΣC) and total nitrogen (ΣN) analyses were carried out on freeze-dried sediment samples at GEOTOP/UQAM using a Carlo-Erba™ Elemental Analyzer. The detection limit for these procedures was approximately 0.1% C and <0.05% N by weight. Inorganic carbon was measured in each sample using a UIC Inc. Model 5011 Coulometer (detection limit <0.06% C per 50 mg sample). Organic carbon values were obtained by subtraction from the ΣC values.

In order to evaluate the efficiency of extraction procedures intended to remove or isolate organic matter from the sediment, analyses were performed for ΣC and C_{inorg} on selected samples (following treatment) using a LECO induction furnace with adsorption bulb to measure CO_2.

4.2.2 Total Mercury

Total mercury (ΣHg) analyses of freeze-dried sediments were carried out by Acme Analytical Laboratories, Ltd.. Sediments (0.5 g) were digested in 3 mL of a HCl-HNO_3-H_2O (3-1-2) solution at 95°C for 1 hour. Dissolved mercury concentrations were determined using cold-vapour atomic adsorption spectrophotometry (CVAAS; reproducibility of ± 5.90%).

These values were confirmed by Hg determinations carried out in the laboratory on selected samples. Freeze-dried sediments (0.5 g) were digested using a microwave procedure (Van Delft and Vos, 1988) in Teflon® bombs in 17 mL of a HNO_3:H_2SO_4:$HClO_4$ (10:5:2) mixture (Agemian and Chau, 1976). The resulting solutions were analyzed by cold-vapour atomic fluorescence spectrometry (CVAFS). Results of the latter procedures were in agreement with those of the commercial laboratory within their stated 5.90% precision.

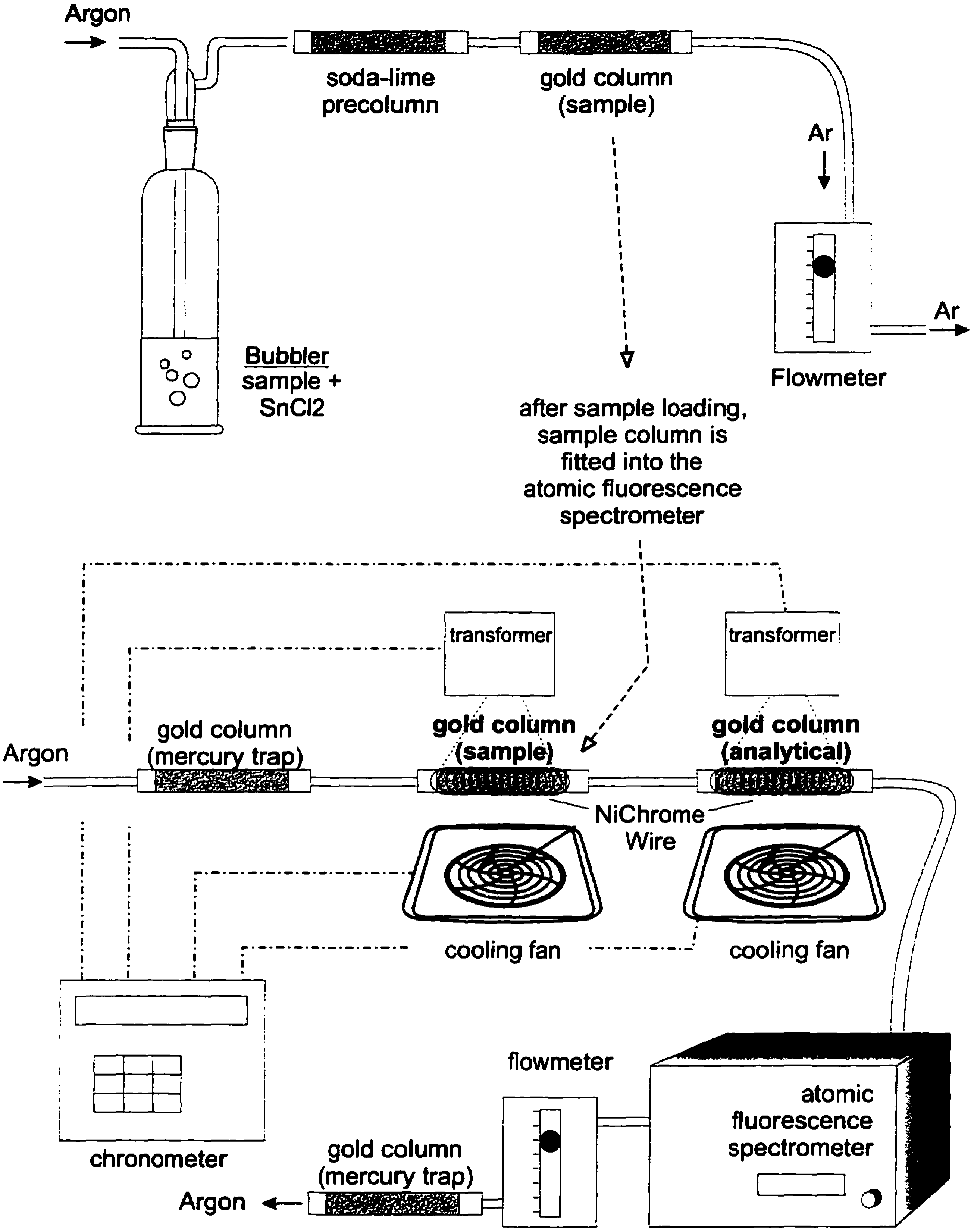

Figure 4.1 Schematic of a two-stage gold-amalgam AFS system

4.2.3 Phase Associated Metals

Mercury concentrations in solutions resulting from the various extraction procedures described in **Section 4.3** were determined following reduction in a $SnCl_2$ reactor, pre-concentration on a two-stage gold amalgamation system (**Figure 4.1**) and detection by a Brooks Rand cold vapour atomic fluorescence spectrometer (AFS) (Nakahara *et al.*, 1978; Bloom and Crecelius, 1983; Gill and Fitzgerald, 1985; Bloom and Fitzgerald, 1988). A saturated $SnCl_2$ solution (500 μL) was added to approximately 100 mL Milli-Q® deionized water in a Teflon® reactor and allowed to purge under Ar flow for 2 hours. Samples were injected into the Teflon® reactor and allowed to react for 10 minutes. Hg(II) was reduced to metallic mercury, volatilized, entrained in the argon stream, and trapped as an amalgam on gold-coated quartz. The gold column was transferred to the AFS system, heated to ~ 500°C, releasing the mercury to the instrument Ar stream. The Hg vapour was trapped on a second, permanent column in order to provide reproducible introduction of Hg to the fluorometer. Precision varied and is presented with the analytical results. Generally, measurements were reproducible within 5%.

Dissolved iron and manganese from the same extracts were analyzed by flame atomic absorption spectrophotometry on a Perkin Elmer 3100. Instrumental precision in most cases was better than ± 3%.

4.3 Sequential Extraction Protocol

The partitioning, reactivity, and bioavailability of environmentally important trace metals in sediments has been investigated by many researchers (Tessier *et al.*, 1979; Robinson, 1984; Canfield 1989; Campbell and Tessier, 1989; Huerta-Diaz and Morse, 1990; Huerta-Diaz *et al.*, 1993; Morse, 1994). Evaluation of *total* trace metal content alone does not permit the examination of chemical associations of trace metals to geological materials. Without an understanding of the chemistry of trace metal and sediment interactions, the fate of trace metals during diagenesis is difficult to elucidate. Furthermore, their response following changes in environmental conditions (seasonal redoxcline migration, dredging, changes in natural and anthropogenic fluxes. etc.) becomes difficult, if not impossible to predict.

The use of reagents to selectively extract soil or sediment components and their associated trace metals permits:

- determination of metal source,
- quantification of biogeochemical availability, and
- elucidation of mechanisms of trace metal mobilization and transport.

By mapping biogeochemical cycles and pathways, quantitative predictions of the fate of trace metals may be refined.

Sequential extractions allow the separation of sediments into operationally-defined reservoirs based on reactivity. Criteria for an ideal extractant includes:

- selectivity, or the ability to solubilize one phase without attacking any other
- the ability to maintain the analyte in solution, in order to prevent analyte re-adsorption to surviving solid phases.

(Tessier *et al.*, 1979; Robinson, 1984; Tipping *et al.*, 1985; Martin *et al.*, 1987; Belzile *et al.*, 1989; Sholkovitz, 1989; Bermond, 1992). As will be discussed below. in the absence of ideal extractants, procedures must be tailored to samples and interpretation of results requires recognition of the limitations of the procedure.

4.3.1 Criticisms and Caveats

This author recognizes the flaws inherent in any sequential extraction procedure. Several major criticisms against the use of sequential extractions have been presented and must be addressed. While specific methodologies are discussed in **Section 4.3.2**, general concerns are expressed here.

4.3.1.1 Bioavailability of Trace Metals

One of the original goals of established sequential extraction procedures was to determine the bioavailability of trace metals in the environment. The very fact that the extraction pools have to be operationally, not mineralogically, defined implies that interpretations of results must be scrutinized with caution. Literature which has been critical of reports quantifying trace metal bioavailability in natural systems note conceptual problems which precede procedural mechanics:

- differences between natural and laboratory conditions (changes in Eh, pH, and ionic strength) which render trace metals bioavailable
- differences between the kinetics of mineral formation and dissolution in natural and laboratory settings

(Martin *et al.*, 1987; Bermond, 1992). The concentrations of metals dissolved in short laboratory protocols cannot properly reproduce natural processes which may occur over entire seasons, years, or decades. Most methods, in order to perform extractions as quickly as possible, use reagents which are much more aggressive than those found in the natural environment. Such extractants may not dissolve the same suite of solid substrates as those which are active during natural processes. Consequently, measurements or predictions of bioavailable metal concentrations in sediments may not be truly representative of the reality.

4.3.1.2 Sample Handling

Criticisms not of the sequential extraction procedure itself, but rather the manner in which samples are handled *prior* to extraction have also been discussed. Researchers (Rapin *et al.*, 1986; Martin *et al.*, 1987) caution against

- exposure of anoxic sediments to atmospheric or dissolved O_2
- drying and grinding sediments

The exposure of anoxic sediments to O_2 obviously results in the partial or complete oxidative destruction of Eh sensitive solids (e.g. monosulphides) and either the formation of new oxic phases or dissolution prior to the appropriate extraction step. Drying and grinding sediments can also cause oxidation, promote the formation of new mineral phases, and accelerate the crystallization of iron and manganese oxides.

The use of fresh frozen sediments for sequential extractions has several drawbacks. Larger sample size must be used to accommodate sample heterogeneity particularly in surface sediments. More importantly, many occluded surfaces may remain protected by resistant coatings until later stages in the extraction sequence. Freeze-drying and grinding allows extractions to be more effective and probably shortens the amount of time necessary to achieve maximum trace metal concentrations. I. Saulnier (pers. comm.) has found that concentrations of mercury extracted from fresh frozen sediments were consistently and substantially lower than those in freeze-dried, ground samples from the same site. It is believed that the difference is due to the increase in available surface area in the ground sediments.

4.3.1.3 Solution / Solid Phase Partitioning

Several researchers report methodological difficulties with sequential extraction protocols which lead them to question the utility of such techniques:

- readsorption of dissolved analyte and redistribution to refractory phases
- ability of extractants to strip metals from or actually degrade supposedly more refractory materials (non-specificity)
- inability of extractants to completely dissolve the targeted phase (non-specificity)

(Tessier *et al.*, 1979; Rendell *et al.*, 1980; Tipping *et al.*, 1985; Martin *et al.*, 1987; Kheboian and Bauer, 1987; Sholkovitz, 1989; Bermond, 1992; Huerta-Diaz *et al.*, 1993).

If the extractants are unable to maintain the metals in solution as soluble species under the procedural pH, Eh, or ligand conditions, then trace metals may be readsorbed to remaining solids or precipitate as a separate phase. As pointed out by Sholkovitz (1989), many of the organic chelation agents, minerals acids, and reducing agents commonly used in many extraction schemes proved unable to prevent readsorption of trace metals to sediment solids. Kheboian and Bauer (1987) reported massive redistribution of trace metals from doped substrates in a synthetic sediment matrix. Other researchers (Tipping, 1981; Canfield, 1989; Kostka and Luther, 1994) have demonstrated that some extractants attack not only the target phase, but also partially solubilize solids which were considered more refractory. In some cases, the reagents desorb trace metals from the surface of residual solids which were not solubilized. Another, more persistent problem is that of incomplete dissolution of the targeted solid (Martin *et al.*, 1987; Cornwell and Morse, 1987; Canfield, 1989; Huerta-Diaz, 1993; Kostka and Luther, 1994). Of particular concern are solids with affinities for trace metals, such as organic matter or crystalline iron and manganese oxides.

Belzile *et al.* (1989) are severely critical of many of the above studies which cite very high trace metal readsorption problems. They note that the study of Kheboian and Bauer (1987) and some others used "model" sediments which included discrete particles of chemical solids intended to represent the chemical constituents of a sediment. In order to evaluate readsorption of trace metals, a single component was doped, the sediments analyzed, and the partitioning evaluated. As Belzile *et al.* (1989) point out, the geochemical properties of model sediments differ significantly from many of the characteristics inherent to natural systems:

- the presence of coatings rather than discrete particles of some substrates,
- the occlusion of many surfaces by coatings,
- the authigenic formation and dissolution of various mineral components
- the presence of mineral phases which are mutually exclusive in natural environments.

In addition, in any system with a single doped phase, the metal will be redistributed as a result of concentration gradients, and the post-equilibrium metal partitioning will reflect relative affinities of the solid phases (Belzile *et al.*, 1989).

Many researchers critical of established sequential extraction techniques have also modified them in ways which emphasize the methodological limitations. Rendell *et al.* (1980), who investigated trace metal readsorption, more than tripled the extraction time, which would promote readsorption of dissolved metals. Several others (Rendell *et al.*, 1980; Tipping *et al.*, 1985; Sholkovitz, 1989) investigated only one extraction step rather than the entire sequence, so that solids which should have been previously extracted potentially interfered with the extraction procedure. For example, both Rendell *et al.* (1980) and Sholkovitz (1989) demonstrated that elevated pH is responsible for the readsorption of trace metals associated with (hydr)oxides, but failed to remove carbonates prior to mineral extraction.

4.3.2 Refinement and Execution of Sequential Extraction Technique

With few exceptions, authors critical of the sequential extraction techniques concede that they are valid tools, but insist that caution in both practice and interpretation is necessary. Obviously, some reagents are better than others, and a discussion of the choice of reagents is included as part of the methodological description.

Tessier *et al.* (1979) defined a number of reservoirs based on the response of a sediment to changes in ionic strength, pH, Eh, and the degradation of organic matter. These operationally defined separations are intended to partition trace metals into the following reservoirs: exchangeable, carbonate, Fe/Mn oxide, organic, and residual (see **Table 4.1**). Huerta Diaz and Morse (1990) provided a more recent modification which addressed many of the drawbacks of the Tessier *et al.* (1979) method. The procedures described in Huerta-Diaz and Morse (1990) have been modified to suit the geochemistry of Saguenay Fjord sediments and to satisfy the particularities of mercury extraction.

Table 4.1 Operationally defined chemical fractions of sediments: reagents and targeted phases from the method of Tessier *et al.* (1979).

Extractant	Targeted Phase(s)
$MgCl_2$ (1 M), pH 7	"Exchangeable" metals sites)
NaOAc (1 M), pH 5	Metals bound to carbonates
$Na_2S_2O_3$ (0.3 M) + Na-citrate (0.175 M) H-citrate (0.025 M)	Metals bound to Fe-Mn oxides
H_2O_2 (30% v/v) + HNO_3 (0.02 M)	Metals bound to organic matter
$HF/HClO_4$ (5:1)	Residual metals

The precise extraction scheme used appears in **Figure-4.2**. All reagents were ultra-pure and all treatments were carried out in sealed Teflon® tubes. Agitation was accomplished by means of a wrist-action shaker.

4.3.2.1 $MgCl_2$ Phase: Easily Exchangeable Metals

Exchangeable ions are those held by electrostatic attraction to non-specific ion adsorption sites. Ammonium citrate (0.1M, pH 8.4), acetic acid (1M), sodium acetate (1M, pH 8.2), and $MgCl_2$ (1N) have all been proposed as suitable extractants (Tessier *et al.*, 1979; Robinson, 1984). Robinson (1984) found, however, that sodium acetate and acetic acid values produced extremes (low and high, respectively) in values for exchangeable metals and recommended the use of ammonium citrate. A choice was made by this author to investigate $MgCl_2$ as an extractant. A 1N $MgCl_2$ solution is least likely to chemically alter freeze-dried sediments and suitably complexes Hg. Application of the $MgCl_2$ extraction procedure to our sediments suggested that there was no "exchangeable" reservoir of Hg, which is in agreement with the work of Eganhouse *et al.* (1978) and Giordano *et al.* (1992). As a result, this step was dropped from the sequence.

4.3.2.2 NaOH Extractable Metal (Humic and Fulvic Acid Reservoir)

The method of Tessier *et al.* (1979) extracts organics late in the separation sequence, using an acidic H_2O_2 solution *following* extraction of Fe/Mn oxides and hydroxides (via hydroxylamine HCl). In our customized protocol, a 1 N HCl solution is used to extract Fe/Mn oxides and hydroxides, but after isolation of the organic fraction. Whereas humins remain insoluble at any pH and humic acids dissolve only at high pH, fulvic acids are soluble in acidic medium. It is therefore necessary to remove fulvic acids prior to treatment with acidic reagents. The use of H_2O_2 to oxidize organic matter is unsuitable for mercury determinations because it also acts as a reductant. As a result, Hg(II) is reduced to Hg(0) and lost to volatilization (Campbell and Tessier, 1989). Schnitzer and Skinner (1968) found that a dilute alkali solution was suitable for the extraction of organic matter. This procedure was used successfully by Dmytriw *et al.*

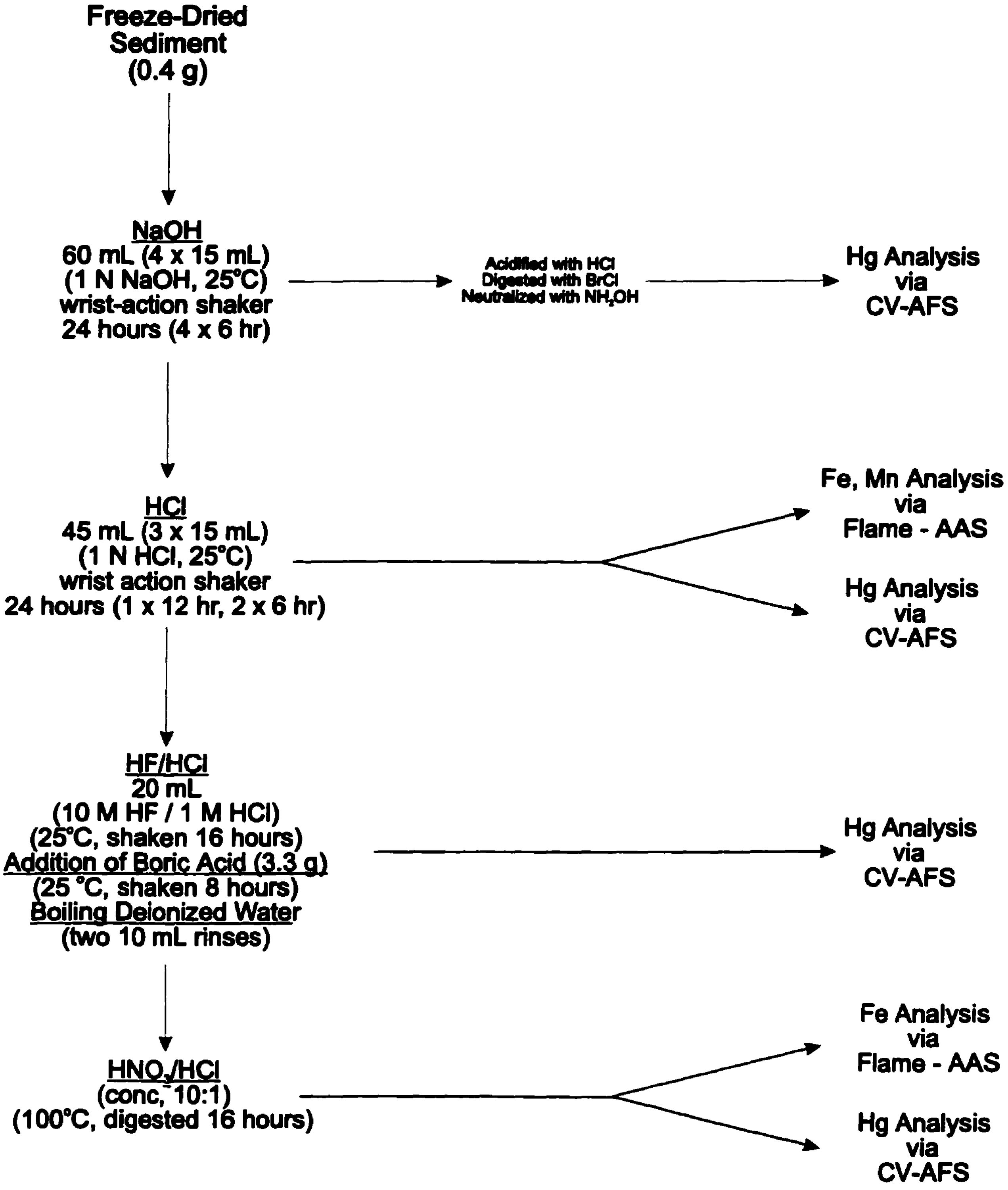

CV-AFS = Cold Vapour Atomic Fluorescence Spectrometry; Flame-AAS = Flame Atomic Absorption Spectrophotometry

Figure 4.2 A sequential extraction protocol for the partitioning of mercury in sediments of the Saguenay Fjord..

(1994) to isolate Hg associated with organic matter in soil profiles. In this study it was found that extraction with dilute NaOH (1N) over 24 hours at 25°C and a solid:solution ratio of 1:120 was optimal for the isolation of organic matter from sediments with the highest C_{org} concentration. This treatment solubilized only minimal amounts of Fe ($\leq$1% Fe_{HCl}), and thus should not significantly mobilize mercury associated with iron-bearing minerals.

It became clear during preliminary experiments that the NaOH solution only extracts 40-70% of the organic matter. Values calculated from DOC concentrations following the NaOH extraction may be underestimated since it has been noted that NaOH solutions can oxidize some organic matter to CO_2 (Schnitzer and Skinner, 1968). Huerta-Diaz *et al.* (1993) recommend the addition of 1% sodium dodecyl sulphate (SDS), a surfactant, to the NaOH reagent to aid in the removal of organics. This author found, however, that it was nearly impossible to remove all the surfactant from the sediments following the NaOH extraction. Even after several (5-8) rinses, large quantities of SDS remained which produced enough CO_2 to overload and damage the LECO adsorption bulb. Alternatively, Huerta-Diaz and Morse (1990) recommended the use of a concentrated H_2SO_4 extraction. Our studies, however, showed no additional removal of organic carbon by this procedure. Huerta-Diaz (pers. comm.) also expressed doubts concerning the effectiveness of the H_2SO_4 (conc.) treatment for sediments containing $\geq$2% C_{org}. Since the separation of refractory organic matter recurs in methodological literature (Martin *et al.*, 1987; Huerta-Diaz and Morse, 1990), it was eventually decided that the potential influence of refractory organic matter extracted in later stages would have to be factored into the interpretation of the results. A further discussion of this latter issue may be found in **Section 5.3.1**.

4.3.2.3 HCl Extractable (Fe, Mn Oxides, Hydroxides, and Monosulphides)

Canfield (1989) defined reactive iron as "that fraction of iron in marine sediments which readily reacts with sulfide to form various iron sulphide minerals". Several techniques have been devised to extract reactive iron, which have commonly included reagents such as: hydroxylamine-HCl in acetic acid (Tessier, 1979; Buckley, 1989; Gobeil and Cossa, 1994), ammonium oxalate (Robinson, 1984), sodium dithionite (Canfield, 1989; Raiswell *et al.* 1993), and HCl at a variety of concentrations and temperatures (Leventhal and Taylor, 1990, Huerta-Diaz and Morse, 1990).

Robinson (1984) reported that hydroxylamine-HCl is capable of dissolving Mn-oxides, but unable to dissolve all Fe-oxides. Tipping *et al.* (1985) and Sholkovitz (1989) reported large-scale readsorption of trace metals in the presence of hydroxylamine-HCl. Ammonium oxalate, while effective for the extraction of poorly crystallized Fe-oxides, does not dissolve well crystallized iron oxides (Canfield, 1989; Kostka and Luther, 1994). A citrate buffered sodium dithionite reagent (CDB) is often recommended as the extractant of choice for reactive iron (Lucotte and d'Anglejan, 1985; Canfield, 1989; Raiswell *et al.*, 1993; Kostka and Luther, 1994). CDB quantitatively dissolves all iron oxides and hydroxides without significantly attacking silicates. Sholkovitz (1989) reported that readsorption of trace metals did not occur with a dithionite solution. Unfortunately, dithionite is not suitable for determination of most trace metals because of metal contamination, precipitation of metal sulphides resulting from the disproportionation of the dithionite, and the tendency of the matrix to clog FAA burners (Tessier, 1979). More specifically, in the case of mercury, dithionite will reduce Hg(II) to Hg(0) with subsequent volatilization and loss to the atmosphere.

Both Canfield (1989) and Kostka and Luther (1994) found that cold dilute HCl ($\leq$ 1N) is capable of complete dissolution of amorphous and partial dissolution of crystalline iron oxides (e.g. goethite and hematite). In contrast to buffered dithionite, iron carbonates (siderite, ankerite) dissolve completely in HCl. A disadvantage, however, is the ability of HCl to attack nontronite, a silicate mineral, and most probably amorphous silicates as well. Minor amounts (<25%) of other silicates (chlorite, biotite, glauconite) can also be dissolved (Canfield, 1989). Higher temperatures and HCl concentrations were found to dissolve iron oxides effectively, but also to attack silicates more aggressively (Raiswell *et al.* 1993; Kostka and Luther, 1994). Leventhal and Taylor (1990) have shown that similar amounts of Fe can be removed from sediments by both the dithionite and cold 24 hour 1N HCl extractions. Finally, Sholkovitz (1989) reported that HCl solutions > 0.2N were capable of preventing any readsorption of trace metals to residual phases.

In preliminary experiments, it was found that a 1 hour, cold 9N HCl extraction yielded roughly similar results to a 24 hour 1N HCl extraction. When expanded to a full 24 hours, however, the 9N procedure was able to dissolve markedly higher concentrations of iron from the same sediment samples. The amount of iron dissolved by 1N and 9N HCl solutions was determined over 27 hour timed-series extractions (see **Figure 4.3**). The concentration of dissolved iron can be empirically described by the equation

(4.1)

$$[Fe]_{HCl} = a \bullet t(1 - e^{\frac{b}{t}})$$

where t is time in hours, and a and b are fitting coefficients. While not intended to be an exhaustive study of the kinetics of iron extractions, it *does* point out the necessity to carry out the 1N HCl extraction for *at least* 24 hours in order to reach a 90% or better extraction efficiency. In further extractions, the reaction time was kept to 24 hours, since it was felt that longer extraction times could promote re-adsorption and further alteration of the sediments with minimal gain in soluble iron. In addition, CDB extractions of Saguenay Fjord sediments taken from the 0-2 cm depth interval were performed by R.

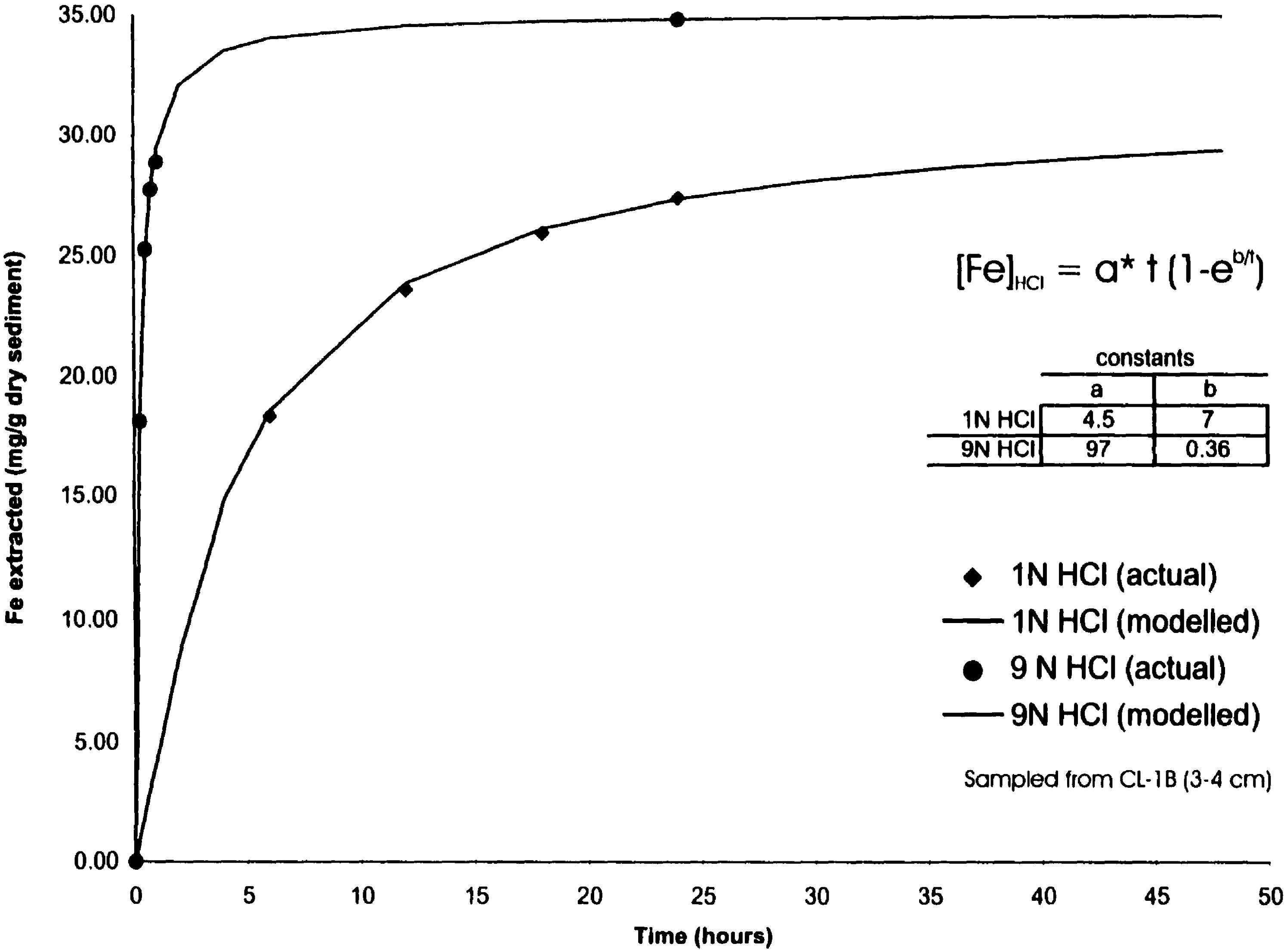

$$[Fe]_{HCl} = a^{*}\, t\, (1\text{-}e^{b/t})$$

	constants	
	a	b
1N HCl	4.5	7
9N HCl	97	0.36

Figure 4.3 Results of a time-series extraction of Fe from sediments by 1N and 9N HCl

Raiswell according to the method of Raiswell *et al.* (1994). In contrast to the findings of Leventhal and Taylor (1990), significantly lower concentrations of iron in surface samples from the Saguenay Fjord sediments were obtained by CDB extraction than by 1N HCl. The implications of non-(hydr)oxide iron extraction by the HCl method are discussed in **Section 5.3.2**.

To summarize, HCl is the only suitable reagent for extraction of mercury associated with Fe and Mn (hydr)oxides. Because 1N HCl-soluble iron already significantly exceeded the CDB-soluble benchmark, it was decided that shorter protocols with more concentrated HCl solutions would only exacerbate the non-specificity. A 24 hour 1N HCl (20°C) method was chosen (Huerta-Diaz and Morse, 1990; Huerta-Diaz *et al.*, 1993; Dmytriw *et al.*, 1994; Gagnon *et al.* 1995).

4.3.2.4 HF Extractable (Clays, Clay-Metal-Organic Complexes)

The silicate fraction of sediments was extracted by HF in the absence of HCl-soluble phases. This procedure may also extract mercury associated with coatings on clays (i.e., clay-metal-organic complexes and some surviving Fe-oxides) which may have been partially protected from previous chemical attack by the silicate underpinning. Several modifications to the HF extraction of silicates have been proposed (Tessier *et al.*, 1979; Lord, 1982; Huerta-Diaz and Morse, 1990). The results of preliminary experiments in this laboratory demonstrated an uptake of mercury *from* a 10N HF extractant *by* the sediments over 24 hours. It was suspected that, in the absence of complexing ligands (F^- binds only weakly to Hg), solubilized Hg(II) had probably been readsorbed to residual solids. HCl was added to the extractant in order to keep Hg in solution (Agemian and Chau, 1976). To the solids remaining after the 1N HCl extraction, 20 mL HF/HCl (10N/1N) reagent was added and the extraction carried out with agitation at room temperature for 16 hours. At the end of 16 hours, 3.3 grams of ultrapure boric acid was added to complex the fluorine and agitation was continued for 8 hours. The solid-solution mixture was separated by means of centrifugation, and the extractants were transferred to sample vessels. The sediments were washed twice with 10 mL boiling Milli-Q® water to dissolve any remaining boric acid and to achieve best quantitative transfer of the extractant solution. The addition of HCl to the HF extraction increased mercury concentrations dramatically, by values exceeding 1000% in the initial test samples.

4.3.2.5 Refractory Phases (pyrite, humins, lignin)

The separation of humins and lignin from pyrite appears nearly impossible via chemical means. As discussed above (**Section 4.3.2.2**), the specific extraction of refractory organic matter is not, at present possible. Huerta-Diaz *et al.* (1993) noted that the persistence of organically-bound metals at the end of the sequential extractions resulted in an overestimation of pyritized metals. Alternatively, Huerta-Diaz *et al.* (1993) determined Fe/metal ratios in pyrite following physical separation via sonication and centrifugation of extraction residues in a heavy liquid (tetrabromoethane, ρ=2.9 g·cm^{-3}). A similar separation was attempted using sodium polytungstate (SPT, ρ=2.9 g·cm^{-3}), a water-soluble, non-toxic and mercury-free heavy liquid. Using an initial 7 g of freeze-dried sediment, no visible pyrite fraction was obtained following centrifugation at speeds as high as 5000 rpm for periods exceeding several hours. Poor pyrite phase recovery is attributable to low sedimentary pyrite content (typically ~ 750 μg pyrite g^{-1} sediment) and low density extraction efficiency (Huerta-Diaz *et al.*, 1993). Other researchers (Mucci and Edenborn, 1992) have reported low concentrations of pyrite (4.8 - 11 μmol·g^{-1} dry sediment) within sediments from the deep basin slope of the Saguenay Fjord.

Huerta-Diaz and Morse (1992) estimated the trace metal content of sedimentary pyrite in a variety of sediments of the Gulf of Mexico. Values for anoxic sulphidic hemipelagic sediments (Green Canyon) were $3.1 \cdot 10^{-5}$ mole Hg per mole pyrite, whereas anoxic sulphidic coastal lagoon (Baffin Bay) sedimentary pyrite contained $8.6 \cdot 10^{-6}$ mole Hg per mole pyrite. Applying these partition coefficients to the relatively pyrite-poor (~ 6 $\mu mol \cdot g^{-1}$) sediments of the Saguenay Fjord, values of pyritized Hg are estimated to be between 10 and 37 ng $Hg \cdot g^{-1}$ sediment, or 1 to 5% of the average total Hg content.

Estimated values for pyritized mercury in the Saguenay Fjord are, however, misleading. The partition coefficients of Huerta-Diaz and Morse (1989) may represent a significant overestimation of Hg content in pyrite due to contamination of their samples by residual organic matter (Huerta-Diaz *et al.*, 1993). In addition, Mucci and Edenborn (1992) suggest that much of the pyrite in Saguenay Fjord sediments may be detrital rather than authigenic in origin based on evidence from source clays in the Saguenay River watershed (e.g. St. Jean-Vianney). Based on the above estimates and field observations, it was decided that the minor contribution of pyritized mercury to the total mercury pool did not warrant the elaborate application of techniques required to isolate it. Any contribution made by pyrite to the mercury reservoir was included in the final HNO_3 (total) digestion of the extraction residue. As in the previous extraction step, HCl (to achieve a mixture of HNO_3:HCl = 10:1) was added to the extractant to keep Hg in solution (Agemian and Chau, 1976). The HNO_3/HCl reagent (15 mL) was added to the remaining solids and reacted overnight at 110°C. Once cooled, the samples were diluted to 25 mL with Milli-Q® water.

In summary, because pyrite concentrations in the Saguenay Fjord are quite low, the inability of the methods investigated to distinguish between refractory organic matter and pyrite may not present a problem. The contribution of pyritic mercury to the total pool were not expected to exceed 5% of total extractable mercury. As a result, extraordinary measures to separate pyritic mercury were not deemed necessary.

4.4 Reduced Sulphur Analyses

A modification of the method of Hsieh and Yang (1989) was used to determine the concentrations of AVS and FeS_2 in the sediments (see **Figure 4.4**; detailed procedure follows). The method permits the analysis of the individual sediment samples in the same reaction chambers for determination of both AVS and pyritic sulphur. This procedure minimizes the potential for oxidation of sulphides, transfer loss, and contamination. The method was altered by performing all sample handling under N_2 (glove bag) rather than by flushing reaction vessels, and by injecting reagents by syringe rather than by overturning round-bottomed flasks. These modifications reduce accidental oxidation of the sample or accidental spillage. The reaction vessels consisted of 250 mL amber glass bottles with threaded caps and fitted silicone stoppers (vulcanized rubber contributes to sulphur contamination). The reaction vessels were covered by plastic screw-on caps, which served as a second seal and prevented popping of corks due to increases in internal pressure. Reagent solutions were stripped of O_2 by bubbling with a stream of N_2 for two hours immediately prior to the procedure. A 2N NaOH/Zn-acetate solution was used to trap evolved H_2S. The high pH of the trap solution facilitates the absorption of H_2S, whereas Zn^{2+} forms highly insoluble ZnS, which is stable under atmospheric O_2.

4.4.1 Acid-Volatile Sulphides

2-4 g of frozen sediment (sampled by minicore) were added to the reaction vessels. Plastic scintillation vials containing 10 mL of a Zn-acetate/NaOH (2N) trap solution were also inserted. The passive distillation was initiated with the addition of a 15 mL HCl (9N) / 20% $SnCl_2$ solution to the reaction vessel by injection with a syringe through the

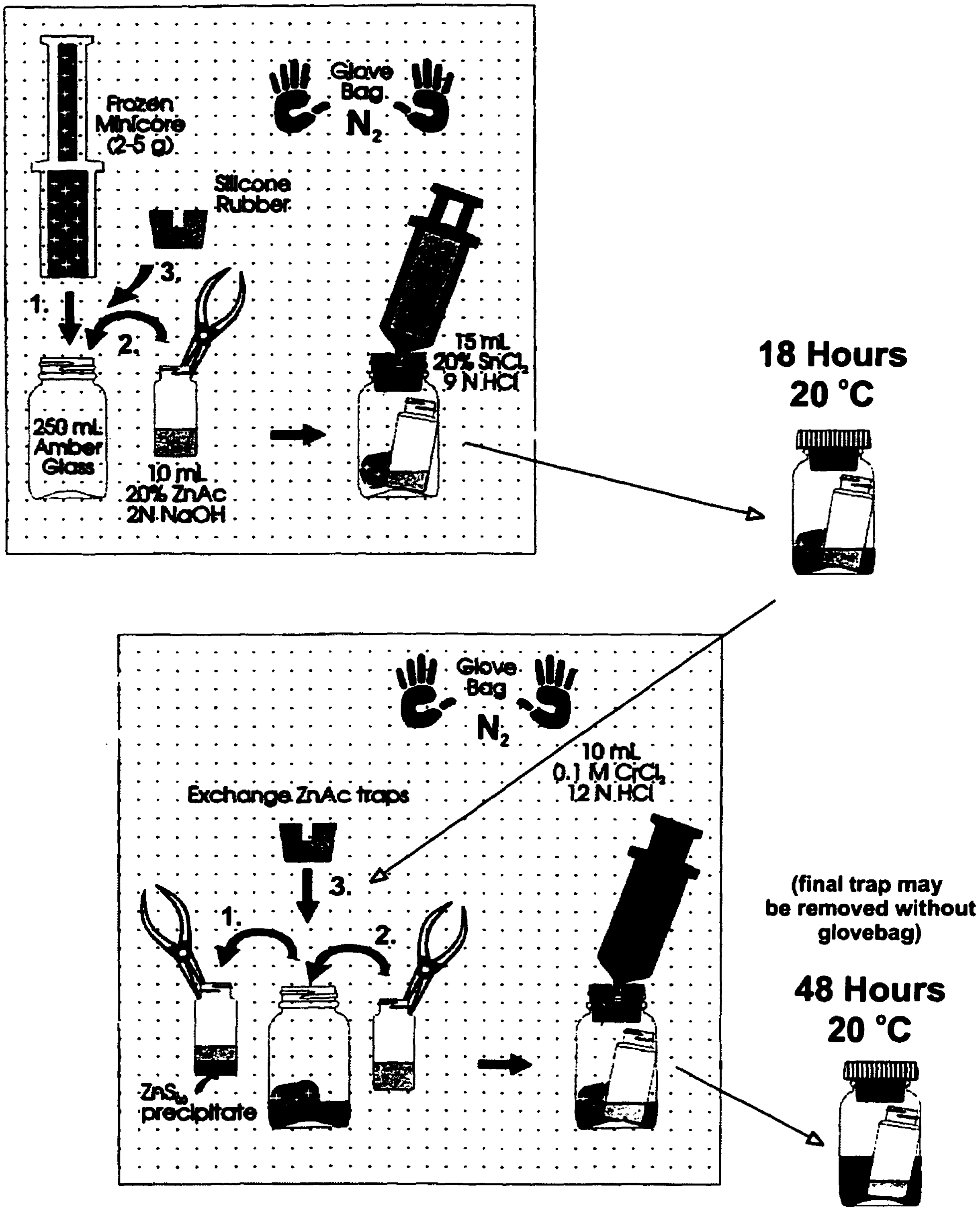

Figure 4.4 A modified passive distillation technique for the determination of AVS and pyrite (after Hsieh and Yang, 1988; modified by A. Bono and T. Arakaki).

silicone stopper. Several authors (Pruden and Bloomfield, 1968; Berner *et al.*, 1979; Chanton and Martens, 1985; Morse and Cornwell, 1987) note that $SnCl_2$ is required to prevent the oxidation of S(-II) to insoluble S(0) via the reduction of Fe^{3+} to Fe^{2+}:

(4.2) $$2\ Fe(III)OOH + H_2S + 4\ H^+ \longrightarrow 2\ Fe^{2+} + S^0 + 4\ H_2O$$

The vessels were capped and allowed to sit overnight, prior to trap retrieval under N_2. It should be noted that pyrite is not attacked by this method, nor is elemental sulphur if the reaction is carried out at room temperature (Hsieh and Yang, 1989).

As pointed out by several authors (Zhabina and Volkov, 1978; Chanton and Martens, 1985; Cornwell and Morse, 1987), treating sediments with a $HCl/SnCl_2$ solution easily dissolves amorphous FeS, mackinawite, and pyrrhotite. These authors, however, also note that more refractory greigite (Fe_3S_4) may only be partially extracted. Since greigite is normally present in trace quantities, its influence on AVS and FeS_2-S values should be negligible.

4.4.2 Chromium Reduced Sulphides

$CrCl_2$ is a powerful reducing agent which efficiently dissolves FeS_2 via reductive degradation (Zhabina and Volkov, 1978) to sulphide. Cornwell and Morse (1987) were able to show 100% recovery of synthetic pyrite (87% recovery of massive pyrite (<50 mesh)) using an acidic $CrCl_2$ reagent. A $CrCl_2$ solution was prepared via addition of $CrCl_3 \cdot 6H_2O$ to a Zn/Hg amalgam. The solution must first be stripped of O_2 and kept under a N_2 stream since Cr(II) oxidizes rapidly (Kolthoff and Sandell, 1952).

Following the reaction of AVS and recovery of the evolved H_2S, fresh traps were placed in the reaction vessels and 10 mL of a concentrated HCl (12N) solution were added to the sediment slurry. The vessels were resealed and 10 mL of the $CrCl_2$ solution were injected to initiate the reaction. The vessels were recapped and allowed to sit 48 hours at room temperature. The traps were removed and analyzed for sulphide.

4.4.3 Iodometric Titration

Trapped ZnS was analyzed via iodometric titration by $Na_2S_2O_3$ using a Radiometer TTT85 Titrator and ABU 80 Autoburette with calomel reference and Pt electrodes. Some difficulties were noted in this procedure, which were traced to the use of the alkali ZnAc traps. It is imperative that the I_2 reagent and S^{2-} analyte be reacted under neutral to acidic conditions in order to achieve the expected stoichiometries and reproducibility in the results.

Under neutral to acidic conditions, the reactions associated with the thiosulphate titration of excess iodine following the reaction with the sulphide analyte proceed as:

(4.3) $$I_2 + HS^- \rightarrow 2\,I^- + H^+ + S^0$$

(4.4) $$I_2 + 2\,S_2O_3^{2-} \rightarrow 2\,I^- + S_4O_6^{2-}$$

The use of alkali traps, however, initially presented some difficulties. Although the thiosulphate titration was carried out under acidic conditions, the sulphide must be reacted with I_2 prior to acidification in order to minimize volatilization and loss of H_2S. Iodine reacts under alkali conditions to form hypoiodite:

(4.5) $$I_2 + 2\,OH^- \rightarrow IO^- + I^- + H_2O$$

(Christian, 1977). The formation of hypoiodite altered the *expected* stoichiometry of the reaction between I_2 and S^{2-} from 1:1 to approximately 3:1, consuming more I_2 reagent and producing a severe overestimation in the S^{2-} concentration. Berka *et al.* (1965) note that the reaction of hypochlorite in the presence of sulphide approximately follows the reaction

(4.6) $$S^{2-} + 4\,ClO^- \longrightarrow SO_4^{2-} + 4\,Cl^-.$$

One or more analogous reactions between sulphide and hypoiodite may occur under basic conditions, producing the observed overestimation of S^{-2}:

(4.7a) $S^{2-} + 4\ I_2 + 8\ OH^- \dashrightarrow SO_4^{2-} + 8\ I^- + 4\ H_2O$

(4.7b) $S^{2-} + 3\ I_2 + 6\ OH^- \dashrightarrow SO_3^{2-} + 6\ I^- + 3\ H_2O$

To circumvent the issue of pH, the required amount I_2 reagent was estimated, added to the reaction flask, and acidified with 5 mL HCl (6N) **prior** to the addition of ZnS from the sample traps.

The thiosulphate titrant was standardized using a KIO_3 standard solution in the presence of excess KI to stabilize I_2 as I_3^-. The efficiency of the reaction vessels procedure was tested using a Na_2S standard. Recovery efficiency of S^{2-} was 98-100% up to concentrations of 600 µmol S. Na_2S standard solutions were prepared from Na_2S crystals washed with Milli-Q® water which had been purged under nitrogen for over two hours and dried. Determinations of 50 µM Na_2S standard solutions were reproducible to within ± 1%.

5. RESULTS

5.1 Distribution of Carbon and Nitrogen

Concentrations of total, inorganic, and organic carbon (ΣC, C_{inorg}, C_{org}) as well as total nitrogen (ΣN) and C/N ratios appear for each station in **Appendix 2**. At each site, carbonates are a very minor component of the ΣC pool, since C_{inorg} rarely exceeds 10% of ΣC. Organic carbon profiles for each site appear in **Figure 5.1**. Total nitrogen values are fairly low and vary little either between stations or with depth.

CL-1B (Laurentian Trough Station)

Concentrations of C_{org} are greatest near the sediment/water interface (~1.70% by weight) and decrease steadily with depth to values as low as 1.38%. Inorganic carbon varies between 0.20 and 0.17%, decreasing steadily with depth. Nitrogen decreases from 0.14 to ~0.09% with depth. The C/N ratio, which shows no apparent relationship to depth, remains between 14 and 18, indicating a mixture of terrigenous and marine organic matter (Rashid, 1985).

SAG-6B (Landward Basin - Upstream Slope)

Sediments on the basin slope are enriched in C_{org} near the sediment/water interface. Unlike Laurentian Trough sediments, sediments at this site are subject to periodic landslide and slumping events, such as the catastrophic 1971 landslide at St. Jean Vianney. Two obvious minima (0.8 and ~1.7%) in C_{org} concentrations occur within two separate clay layers which were visually identified as distinct grey layers within black and brown muds. These layers record the deposition of sediments from the St. Jean Vianney landslide (21-27 cm) and deposition of a more recent submarine debris flow (11-14 cm). Although C_{inorg} typically represents <5% of ΣC in the organic-rich muds, it comprises as much as ~10% and 42% of ΣC in the upper and lower clay layers, respectively. ΣN values decrease below surface sediments as nitrogen-bearing organic matter, which is more labile, is preferentially mineralized. C/N ratio values range from 18 to 33, indicating a more terrigenous source relative to the trough sediments.

SAG-30B (Landward Basin - Bottom)

At the bottom of the basin, landslide and submarine flow debris are less abundant or well mixed with the indigenous sediments; they are not present as visually distinct layers. Carbon values are enriched near the sediment-water interface (C_{org} ~ 2.5-2.8%) and decrease with depth to <2.0%. In contrast to the other sampled sites, inorganic carbon concentrations are nearly constant and significantly lower. Inorganic carbon levels range between 0.75 and 0.89% and decrease with depth. Similarly, nitrogen content is low and decreases with depth (0.13% to 0.07%). C/N ratios vary between 21 and 28 and reflect the relative importance of the terrigenous organic matter input.

5.2 Acid-Volatile Sulphides

Acid volatile sulphides include amorphous FeS, mackinawite, and poorly crystallized greigite. Their distribution is presented in **Appendix 2**. Although the determination of Na_2S standards by iodometric titration (**Section 4.4.3**) was fairly precise (±<1%), sample heterogeneity and intersample variations yielded analytical results which were reproducible to approximately ± 12%

CL-1B

AVS are nearly absent (<5 $\mu mol \cdot g^{-1}$) in surficial sediments at CL-1B. A peak (27 $\mu mol \cdot g^{-1}$) is observed at 6.5 cm, beneath which values increase almost linearly with depth from 11 to 36 $\mu mol \cdot g^{-1}$ (**FIGURE 5.1**).

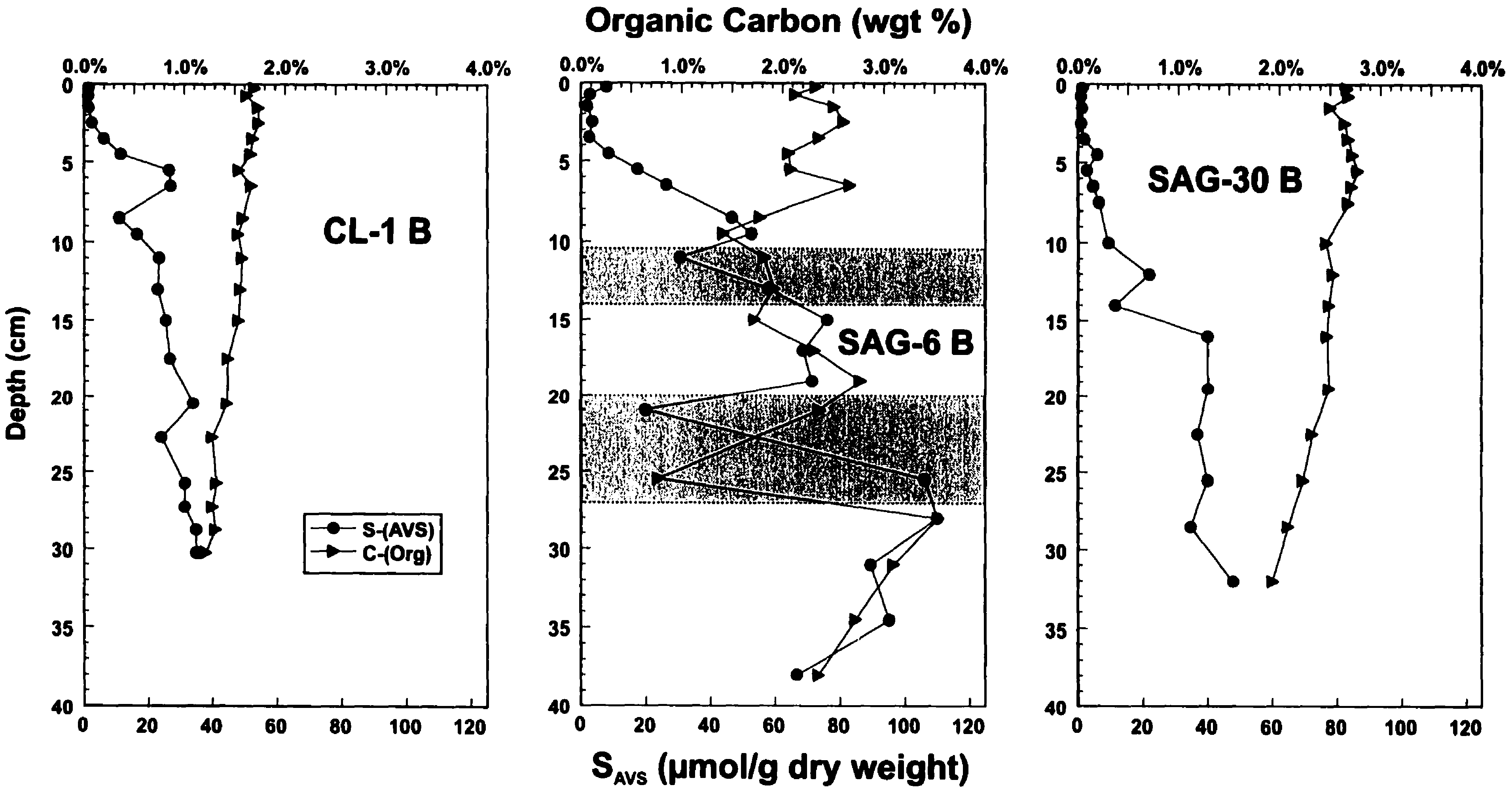

Figure 5.1 Distribution of organic carbon and acid-volatile sulphide in sediments of the Saguenay Fjord and Laurentian Trough

SAG-6B

Sediments at station SAG-6B are characterized by a very thin (few mm) oxic layer below which there is rapid onset of sulphate reduction. The concentration of AVS increases with depth to about 53 $\mu mol \cdot g^{-1}$ at 9.5 cm. There are AVS peaks both above and below each clay layer, with remarkably low concentrations within the layers themselves. Beneath the upper clay layer, concentrations of AVS reach values of 76 $\mu mol \cdot g^{-1}$, whereas values beneath the deeper clay layer reach 110 $\mu mol \cdot g^{-1}$ and decrease gradually with depth. Further discussion of the distribution of AVS in basin slope sediments appears in **Section 6.1.2.**

SAG-30B

Compared to basin slope sediments, the AVS profile at the bottom of the basin (SAG-30B) is relatively featureless and resembles the profile at CL-1B. AVS concentrations are negligible near the sediment/water interface and increase slowly with depth, with the exception of a trough at about 14 cm. Below ~16 cm, AVS concentrations remain fairly constant with depth at about 40 $\mu mol \cdot g^{-1}$.

5.3 $\mathbf{Mn_{HCl}}$

Vertical profiles of 1N HCl-extractable Mn (Mn_{HCl}) are presumed to represent the distribution of this element in Mn oxides and oxihydroxides. The Mn_{HCl} profiles are reproduced for each station in **Figure 5.2** and are tabulated in **Appendix 2**. At each station, sediments exhibit surface enrichment of Mn_{HCl} prior to the onset of suboxic conditions. A peak occurs where dissolved Mn(II), which has migrated from the deeper suboxic and anoxic sediments, is oxidized to Mn(IV) and re-precipitated. Because of the slow kinetics of the oxidation reaction, Mn(II) often migrates slightly into oxygenated sediments, and the dissolved Mn maxima (reported in Gagnon *et al.*, 1997) thus serve to better define the redoxcline (Gagnon *et al.*, 1995). The redox boundary occurs slightly below the depth of the Mn_{HCl} (Mn reoxidation) peak in each profile. Concentrations of Mn_{HCl} in suboxic sediments decrease dramatically, demonstrating marked depletion as a result of reductive dissolution and remobilization below the redoxcline.

5.4 Fe_{HCl}

The profiles of 1N HCl-extractable iron (Fe_{HCl}) like those of Mn_{HCl}, have few sharply defined features aside from the formation of a broad peak approximately marking the position of the redoxcline (**Appendix 2, Figure 5.2**). Suboxic Fe_{HCl} depletion also results from the reduction, dissolution, and remobilization of iron oxides, hydroxides, and oxihydroxides to the redoxcline, where Fe^{2+} diffusing from below is rapidly oxidized and re-precipitated as Fe(III) oxihydroxides upon encountering O_2. Below the redoxcline, Fe_{HCl} concentrations exhibit minor depletion compared to Mn_{HCl}, as much of the Fe_{HCl} is bound to phases which are more resistant to reduction (i.e., silicates and well crystallized oxides; Canfield, 1989; Canfield *et al.*, 1992). AVS concentrations account for less than 10% of the Fe_{HCl} and do not significantly affect the shape of the Fe_{HCl} profiles.

CL-1B

Fe_{HCl} concentrations in Laurentian Trough sediments vary between 430 to 520 $\mu mol \cdot g^{-1}$ dry sediment (2.4 to 2.9% by weight). They do not change markedly across the redoxcline and the Fe_{HCl} peak at the redoxcline is weak.

SAG-6B

Reactive iron concentrations in sediments of the basin slope are much lower (285 - 500 $\mu mol \cdot g^{-1}$, or 1.6 - 2.8% by weight) than at the other stations, and a strong Fe_{HCl} peak

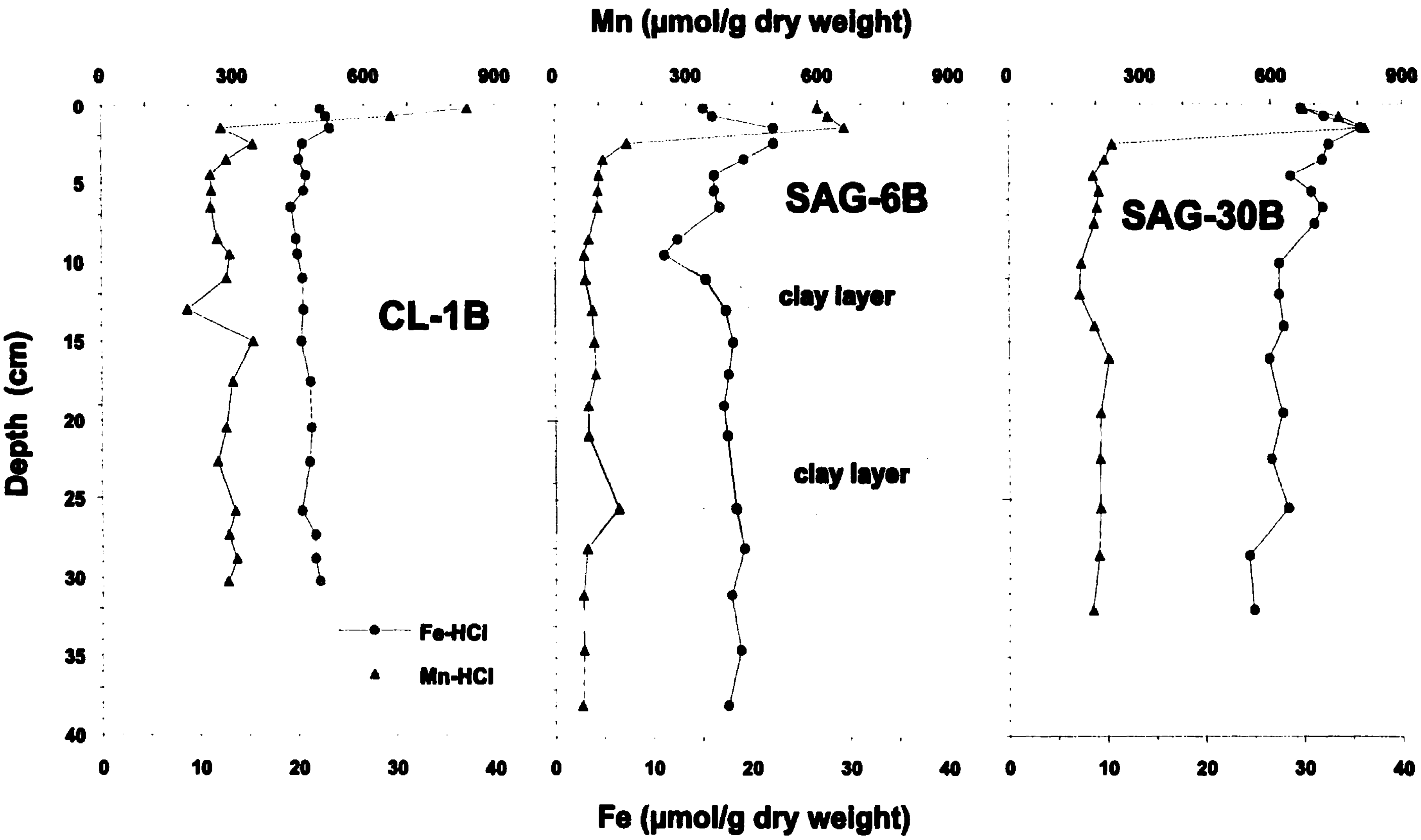

Figure 5.2 Distribution of HCl(1N)-extractable Fe and Mn in sediments of the Saguenay Fjord and Laurentian Trough

is obvious at the redoxcline. With the exception of a Fe_{HCl} minimum above the upper clay layer, HCl-soluble iron concentrations below the redoxcline are nearly constant with depth. The lower clay layer does not coincide with any distinguishable feature in the Fe_{HCl} profile.

SAG-30B

Sediments from the bottom of the deep basin also exhibit a large Fe_{HCl} peak associated with the re-precipitation of iron oxihydroxides at the redoxcline. Concentrations below the redoxcline change little with depth. Fe_{HCl} concentrations at SAG-30B (570 - 805 $\mu mol \cdot g^{-1}$, or 3.2-4.5% by weight) are much higher than those in basin slope or Laurentian Trough sediments.

5.5 Chromium Reducible Sulphur (S_{CRS})

As discussed previously (**Section 4.4.2**), S_{CRS} concentrations are presumed to represent the pyritic sulphur content of the sediments. Vertical distributions of S_{CRS} are presented in **Figure 5.3** and tabulated for each station in **Appendix 2**.

CL-1B

Sediments from the Laurentian Trough show markedly different distributions of S_{CRS} above and below 10 cm depth. In the uppermost sediments, the concentration of S_{CRS} ranges from 7 to 25 $\mu mol \cdot g^{-1}$ and fluctuates considerably, exhibiting several peaks and troughs. Beneath 10 cm, S_{CRS} levels vary between 7 and 11 $\mu mol \cdot g^{-1}$ and present a much more monotonous profile. Significant quantities (7-9 $\mu mol \cdot g^{-1}$) of S_{CRS} are also present in the top 2 cm of the sediment profile, which consists of oxic sediments, suggesting that much of this pyrite is, in fact, detrital.

SAG-6B

The profile of S_{CRS} in basin slope sediments fluctuates considerably, partly because of the inter-layering of the clay deposits. Concentrations of chromium-reduced sulphur near the sediment-water interface (0-3 cm) range between 12-14 $\mu mol \cdot g$. A sharp peak (38 $\mu mol \cdot g^{-1}$) occurs at about 4.5 cm and is followed by a second, broader peak (25 $\mu mol \cdot g^{-1}$) around 8-9 cm depth. S_{CRS} peaks (~22 $\mu mol \cdot g^{-1}$) also occur in association with each clay deposit, while concentrations *decrease* within the organic-rich mud deposits.

SAG-30B

In the sediments of the deep basin, the S_{CRS} concentrations are considerably lower than at the other stations. In addition, the S_{CRS} profile is nearly featureless. Near the sediment/water interface (0-2 cm), the concentration of S_{CRS} *decreases* with depth from 6.5 to 5.3 $\mu mol \cdot g^{-1}$. In deeper sediments, however, (2-32 cm) S_{CRS} levels gradually *increase* to ~9 $\mu mol \cdot g^{-1}$.

5.6 Fe_{pyr}

The final step of the sequential extraction protocol for mercury, described in **Section 4.3.2.5**, was intended to dissolve pyrite and is modified from Lord (1982). Iron extracted here is defined as Fe_{pyr} and serves as a second means of evaluating pyrite distribution, independent of the reduced sulphur distillation procedures. Fe_{pyr} concentrations are presented in **Appendix 2** and are compared graphically to S_{CRS} in **Figure 5.3**. Further comparison and discussion of the efficiency of these techniques appears in **Section 5.8.4**. According to the stoichiometry of pyrite (FeS_2), and if both CRS and sequential extraction procedures dissolved equivalent amounts of the mineral

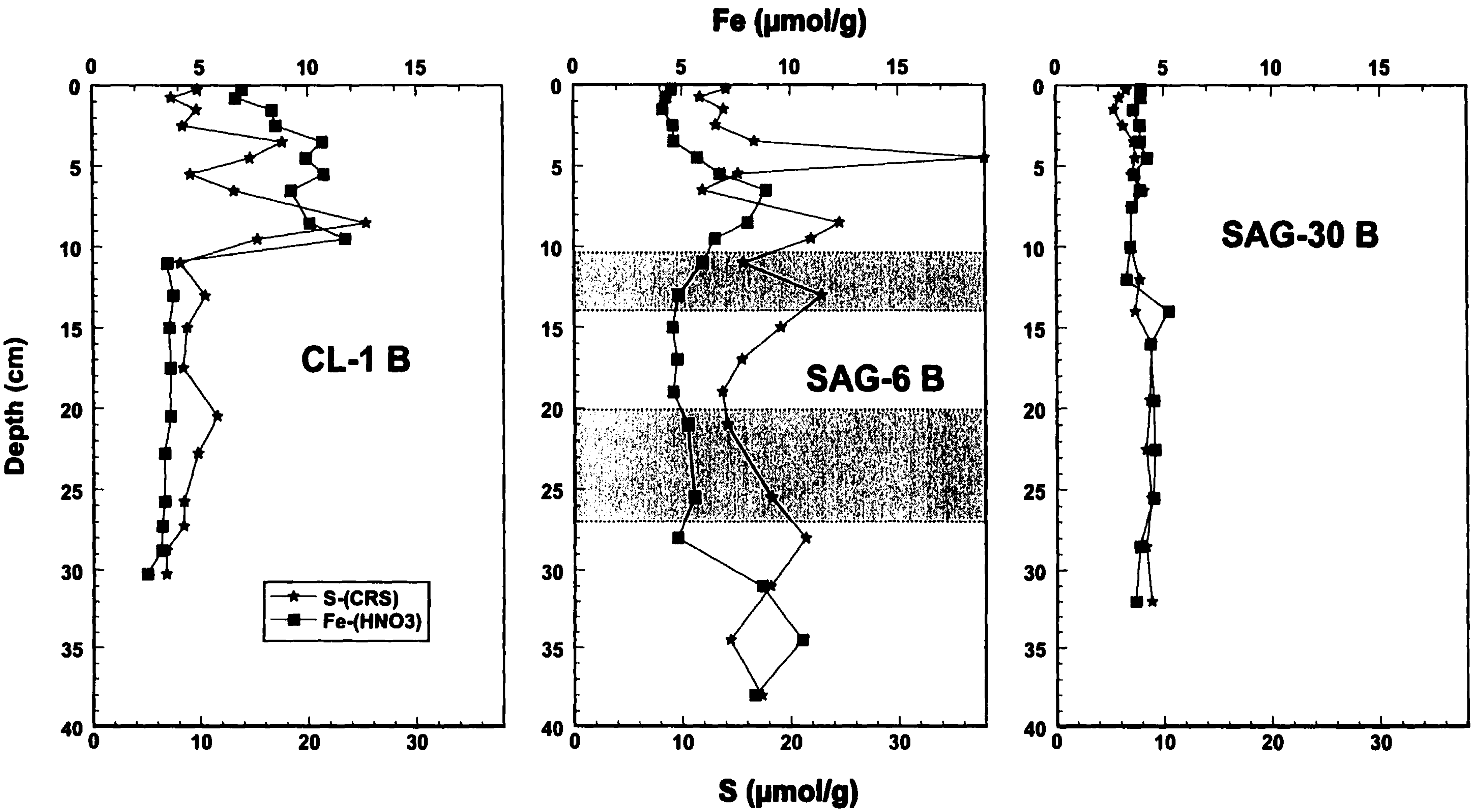

Figure 5.3 Distribution of chromium-reducible sulphur (method after Hsieh and Yang, 1988) and pyritic Fe isolated using a modified sequential extraction procedure (after Lord, 1982) in sediments of the Saguenay Fjord and Laurentian Channel.

from the sediments, the molar ration of S_{CRS} to Fe_{pyr} should be 2. The scaling of the horizontal axes in **Figure 5.3** were adjusted to reflect this relationship.

CL-1B

The distribution of Fe_{pyr} in Laurentian Trough sediments shows pronounced pyrite enrichment in surface sediments (7-12 $\mu mol \cdot g^{-1}$). Below the pyrite maximum at ~10 cm. values decrease markedly (~4.5 $\mu mol \cdot g^{-1}$) and remain nearly constant with depth. While smoother than the S_{CRS} profile, Fe_{pyr} concentration profiles are stoichiometrically very similar.

SAG-6B

In basin slope sediments, the concentration of Fe_{pyr} remains roughly constant at 4 $\mu mol \cdot g^{-1}$. Notable exceptions are the two small maxima (~9 and ~11 $\mu mol \cdot g^{-1}$), which occur, respectively, at the 6-7 and 33-36 cm depth intervals. At SAG-6B, the distribution of Fe_{pyr} differs markedly from S_{CRS}. As well, Fe_{pyr} and S_{CRS} profiles exhibit perceptible differences in their relative stoichiometric ratios.

SAG-30B

The profile of Fe_{pyr} in the sediments at the bottom of the basin shows much less variation than at either of the previous stations. Concentrations remain fairly constant around 4 $\mu mol \cdot g^{-1}$, with the exception of a small peak at 14 cm.

5.7 Results - Mercury Analyses

All results from the mercury analyses (partitioned, summed, and total) are presented in **Appendix 3**. Profiles of mercury concentrations (i.e., Hg_{sum} and Hg_{tot} with depth appear in **Figure 5.4**. Profiles of Hg sequential extractions for each station are

Table 5.1: Definition of Hg fraction denotations used in text

Term	Definition
Hg_{TOT}	Total Hg as determined by *digestion technique* (**Section 4.2.2**)
Hg_{SUM}	Sum of Hg content of the four extraction phases (NaOH, HCl, HF/HCl, and HNO_3). Also **total *extractable* mercury**.
$Hg_{Fraction}$	Generally, the amount of Hg solubilized during a given sequential extraction treatment (**Section 4.3.2**); specifically: Hg_{NaOH}, Hg_{HCl}, $Hg_{HF/HCl}$, or Hg_{HNO3}.

presented in various forms (Section 5.7.2) in **Figures 5.5 - 5.8**. The nomenclature used to refer to the different mercury fractions is defined in **Table 5.1**.

5.7.1 Total Mercury (Hg_{tot})

Results of the Hg_{tot} analyses of these samples have already been presented and discussed by Gagnon (1994). The profiles of mercury within the Saguenay Fjord and adjoining Laurentian Trough (**Figure 5.4**) bear the strong temporal signature of Hg input during the years of operation of the chlor-alkali plant at Arvida (1947-1971). The differences between Hg_{tot} and Hg_{sum} are discussed below (**Section 5.2.5**).

CL-1B

Mercury concentrations in Laurentian Trough sediments appear as a broad hump, over which concentrations double (230 - 575 $ng \cdot g^{-1}$) with depth. Because the sedimentation rate in the trough is slow (~0.1 $cm \cdot a^{-1}$; Silverberg *et al.*, 1986), the history of mercury contamination of these sediments over the entire period of operation of the Arvida plant, as well as some time prior to its opening, is recorded in the CL-1B core.

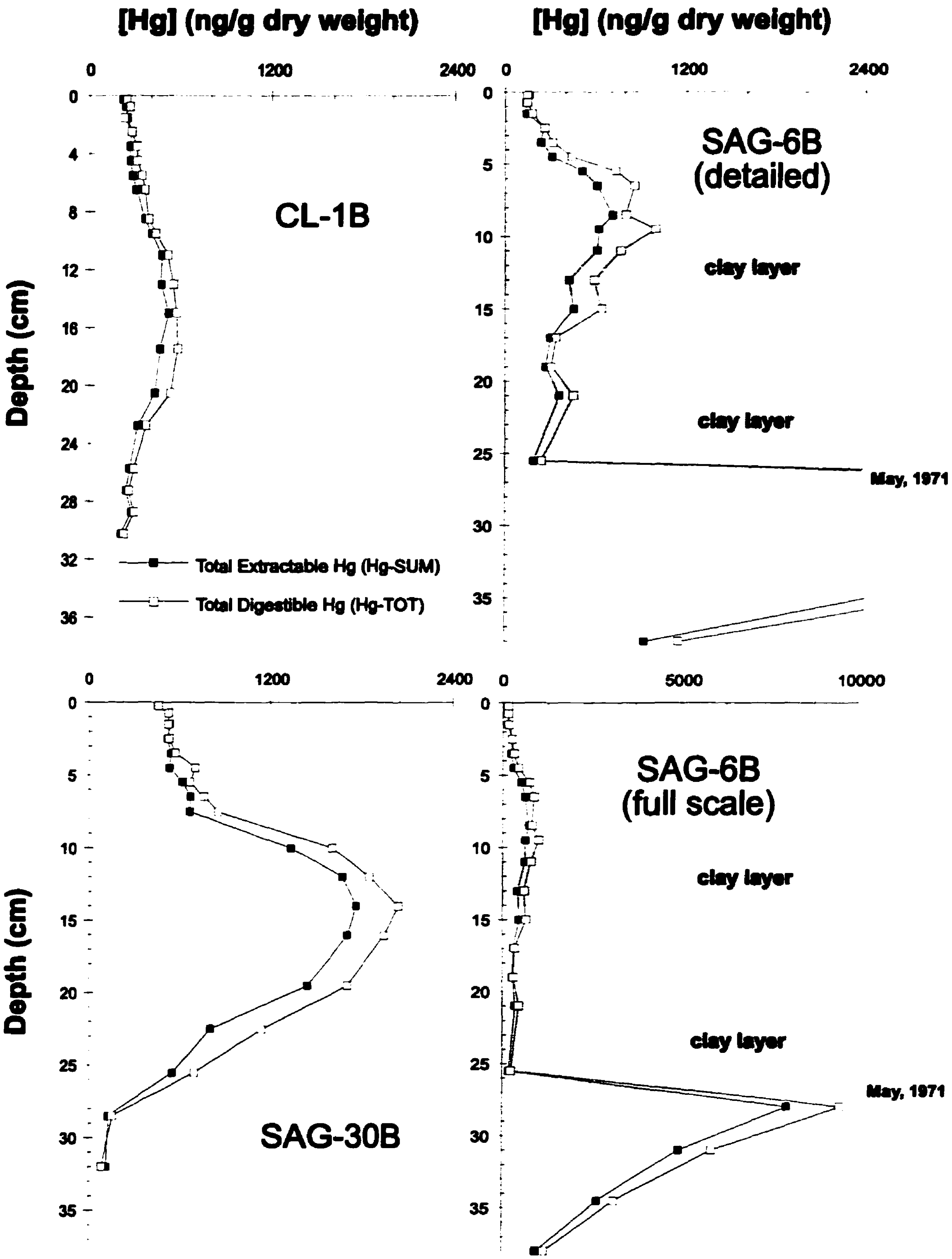

Figure 5.4 Distribution of Hg_{ex} in the sediments of the Saguenay Fjord and Laurentian Trough.

Hg concentrations at the bottom of the core at this station remain elevated compared to pre-industrial Saguenay Fjord sediments (~ 150 ng·g^{-1}; Loring, 1975; Smith and Loring, 1981; Barbeau *et al.*, 1981b). This indicates an historically elevated input of mercury to Laurentian Trough sediments, relative to the Saguenay Fjord, as a result of other contaminant sources. In addition to Hg input from the Arvida plant (through the Saguenay Fjord), mercury is transported to Trough sediments via the St. Lawrence River as well as by atmospheric input (Gobeil and Cossa, 1993; Gagnon *et al.*, 1997). Mercury concentrations in surface sediments (0-3 cm) of the Laurentian Trough are similar to those beneath the zone of contamination.

SAG-6B

Values of Hg_{tot} measured in the uppermost layers of sediment (0-2 cm) of the basin slope are close to pre-industrial Hg concentrations (~ 150 ng·g^{-1}; Loring, 1975; Smith and Loring, 1981; Barbeau *et al.*, 1981b). With depth, however, Hg_{tot} values rise considerably, and two major Hg_{tot} peaks are visible. A broad band of contaminated sediment rests between 4 to 18 cm with a peak of 1000 ng·g^{-1} which coincides with the top of the shallower clay layer (9-10 cm). A much larger peak, reaching 9500 ng·g^{-1}, underlies the bottom clay layer (27-29 cm). The deeper clay layer represents a massive input of post-Wisconsinian clays following the 1971 St. Jean-Vianney landslide. The landslide coincided with maximum Hg output at the chlor-alkali plant, and occurred just prior to sharp reductions in Hg concentrations in the effluents as a result of the implementation of new government regulations in 1971-72. Highly contaminated sediments are found beyond the sampling depth of this core.

SAG-30B

Sediments recovered from the bottom of the basin (SAG-30B) bear concentrations of mercury significantly exceeding pre-industrial concentrations even in surficial sediments. Values increase with depth, forming a broad Hg_{tot} peak which reaches a maximum at 2050 $ng \cdot g^{-1}$ at around 15 cm depth. Because sedimentation rates prior to the 1971 landslide were slow (~ 0.1 $cm \cdot a^{-1}$), this core provides a complete historical record of recent anthropogenic inputs of Hg to the fjord. Pre-industrial Hg concentrations are found below the zone of severest mercury contamination (>27 cm).

Values presented here agree with those reported by other authors (Loring, 1975; Barbeau *et al.*, 1981b; Smith and Loring, 1981; Mucci and Edenborn, 1992; Gobeil and Cossa, 1993; Gagnon *et al.*, 1997). Hg_{tot} concentrations (site averages only) reported by Loring (1975) for sediments collected in 1974 in the vicinity of our stations nearly correspond with maximum mercury levels measured at each site. Similar mercury profiles in sediments recovered in previous and later years at identical or nearby sites have been presented by Smith and Loring (1981), Mucci and Edenborn (1992), Gobeil and Cossa (1993), and Gagnon *et al.* (1996b, 1997). Markedly lower mercury concentrations (<6 $\mu g \cdot g^{-1}$) reported by Barbeau *et al.* (1981b) from the basin slope appear to be an artifact of the analytical procedure (i.e., H_2O_2 digestion) they employed, which reduces and volatilizes mercury (Campbell and Tessier, 1989). Surface sediments (0-2 cm) from stations SAG-6B and SAG-30B have slightly lower concentrations of Hg_{tot} relative to comparable samples taken from nearby sites in 1986 (Pelletier and Canuel, 1988). The results of this study and more recent measurements indicate that despite a significant decrease in Hg concentration since 1972 and the closure of the plant in 1976, surficial sediment concentrations remain higher than pre-industrial levels. The source of Hg to these sediments has been (Gagnon *et al.*, 1996b; 1997) and continues to be investigated.

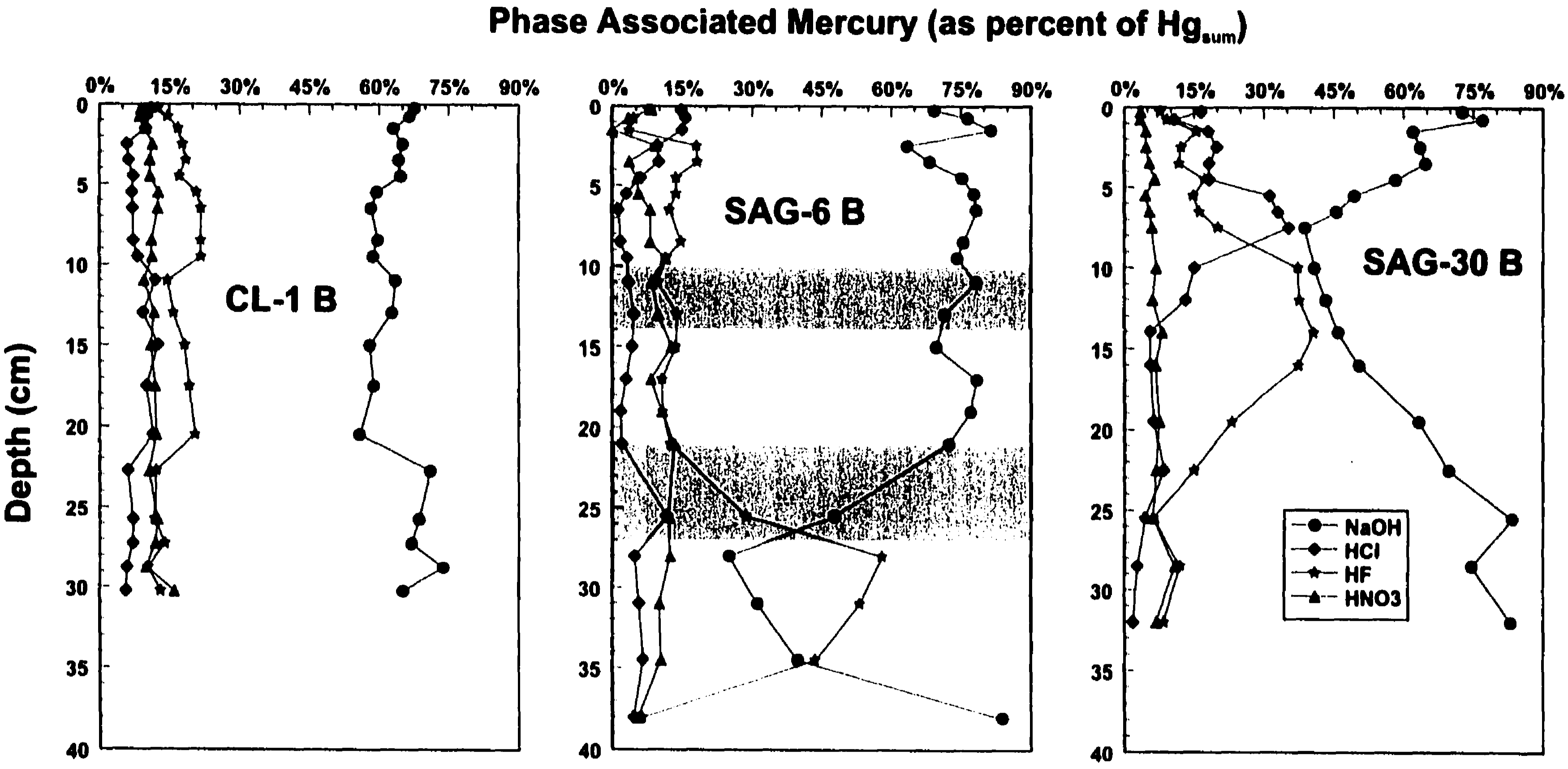

Figure 5.5 Relative distribution of mercury ($Hg_{fraction}:Hg_{sum}$) among operationally defined extraction pools in sediments of the Laurentian Trough and Saguenay Fjord

5.7.2 Extracted Mercury

Because the vertical distribution of Hg principally reflects temporal input of mercury to the sediments, a comparison of the absolute concentrations of the various fractions of mercury extracted from the cores provides limited insight on factors responsible for the partitioning. Consequently, relative concentrations with respect to the total and between stations are compared and discussed. Profiles of the relative concentration ($Hg_{fraction}/Hg_{sum}$) of the extracted mercury at each station appear in **Figure 5.5**. Profiles of the absolute concentrations of the various $Hg_{fraction}$ pools appear separately with each station (**Figures 5.6 - 5.8**)

CL-1B

In the Laurentian Trough sediments, Hg_{NaOH} remains the dominant mercury phase throughout the profile (**Figure 5.6**). The fraction of Hg extractable in NaOH constitutes between 56% to 74% of the total extractable mercury (Hg_{sum}) (**Figure 5.5**). The remaining fractions of mercury are comparatively minor, with few easily interpretable features within their profiles. The ratios of Hg_{HCl}/Hg_{sum} are slightly elevated at the surface, but remain between 6 and 13% with subsurface maxima at ~11 and 20.5 cm. The contribution of $Hg_{HF/HCl}$ changes little with depth, ranging between 10 and 22% and is consistently the greatest fraction after Hg_{NaOH}. The distribution of $Hg_{HF/HCl}$ closely follows that of Hg_{sum}, and $Hg_{HF/HCl}/Hg_{sum}$ mirrors the profile of Hg_{NaOH}/Hg_{sum}. With the exception of a small peak at 30 cm, Hg_{HNO_3}/Hg_{sum} ratios at this station are nearly constant, varying only between 9 and 13%.

SAG-6B

The presence of a highly contaminated mercury layer requires that absolute values be presented in two separate diagrams (**Figures 5.7a, 5.7b**), so that details at lower Hg concentrations are visible. Whereas the NaOH-associated mercury pool remains the most

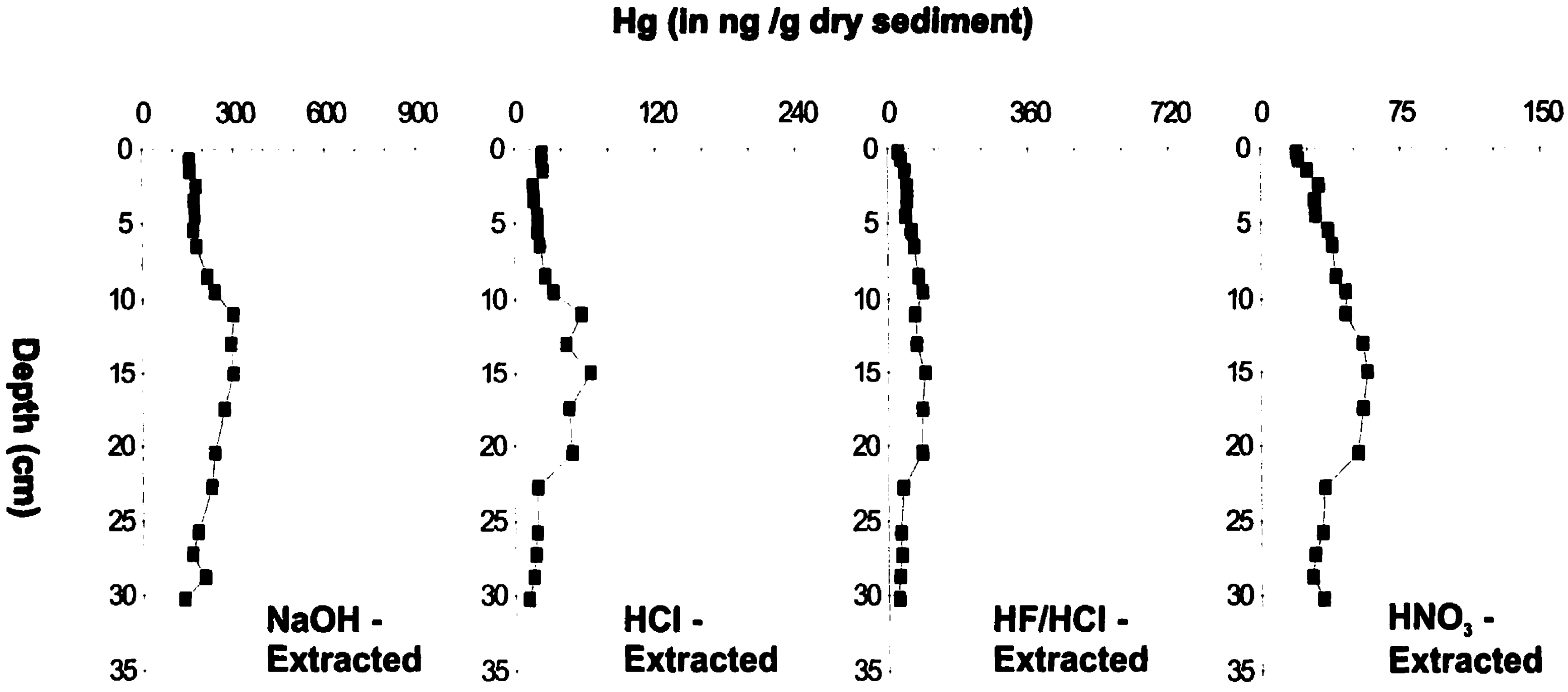

CL-1B

Figure 5.6 **The distribution of mercury among operationally defined extraction pools in sediments of the Laurentian Channel (Station CL-1B).**

significant fraction, the association of Hg to other substrates is significant in the basin slope sediments. Above the lower clay layer, the Hg_{NaOH}/Hg_{sum} ratio varies between 63 and 81% (**Figure 5.5**). A marked decrease in Hg_{NaOH}/Hg_{sum} occurs with the onset of the deeper clay layer (21 cm) from 70% to 25% of Hg_{sum} at the base of the landslide deposit. With depth (36-40 cm), the contribution of Hg_{NaOH} increases and ratios return to similar to those *above* the deeper clay deposit.

In comparison, other fractions of mercury generally play a minor role. There is surface enrichment of Hg_{HCl} (15% of total), and a small peak in the lower clay layer, but otherwise the contribution of HCl-soluble Hg remains $\leq$ 6%.

The ratio of $Hg_{HF/HCl}$ to Hg_{sum} is also small (11-18%) above the deeper landslide layer. The importance of HF/HCl extractable mercury increases dramatically within and slightly below the deep clay layer. $Hg_{HF/HCl}$ increases to nearly 60% of Hg_{sum}, at the expense of Hg_{NaOH}, between 24-36 cm, but decreases again with depth (36-40 cm). Again, the distribution of $Hg_{HF/HCl}$ shadows Hg_{sum}, and $Hg_{HF/HCl}/Hg_{sum}$ profiles seem to mirror those of Hg_{NaOH}/Hg_{sum}.

The vertical distribution of Hg_{HNO3} in basin slope sediments ranges between 0 and 13% of Hg_{sum}. Hg_{HNO3}/Hg_{sum} ratios are low and erratic in surface sediments, then increase slightly and remain relatively constant with depth.

SAG-30B

At SAG-30B, changes in mercury partitioning occur in the absence of any visible allochthonous clay layer. Although Hg_{NaOH} remains the predominant mercury fraction at this site, other fractions comprise a significant proportion of Hg_{sum} (**Figure 5.8**). Ratios of Hg_{NaOH} to Hg_{sum} are highest in surface and deeper (>19 cm) sediments, whereas they are greatly depressed between 5 and 19 cm. Hg_{HCl} comprises ~15% of Hg_{sum} near the sediment/water interface, and values increase dramatically to peak at ~33% between 5 and

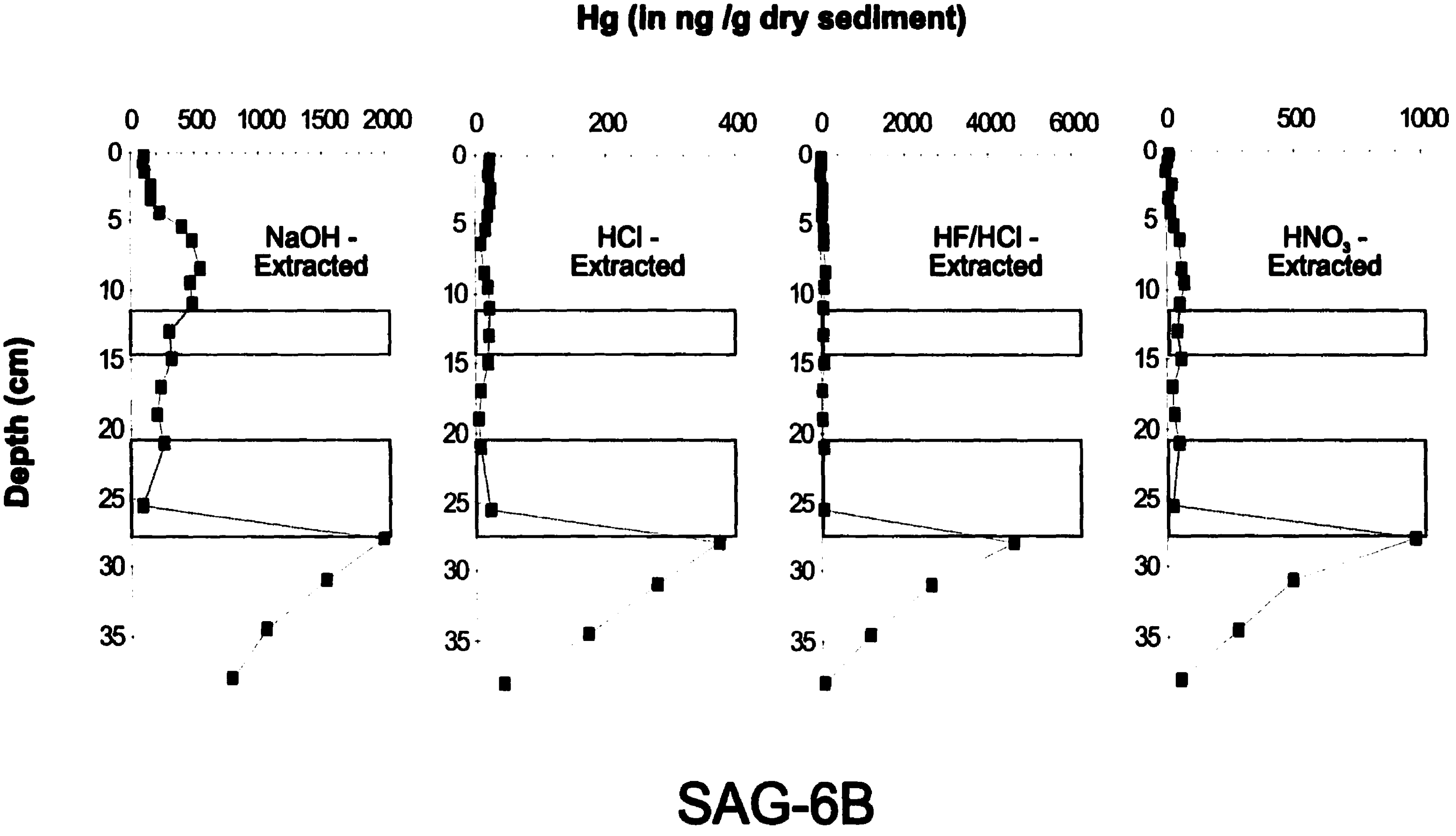

Figure 5.7a Distribution of phase associated mercury among operationally defined extraction pools in sediments of the Saguenay Fjord (SAG-6B), full scale.

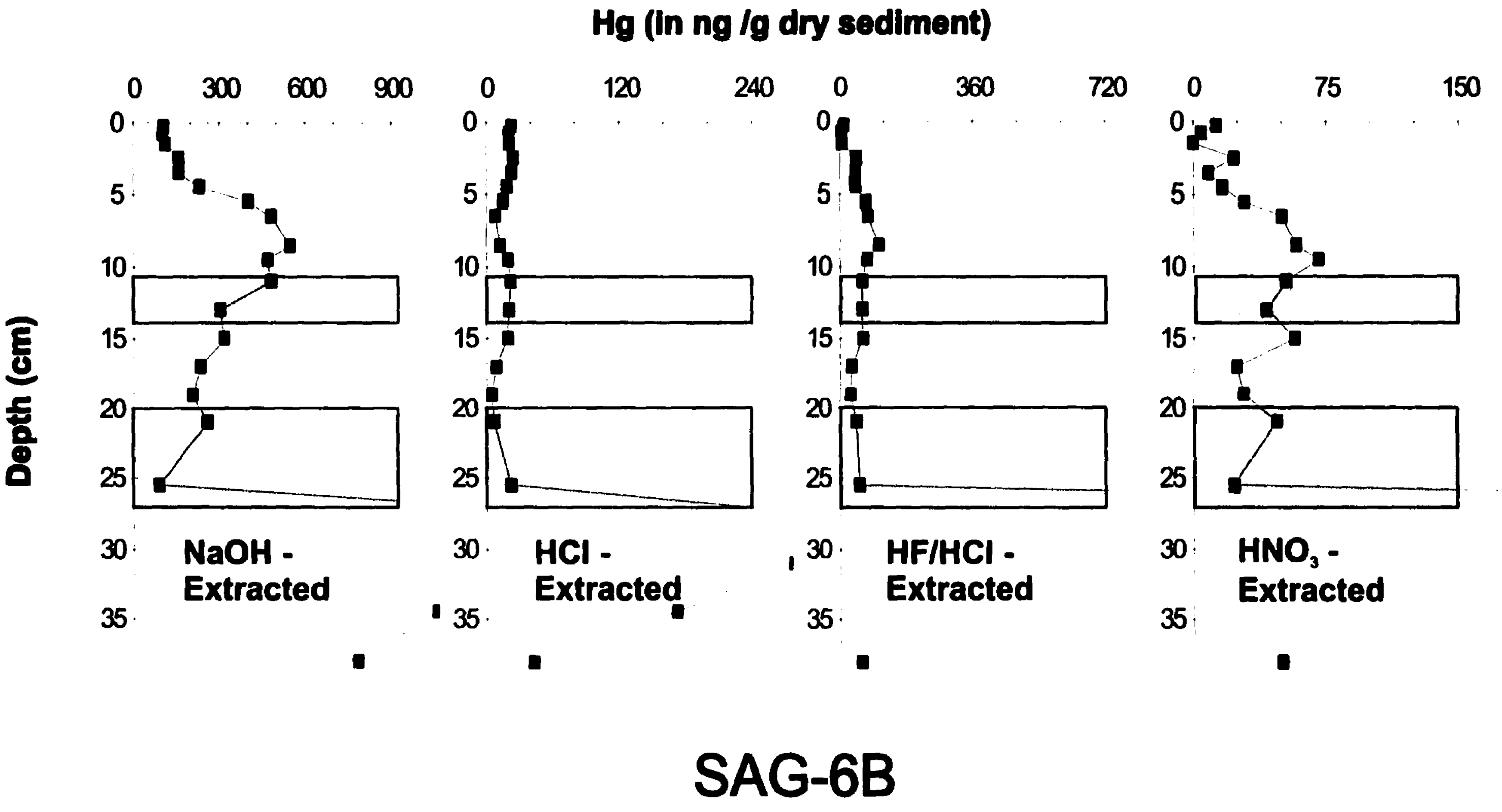

Figure 5.7b Distribution of phase associated mercury among operationally defined extraction pools in sediments of the Saguenay Fjord (SAG-6B), exploded view.

8 cm depth, whereas Hg_{NaOH}/Hg_{sum} ratios decrease markedly at these depths. Below 10 cm, the contribution of Hg_{HCl} is negligible and the smallest of all extractable fractions (≤8%). Little Hg is solubilized by the HF/HCl reagent (~15%) between the sediment/water interface and 10 cm depth. As Hg_{HCl}/Hg_{sum} ratios drop off, however, $Hg_{HF/HCl}/Hg_{sum}$ ratios increase dramatically to values as high as 41%, whereas Hg_{NaOH}/Hg_{sum} remain low, and only increase when $Hg_{HF/HCl}$ values subside with depth. At this site, Hg_{NaOH}/Hg_{sum} profiles mirror the combined profiles of Hg_{HCl}/Hg_{sum} and $Hg_{HF/HCl}/Hg_{sum}$. In sediments recovered from the bottom of the basin, Hg_{HNO3}/Hg_{sum} increases from 3% near the sediment/water interface to 7% at depth (<34 cm), with the exception of a small (11%) peak at 27-30 cm.

5.8 Critical Evaluation of the Methodology

5.8.1 NaOH Extraction

Organic Carbon

Organic matter is believed to be one of the more reactive sediment materials with respect to mercury sorption. The distribution of C_{org} in the various extractant pools (NaOH, HCl, HF/HCl, and HNO_3) is, therefore, critical to the interpretation of Hg partitioning. Determinations of organic carbon content in selected samples were performed both on solid residues following extraction, as well as on the extract solutions themselves. The distribution of organic carbon within the operationally defined sequential extraction pools appears in **Table 5.2**. These values are *not* meant as a detailed accounting of organic carbon in each extraction pool, but rather are intended to serve as a rough estimate and point of discussion.

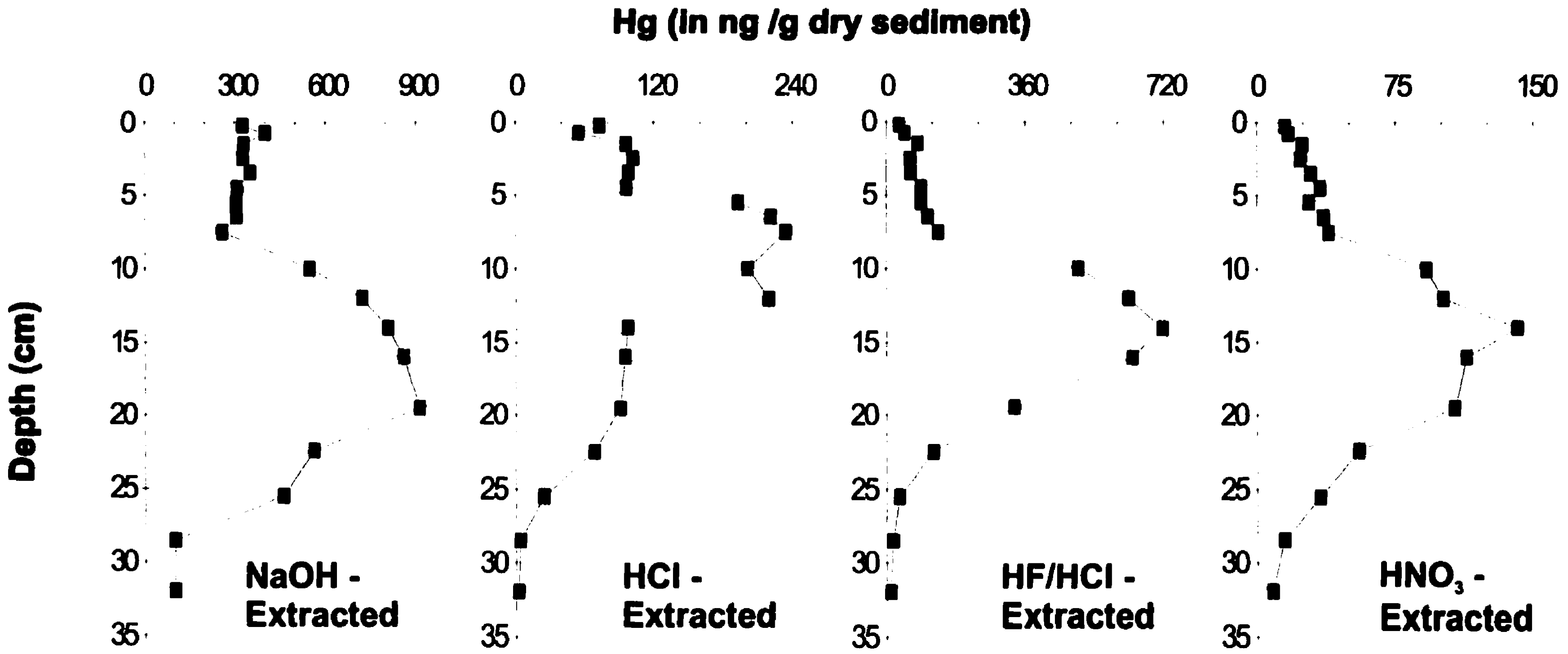

SAG-30B

Figure 5.8 Distribution of phase-associated mercury among operationally defined extraction pools in sediments of the Saguenay Fjord (SAG-30B).

Table 5.2 **Distribution of organic carbon among operationally defined fractions in the Laurentian Channel and Saguenay Fjord sediments.**

Analyzed Phase	ΣCorg Extracted, by phase (in % of total)			
	NaOH	HCl	HF/HCl	HNO_3
Supernatant DOC	36-55%	10-20%	5-10%	10-20%
Residual Solid	35-74%	7-20%	11%	Not Determined

As discussed previously, the NaOH (1N) extraction step was clearly incapable of extracting all organic carbon. Alkali has been shown to solubilize some lipids, hemicellulose and starches, as well as fulvic and humic acids (Flaig *et al.*, 1975). Other compounds which normally make up a smaller component of the organic carbon pool, including cellulose, lignin, and humin, are *not* soluble in dilute base and would therefore be extracted in later phases. In addition, the susceptibility of organic matter to chemical attack and solubilization may be significantly reduced as a consequence of binding to other sedimentary solid surfaces. The following step, HCl (1N) should release any organic substances co-precipitated with, or covered over by iron hydroxide coatings or carbonate minerals. The quantity of organic matter soluble in HCl was not expected to be important, since only a small percentage (6-11%) of estuarine organic matter is precipitated with iron hydroxide flocs (Sholkovitz, 1976; Sholkovitz *et al.*, 1978). On the other hand, organic matter bound to clay surfaces has been found to resist both alkali and acidic attack and may only be extracted when concentrated HF is used to dissolve the clay substrate (Hatcher *et al.*, 1985; Stevenson, 1994). Lignins and humins should survive the preceding steps and solubilize only following treatment in concentrated HNO_3. According to Louchouarn *et al.* (1995), lignin may account for 5-10% of the Saguenay Fjord sedimentary particulate organic matter. Accordingly, the bulk of the organic matter degraded in the HNO_3 step may be of ligneous origins. It is possible that some highly resistant organic matter may survive even the HNO_3 step, since a minute quantity of combustible solid survived the final hot HNO_3 (conc.) extraction step. Although it has not been confirmed, the loss of ~ 60% of the mass of the residue during combustion suggests that the residue may partly consist of highly refractory organic matter (T. Ahmedali, pers. comm.), possibly ligneous in origin. The post-extraction residues did not exceed 650 μg per gram dried sediment. It was impossible to evaluate the organic content of these samples because the sample size was so small. In addition, sources of error, such as the loss during sample transfer, can become large late in the extraction protocol due simply to the number of manipulations which have been performed on each sample. Because there is at present no method which can be applied to completely isolate inorganic and organic components of estuarine sediments **(Section 4.3.2)**, the relative contribution of organic matter *in each extractant pool* has been considered in the interpretation of mercury partitioning.

Iron and Manganese

The 24 hour, 1N NaOH extraction solubilized little iron or manganese. Concentrations of Fe_{NaOH} did not exceed 1% of Fe_{HCl} values, while Mn leached by the NaOH solution was less than 2% of Mn_{HCl}. Under the conditions of the extraction (i.e. pH ~ 13), the metal oxyhydroxides are highly insoluble. The high concentration of dissolved organic matter in the NaOH extract suggests that the dissolved metals were organically chelated. It is impossible to determine whether the chelation occurred naturally *in situ*, or as an artifact of the procedure itself.

5.8.2 Comparison of HCl and CDB Extraction Techniques

The relative merits of the HCl and CDB extractants, as well as the criteria for the choice of HCl over other reagents for the selective dissolution of Fe/Mn (hydr)oxides have already been discussed (**Section 4.3.2.3**).

The concern expressed by Raiswell *et al.* (1993) arose from the apparent inability of the HCl extraction procedure to solubilize crystalline iron oxides phases (haematite, goethite, and magnetite). In addition, Morse (1994) found that the oxidation products of iron monosulphides which resulted from freeze-drying sediments were not dissolved by treatment with dilute HCl. Given the small contribution of Fe_{AVS} to Fe_{HCl}, the inability of HCl to extract all products of AVS oxidation should be insignificant to Fe_{HCl} results. In contrast, the effects of AVS oxidation on trace metal (mercury in this study) partitioning as determined by the sequential extraction procedure are unclear. The identification and reactivity of the oxidation products of reactive iron sulphides (FeS, mackinawite, and greigite) have received insufficient attention in the literature. It is possible that mercury associated with AVS minerals may be partly extracted in the HCl step as well as in the more aggressive steps (HF/HCl, HNO_3).

Iron concentrations in extracts of dilute HCl and citrate/dithionite/bicarbonate (CDB) of surface sediments (0-1.5 cm) from each station, and SAG-15B (see **Figure 3.1** for site location) were compared. Fe_{HCl} concentrations were invariably higher than Fe_{CDB}, generally more than twice the CDB values. The difference between the extraction results is believed to be caused by chemical attack of iron-bearing silicates and the leaching of Fe into solution (Kostka and Luther, 1993; Raiswell *et al.*, 1993). As a result, the very low DOS and DOP values described above may be underestimated compared to the literature definition. Alternatively, these numbers may be a more realistic representation of the system if, over time, all of the Fe_{HCl} is available for sulphidization and pyritization.

Both Fe_{HCl} and Fe_{CDB} exhibit a negative correlation to AVS (**Figure 5.9**), similar to observations reported by Kostka and Luther (1995) in salt marsh sediments. The relationship arises from the formation of AVS at the expense of Fe_{HCl} as sediments become anoxic. Although Fe_{HCl} includes FeS solids, the contribution of AVS is minute compared to total reactive iron and therefore effects little noticeable influence on the curve.

The *difference* between Fe_{HCl} and Fe_{CDB} is also plotted against AVS (**Figure 5.9**) and likewise exhibits a negative correlation to AVS. About 100 $\mu mol \cdot g^{-1}$ of iron seems reactive to sulphide in excess of what is extracted by CDB. This may be interpreted as the remobilization and sulphidization of iron associated with silicates. Several authors (Canfield, *et al.*, 1992; Raiswell *et al.*, 1993) report that iron associated with silicates can react with sulphide, but at exceedingly slow rates. It is not known which silicates may be leached, but minerals such as biotite, chlorite, and amorphous silicates are markedly more soluble in 1N HCl than in dithionite (Kostka and Luther, 1993; Raiswell *et al.*, 1993). In addition, these solids are common to the mineralogy of the suspended particulate matter and sediments of the Saguenay Fjord (Sundby and Loring, 1977; Mucci and Edenborn, 1992; Gagnon *et al.*, 1993).

5.8.3 Extraction of AVS

The extraction of iron monosulphides was performed on wet frozen sediments, not as part of the sequential extraction techniques, and thus suffer from none of the complications resulting from freeze-drying. The procedure used to determine AVS completely extracts sulphur from amorphous FeS and mackinawite, but only partially extracts (~60%) greigite (Cornwell and Morse, 1987). Any greigite which is not dissolved may be extracted with pyrite following reduction with Cr^{2+}. It is possible that

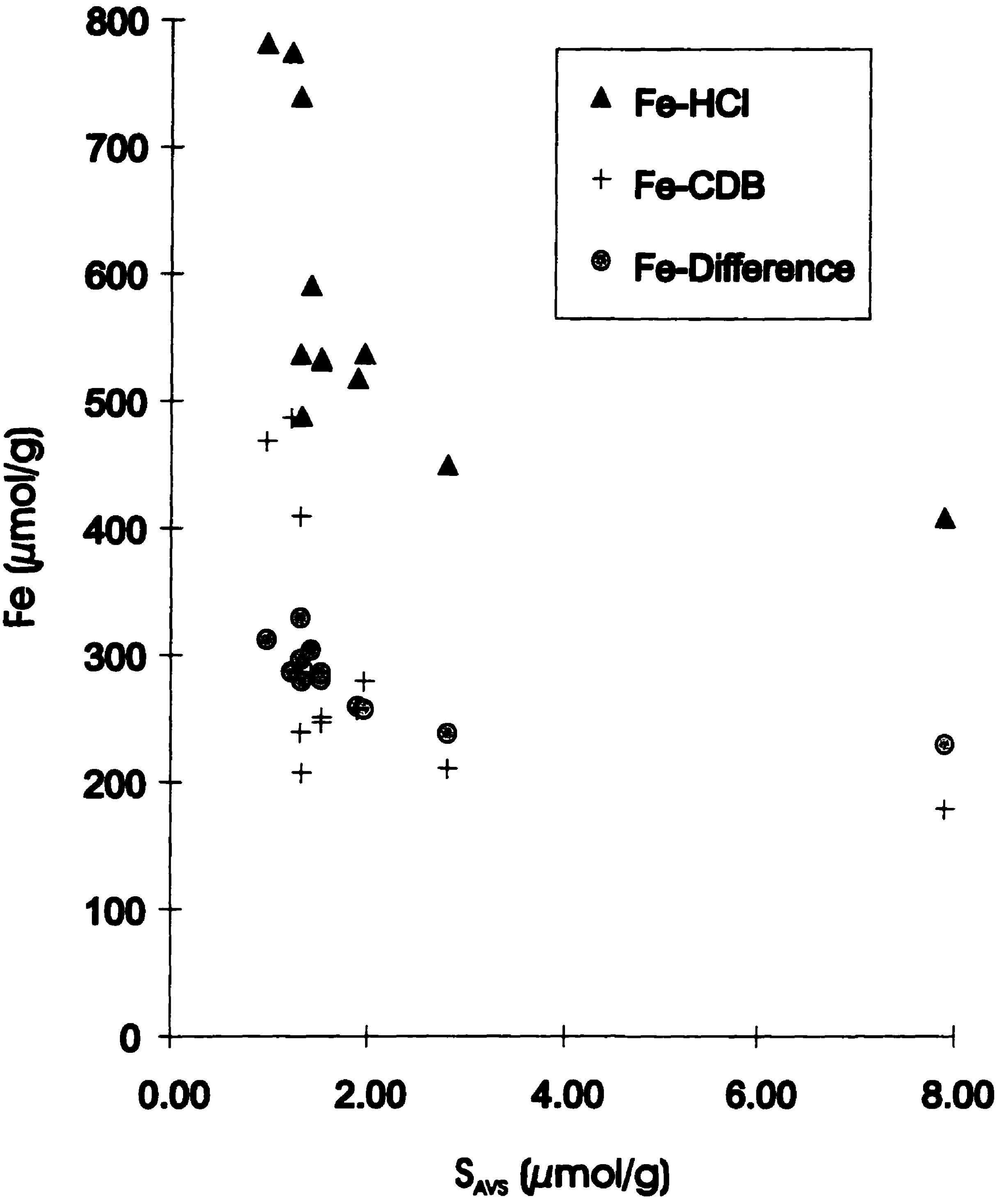

Figure 5.9 The relationship of Fe_{HCl} and Fe_{CDB} to S_{AVS} in sediments of the Laurentian Trough and Saguenay Fjord.

greigite partially oxidizes to zero valence sulphur, but this is less likely in the presence of powerful reductants (i.e. $SnCl_2$ and Cr^{2+}). Neither elemental sulphur nor organic sulphur are solubilized during these treatments. To define AVS as all monosulphides, greigite is assumed to be absent or comparatively insignificant. Howarth and Jorgensen (1984) reported only minute amounts of greigite in sediments from two Danish fjords, whereas Morse and Cornwell (1987) reported greigite in only one of fourteen anoxic sediments. To date, no attempt has been made to quantify greigite in the anomalously AVS-rich Saguenay Fjord sediments.

5.8.4 Contrasts between Fe_{pyr} and S_{CRS} in basin slope sediments

The Lord (1982) method ($Fe_{Lord} \approx Fe_{pyr}$) and the Zhabina and Volkov (1978) chromium-reduction technique (S_{CRS}) are each designed to extract pyrite. The two methods have been found to be equally effective for the dissolution of sedimentary pyrite and nearly equivalent for the degradation of massive pyrite (Cornwell and Morse, 1987; Huerta-Diaz and Morse, 1990). Consequently, the determination of pyrite content by the quantification of *both* iron and sulphur serves as a useful check of the methodology.

Although concentrations of pyritic iron and sulphur are similar in sediments of CL-1B and SAG-30B, there is a marked discrepancy between them at SAG-6B (**Figure 6.3**). Here, Fe_{pyr} concentrations are consistently lower than the corresponding CRS values, except at the two Fe_{pyr} maxima. In addition, the Fe_{pyr} profile seems stripped of the detail exhibited by the S_{CRS} distribution. The maxima of Fe_{pyr} and S_{CRS} occur at different depths. The distribution of S_{CRS} in this study agrees with results determined independently on samples from the same core by Gagnon *et al.* (1995). Mucci and Edenborn (1992) also reported similar pyrite concentrations at a station near SAG-6B using the method of Lord (1982). In this study, however, Fe_{pyr} exhibits maxima above and below the clay layers, as opposed to within them, as is evident in the S_{CRS} results as well as the pyrite concentrations reported by Mucci and Edenborn (1992) and Gagnon *et al.* (1995). The contrast between the iron and sulphur profiles could arise from particularities specific to each technique. Some possibilities include:

- incomplete pyrite extraction by HNO_3 (Fe_{pyr} only),
- differences in homogeneity and grain-size between frozen (S_{CRS}) and freeze-dried/ground (Fe_{pyr}) samples,
- oxidation or solubilization of pyrite during pre-treatment or extraction prior to the HNO_3 step (Fe_{pyr} only), and
- extraction of a sulphide phase by the CRS method which, in the sequential extraction technique, is extracted prior to the HNO_3 step.

The first is easily dismissed upon examination of pyrite extraction methodologies (Lord, 1982; Huerta-Diaz and Morse, 1990). The more intense compression of the redox profile at SAG-6B relative to the other stations reduces the spatial resolution of sampling techniques and increases the effect of sediment heterogeneity at this site. The frozen sediments are discrete samples and may not always be representative of a more integrated sampling. Nevertheless, sample heterogeneity is probably only responsible for occasional erratic data points at each station, but not the systematic differences between pyritic iron and sulphur at SAG-6B.

Smaller grain-size would facilitate solubilization of pyrite particles. Were grain-size alone a factor, the ground samples (Fe_{pyr}) would bear higher pyrite concentrations compared to the frozen counterparts (S_{CRS}), but in fact, the reverse is true.

Oxidative destruction of some pyrite prior to the HNO_3 step in the sequential extraction of freeze-dried sediments could have resulted from the freeze-drying alone, or during treatment with other reagents. Lord (1982) reported the necessity of a conversion factor to account for the dissolution by HF alone (~8% of FeS_2). The addition of HCl to the HF solution may increase pyrite solubility by forming soluble chloro complexes of iron. The similarity in pyrite concentrations among the other stations and the Fe_{pyr}/S_{CDB} discrepancy at SAG-6B alone, however, suggest that premature non-specific pyrite solubilization is not the principal cause of the iron/sulphur discrepancy.

Because greigite is only partially solubilized by the AVS extraction technique, reductive dissolution of greigite by reduced chromium (CRS) could produce the discrepancies between Fe_{pyr} and S_{CRS} which appear in the profiles of SAG-6B. Greigite is a common intermediate phase between pyrite and mackinawite that requires partially oxidized sulphur (POS) to convert to pyrite (Schoonen and Barnes, 1991) except at very low pH (Rickard and Luther, 1996; Rickard, 1996). In sediments depleted in POS, the final conversion of greigite to pyrite might be seriously retarded resulting in significant greigite preservation. In this instance, S_{CRS} values could overestimate pyrite concentrations. It is noteworthy that serious discrepancies between pyritic iron and sulphur occur only at SAG-6B, where AVS preservation is highest.

5.8.5 Differences between Hg_{sum} and Hg_{total}

Summed values from the sequential extraction procedure achieved 80 - 108% efficiency in the Laurentian Trough sediments and 70-107% in Fjord sediments (**Figure 5.4**). One notable exception is the sample in SAG-30 which showed 133% extraction, but where the ΣHg was very low (120 $ng \cdot g^{-1}$). In general, the few instances of overestimation occurred in samples with ΣHg are less than 250 $ng \cdot g^{-1}$, and are associated either to cumulative analytical errors or to contamination.

There are several possible sources of mercury loss. Some of the difference has to be attributed to the cumulative analytical uncertainties and to heterogeneity of individual samples. Loss to sorption by the reaction vessel should have been negligible since all extractions were performed in Teflon™ test tubes. Furthermore, volatilization of mercury is considered unlikely since none of the extraction solutions were reducing and there was sufficient ligand concentrations (OH^- or Cl^-) to keep Hg(II) in solution. Loss during supernatant transfer in the sequential extraction procedure certainly contributed to the missing mercury, particularly since the highest concentrations of mercury are found with the smallest particles (Loring, 1975). It seems doubtful, however, that there was sufficient solid discarded with unused supernatant to account for as much as 20-30% loss in some samples. The minute amount of solid remaining in most samples following the final HNO_3 treatment could have contained adsorbed mercury. The residue was not analyzed for Hg simply because it could not be solubilized and therefore was not appropriate for injection into the CVAFS. The only likely refractory phase with significant reactivity toward mercury might be the remnants of high molecular weight aromatic organic compounds. In sediments where the total mercury concentration exceeds 1000 $ng \cdot g^{-1}$, the amount of "missing" mercury, while low as a percentage of the total. becomes quite large in absolute terms. Under these conditions, it becomes questionable whether such a small quantity of refractory organic matter, already subjected to highly oxidative and acidic conditions, could retain extremely high concentrations of mercury by weight.

6 DISCUSSION

6.1 Diagenetic Parameters

6.1.1 Diagenetic Environments in this Study

CL-1B (Laurentian Trough Station)

The organic carbon, S_{AVS}, and Fe_{HCl} profiles from the Laurentian Trough site **(Figures 5.1 and 5.2)** are typical of a steady state sedimentary environment, with little perturbation of sediments by slumping or landslide events. The redox boundary occurs near the sediment/water interface (~2 cm), which indicates the rapid consumption of O_2 from microbial attack of organic matter. The presence of small Fe_{HCl} and Mn_{HCl} peaks near the sediment/water interface indicates that oxidation of organic matter driving the cycling of Fe and Mn across the redox boundary (and the consequent accumulation of Fe and Mn oxides near the redoxcline) is much less than in the sediments of the Laurentian Trough than in the Saguenay Fjord (SAG-6B and SAG-30B - see below). The sedimentary redox chemistry is largely determined by the quantity and reactivity of organic matter, as well as by the rate of burial (i.e., sedimentation rate). Although the organic matter in the Laurentian Trough has a larger marine component and is therefore more labile, the quantity of organic matter reaching the sediment/water interface is greater in the Saguenay Fjord. Additionally, the slower sedimentation rate in the Laurentian Trough (0.1 cm a^{-1}; Silverberg *et al.*, 1986) compared to the Saguenay Fjord (between 0.3 and 0.5 cm a^{-1}; Smith and Walton, 1980) permits substantially greater degradation of organic matter in the sediments of the Laurentian Trough prior to burial. The quantity and reactivity of organic matter that remains available to drive suboxic and anoxic microbiotic metabolism is therefore less than at sites with more rapid burial. High porewater concentrations of SO_4^{2-} and lower rates of sulphate reduction in sediments from the Laurentian Trough relative to the Saguenay Fjord confirm that anaerobic processes at

CL-1B are less active and remineralize a smaller fraction of the organic matter (Edenborn *et al.*, 1987; Gagnon *et al.*, 1996a, 1995).

Increasing and elevated concentrations of pyrite (both S_{CRS} and Fe_{HNO3}) to a depth of 10 cm suggest a change in the sedimentary regime over the last century. Pyrite is a stable end-product of anaerobic diagenetic mineralization and accumulates in sediments. A similar distribution of pyrite in the top 10 cm of the Trough sediments was also reported by Gagnon *et al.* (1995) in samples taken from the same station in 1991. An increase in either the rate of deposition or the reactivity of sedimentary organic matter could explain these observations.

SAG-6B (Landward Slope Inner Basin Station)

The diagenetic behaviour of the sediments at SAG-6B is complicated by the presence of allochthonous, organic-poor clay layers within the profile. Near the sediment/water interface, profiles of Fe_{HCl} and Mn_{HCl} attest to the presence of a shallow, intense redoxcline, which is the result of high input and rapid burial of terrestrial organic matter at the basin slope. Large, sharp peaks of HCl-soluble iron and manganese at ~1-2 cm reflect the active remobilization of these metals following reductive dissolution upon burial and subsequent oxidative re-precipitation in the O_2 penetration zone. The presence of S_{AVS} in the top 0.5 cm of sediment indicates that the sequence of diagenetic oxidation reactions is severely compressed in these sediments, and sulphate reduction takes place just millimeters below the sediment/water interface. The presence of Fe and Mn (hydr)oxides below the depth of S_{AVS} accumulation may be the result of O_2 transport by bioturbation and bioirrigation (Gagnon *et al.*, 1996a), but more likely reflects, on the basis of the porewater chemistry (i.e., pH, dissolved Fe^{2+} and sulphide) the stability of iron (hydr)oxide minerals (Canfield *et al.*, 1992; Postma and Jakobsen, 1996). Similar S_{CRS}

distribution and concentrations in surface sediments (i.e., post-landslide) were reported by Gagnon *et al.* (1995) at a nearby site (SAG-5B 1992).

As a result of slumping and landslide events, organic rich muds were buried under a thick layer of allochthonous clays. Because the clay layers are organic-poor, sulphate reduction rates within them are extremely low (Edenborn *et al.*, 1987; Mucci and Edenborn, 1992). Beneath them, however, the nearly instantaneous burial of fresh organic matter at the former sediment/water interface promoted high sulphate reduction rates and the accumulation of large quantities of acid-volatile sulphide. Following burial and the re-establishment of the surface redox boundary, the clay layers served as a source of dissolved Fe^{2+} to both the overlying and underlying sulphate-reducing muds. Consequently, a zone of AVS enrichment occurs *above* each clay layer as well as beneath it. Because of the alternating layers of mud and clay, the profiles of S_{AVS} and C_{org} correlate well beneath the first clay layer (**Figure 5.1**). High AVS concentrations extend into the lower boundaries of the clay layers following the precipitation of HS^- (which diffused from underlying muds) with Fe^{2+} (released to porewaters within the clay layer). The elevated S_{CRS} and inorganic carbon concentrations which also distinguish the clay layers are partly of detrital origin and are found in similar concentrations in the original post-Wisconsinian clays of St. Jean-Vianney (Mucci and Edenborn, 1992; Gagnon *et al.*, 1995). The HCl-soluble iron and manganese profiles are apparently affected little by the presence of the clay layers. Mucci and Edenborn (1992) reported significant remobilization of reducible iron to the oxic layer, but the lack of specificity afforded by the use of an HCl extractant has somewhat obscured the vertical distribution of iron and manganese (hydr)oxides. A Mn_{HCl} peak is visible in the lower clay layer, which corresponds to sharp carbonate and S_{AVS} maxima, which suggests the incorporation of manganese into carbonate (Mucci, 1988) or monosulphide phases (Arakaki and Morse, 1993; Morse and Arakaki, 1993).

SAG-30B (Inner Basin Bottom Station)

Sediments in the basin bottom, in contrast to those at much shallower SAG-6B, are scarcely affected by landslide and slumping events. The organic carbon profile shows no significant changes which would reveal sudden, massive deposition of allochthonous organic-poor clays (**Figure 5.1**). Pyritic iron and S_{AVS} distributions also appear featureless, with the exception of a discontinuity at ~14-15 cm (**Figures 5.2 and 5.3**). The simultaneous pyrite spike and marked decrease in AVS coincident with the maximum Hg_{tot} values may be geochemical markers of the 1971 St. Jean-Vianney landslide and the period of maximum Hg discharge from the Arvida chlor-alkali plant. The effects of the landslide here are obviously more difficult to identify, both visually and chemically, compared to basin slope sediments. The Saint Jean-Vianney landslide deposit is much thinner at SAG-30B because this site is about 20 kilometers downstream and significantly deeper (>100 m) than SAG-6B.

The sharp peak of HCl-extractable Fe and Mn at 1.5 cm depth indicates a strong redoxcline and the significant remobilization of reducible metals. The more gradual accumulation of iron monosulphides (~5 cm) reflects the lower catabolic rates at this station. Despite comparable C_{org} concentrations, the increased settling time through the deeper water column above the basin and a significantly slower sedimentation rate (Edenborn *et al.*, 1987; Gagnon *et al.*, 1995) promotes the aerobic degradation of the most labile organic matter prior to burial. The near constant concentration of S_{AVS} below 16 cm is consistent with an observed decrease in SRR values below ~17 cm (Edenborn *et al.*, 1987). The nearly vertical pyrite profiles (both S_{CRS} and Fe_{HNO3}), within both oxic and anoxic sediments could result from the steady input of detrital pyrite. Alternatively, pyrite may also have formed authigenically in anoxic sediments or in oxic strata as a result of bioturbation or sulphate reduction in microenvironments. It is interesting to note that S_{AVS} concentrations do not *decrease* with depth, which indicates that the conversion rate of monosulphides to pyrite is atypically low at this site (Ouellet, 1978; Gagnon *et al.*, 1995).

HCl-extractable iron concentrations are higher at SAG-30B than at either the CL-1B or SAG-6B sampling stations. Although the flux of particulate iron from flocculating particulates at the halocline may be lower than at SAG-6B (Sundby and Loring, 1978), less reducing conditions in the surface sediments permit greater preservation of authigenic Fe oxides. The same reasoning applies to Mn_{HCl} which usually diffuses further into oxic sediments before being oxidized and therefore can more easily escape to the overlying waters if the O_2 penetration zone is very thin. The high concentrations of particulate Mn in bottom waters of the Saguenay Fjord observed by Sundby and Loring (1978) may originate from the diffusion of Mn(II) out of the sediment and its oxidation in the water column. In addition, a mid-column (~120 m) dissolved Mn maximum was observed (A. Mucci, pers. comm.) which could be attributed to the dispersion of dissolved Mn along an isopycnal which intersects reducing sediments.

6.1.2 Diagenetic Behaviour of Sulphur

Sediments of the Saguenay Fjord and the adjoining St. Lawrence Estuary exhibit an enrichment of monosulphides relative to pyrite that is uncharacteristic of most estuarine sediments (Gagnon *et al.*, 1995). The ratio of S_{AVS}:S_{CRS} within sediments varies between 0.14 and 5.82 in the Saguenay Fjord and Laurentian Trough but generally exceeds unity (**Appendix 2**). In general, S_{AVS}:S_{CRS} ratios in coastal marine sediments are typically much less than 1, reflecting the efficient conversion of iron monosulphides to pyrite. In addition to the Saguenay/St. Lawrence system, other notable exceptions include the anoxic basins of Skan Bay, Denmark where ratios reach 5.1 (Morse and Cornwell, 1987), and, to a lesser degree, those of Orca Basin (Gulf of Mexico) and Kau Bay, Indonesia where maximum values reach 1.9 and 1.6, respectively (Morse and Cornwell, 1987; Middelburg, 1991).

Examination of freeze-dried Saguenay Fjord sediments mounted on a polished thin section using a JEOL 8900™ Electron Microprobe seem to confirm the hypothesis of Mucci and Edenborn (1992), who suggested that a significant fraction of the pyrite in Saguenay Fjord sediments may be of detrital origin. Pyrite grains were typically small (1-4 μm diameter) and mostly appeared as fragments. Only a small fraction of pyrite grains examined were framboidal, although observations of the smaller particles was often difficult or beyond instrumental resolution. Authigenic (framboidal) pyrite was most easily distinguished from detrital pyrite by its high As (up to 1000 ppm) content. Given that a significant fraction of sedimentary pyrite is detrital, rather than authigenic, actual S_{AVS}:S_{CRS} are underestimated.

As defined in **Section 2.4.2.1**, DOP is a measure of the fraction of "reactive" iron which has combined with sulphide to form pyrite. A high DOP value indicates that the depletion of available reactive iron limits the formation of pyrite. In contrast, a low DOP suggests that other factors limit pyrite production, such as the quantity and quality of organic matter, or the availability of sulphide, polysulphides, and elemental sulphur. The latter two species are thought to be required for the conversion of AVS to pyrite in marine sediments (Berner, 1970; Rickard, 1975).

DOP is much less useful to describe the geochemistry of iron and sulphur in sediments that exhibit poor conversion of AVS to pyrite. Degree of sulphidization (DOS) is a term similar to DOP but is used for sediments that show significant preservation of

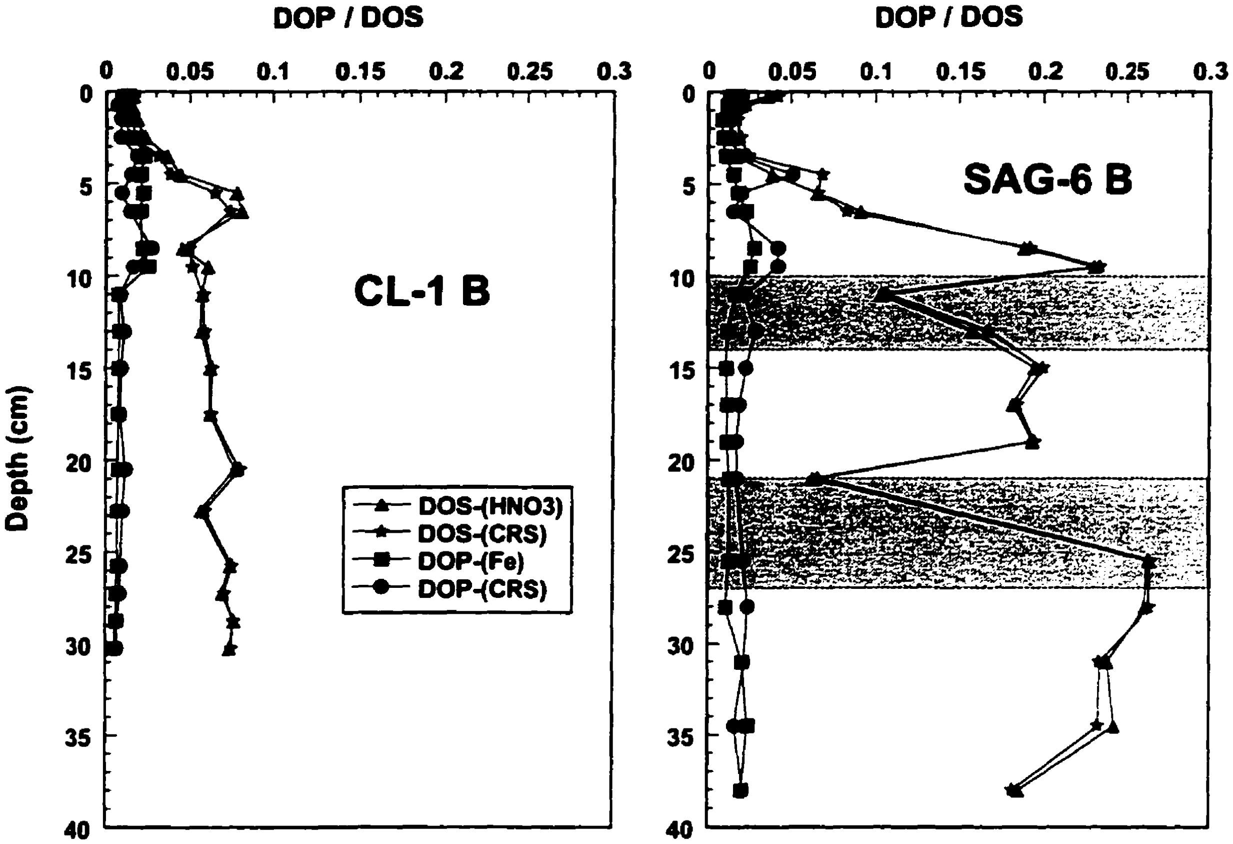

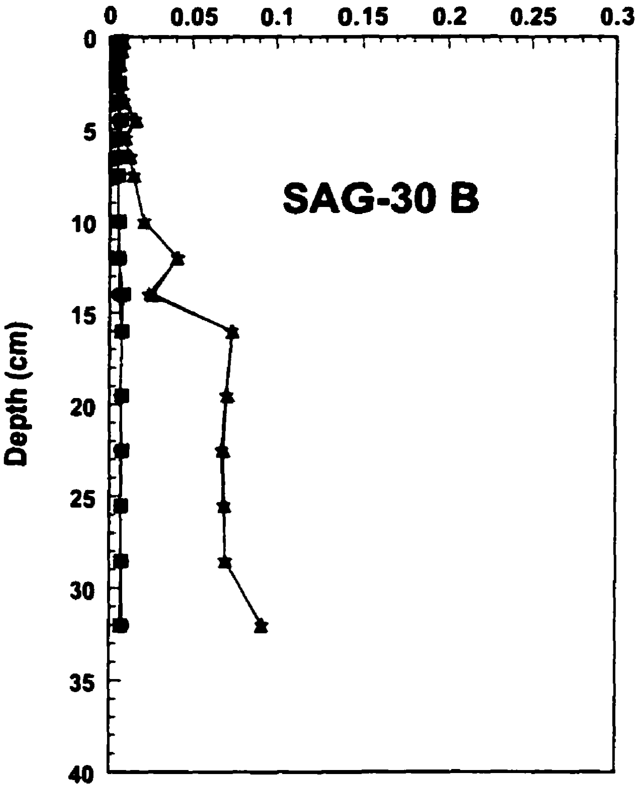

Figure 6.1: DOS and DOP profiles of Saguenay Fjord & Laurentian Trough sediments.

iron monosulphides. First introduced by Boesen and Postma (1988), DOS is defined in **Equation 6.1**.

$$DOS = \frac{Fe_{AVS} + Fe_{pyrite}}{Fe_{HCl} + Fe_{pyrite}} \qquad 6.1$$

Both DOP and DOS values were calculated, and profiles for each station appear in **Figure 6.1**. DOP values for the Saguenay Fjord and Laurentian Trough sediments are uniformly low. As a result of the high reactive iron and low pyrite concentrations, DOP values remain below 0.05 in all samples and never exceed 0.01 in SAG-30B. In the bottom of the inner basin and Laurentian Trough sediments, however, DOS values reach 0.10 and as high as 0.30 in basin slope sediments. Because the contribution of pyrite to the sulphide pool is so small, DOS values principally reflect the influence of AVS precipitation.

Clearly, diagenetic conditions in the Saguenay Fjord and nearby Laurentian Trough sediments favour the preservation of monosulphides over the formation of pyrite. According to Gagnon *et al.* (1995), the formation of pyrite in these sediments is limited by the dearth of species bearing S(0) (i.e., elemental sulphur, polysulphides). The abundance of reactive iron phases in Saguenay Fjord sediments results in the rapid precipitation of iron monosulphides and near depletion of dissolved HS^- (Gagnon *et al.* 1996a). The conversion of monosulphides to pyrite in marine and most estuarine sediments requires partially oxidized sulphur (POS) compounds, which form as a result of the oxidation of S(-II) through:

- redoxcline migration,
- benthic mixing and bio-irrigation, or
- the migration of dissolved sulphide into suboxic porewaters

(Berner, 1970; Pyzik and Sommer 1981; Luther, 1991). In these sediments, the rapid onset of anoxia and near-complete precipitation of dissolved sulphide as iron monosulphides precludes the production of POS compounds, which in turn retards conversion of the monosulphides to pyrite.

Geographic variations in S_{AVS}:S_{CRS} ratio within the Saguenay Fjord and Laurentian Trough sediments have been discussed in greater detail by Gagnon *et al.* (1995). They proposed that the lower maximum S_{AVS}:S_{CRS} ratios in the Gulf of St. Lawrence are probably attributable to differences in sedimentation rates, the reactivity of organic matter settling at the sediment/water interface, and the intensity of bioirrigation (Gagnon *et al.*, 1996a, 1995). The formation of pyrite is more favourable in the Gulf of St. Lawrence, where burial rates are slower, organic matter is more labile, and both bioturbation and bioirrigation are more intense (Belzile, 1986). Slower burial of AVS leads to longer residence time near the redoxcline, and greater bioturbation increases the flux of oxidizers (O_2, Fe/Mn (hydr)oxides) to anoxic sediments. As a result, the sediments of the Gulf of St. Lawrence are a more conducive environment for the formation of intermediate sulphur compounds and consequently foster the conversion of AVS to pyrite (Howarth, 1984; Luther, 1987; Aller and Rude, 1988; Luther *et al.*, 1992).

6.2 Distribution of Mercury

6.2.1 Operationally Defined Hg Fractions and Sediment Solids

The goal of the sequential extraction protocol was to separate mercury associated with different sedimentary solids. The use of non-specific extraction reagents in a natural system, however, requires that each fraction be defined operationally. Cautious evaluation of the results is needed to resolve the actual relationships of extracted trace metals to the targeted solids before the factors controlling their distribution can be discussed.

NaOH Extractable Mercury

Hg_{NaOH} represents the largest fraction of mercury at each station (**Figure 5.5**) and consists of mercury associated with organic matter. Originally, following effluent release, mercury was scavenged from the water column by, and transported to the sediment/water interface by particulate organic matter, which thus served as the carrier phase and primary associated solid for Hg (Loring, 1975). Consequently Hg_{NaOH} reflects the temporal variations in Hg effluent from the Arvida chlor-alkali plant (Loring, 1975; Gobeil and Cossa, 1993). Mercury is slowly released as organic matter is degraded, so that much of the transfer of Hg to other sedimentary phases appears to occur *at the expense* of $Hg_{NaOH.}$ Hg concentrations in each phase, however, remain largely dependent on the temporal variations in total mercury input (**Figure 6.2a-d**). As a result, positive correlations between C_{org} (**Figure 5.1**) and the Hg_{NaOH}:Hg_{sum} ratio (**Figure 6.2a**) are not easily established.

HCl Extractable Mercury

In general, HCl-extractable mercury (**Figure 5.5**) constitutes only a small portion of the total mercury. At each station, elevated Hg_{HCl}:Hg_{sum} ratios occur near the sediment/water interface. This distribution is consistent with the adsorption or co-precipitation of mercury with Fe and Mn (hydr)oxides formed authigenically or precipitated within the water column, which accumulate at or just below the sediment/water interface. In deeper sediments, peaks in the Hg_{HCl}:Hg_{sum} ratio are few and weak. Our data are in agreement with the observations of Gobeil and Cossa (1993) concerning the vertical distribution of Hg_{HCl}, but, considering the overall low Hg_{HCl}:Hg_{sum} ratios, do not indicate that Fe and Mn (hydr)oxides serve as an overall major sink within the sediments of the Saguenay Fjord and Gulf of St. Lawrence, as they propose (see **Section 6.3.3**).

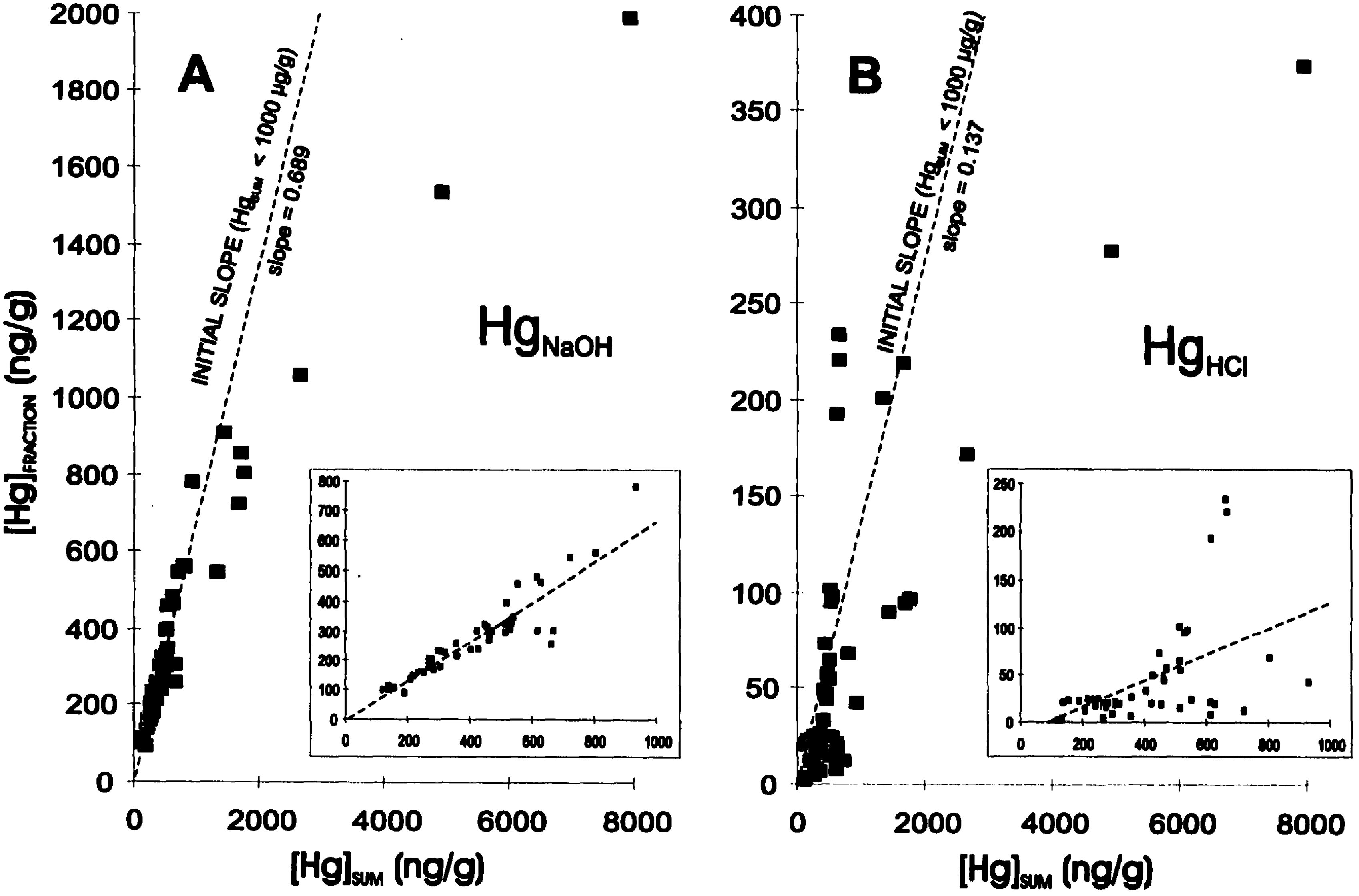

Figure 6.2 [$Hg_{FRACTION}$] as a function of [Hg_{SUM}]; exploded views appear as shaded boxes. Dashed line represents the slope derived below [Hg_{SUM}] = 1000 ng/g. A = Hg_{NaOH}; B = Hg_{HCl}; C = $Hg_{HF/HCl}$; D = Hg_{HNO3}.

HF/HCl Extractable Mercury

Mercury extracted in the HF/HCl step is probably not associated directly with clays, but with a variety of refractory organic and inorganic substrates which may include coatings on clays and other solids:

- clay-metal-organic (CMO) complexes,
- naturally occurring refractory crystalline Fe and Mn oxides
- AVS oxidation products (refractory iron oxides and elemental sulphur)
- pyrite.

Because little mercury is associated with the bulk pyrite extraction (HNO_3 step), the contribution of pyritic mercury to $Hg_{HF/HCl}$ is probably not a significant source of Hg in this fraction. Alternatively, the potential importance of CMO complexes is difficult to evaluate. Precise DOC analyses on most HF/HCl samples were not possible because of instrumental incompatibilities with the HF (10N) matrix. In any case, there would be no way to quantify the relative contribution of CMO complexes to HF-extracted organic matter.

Marked similarities were found between the proportion of total mercury extracted by HF/HCl (**Figures 5.5**) from subsurface sediments and AVS distribution (**Figure 5.1**), although overall numerical correlations are not useful. The relationship between S_{AVS} and $Hg_{HF/HCl}$:Hg_{sum} seems obvious in the sediments at SAG-6B, although C_{org} and S_{AVS} distributions at this site are similar. Clearer evidence is found at station SAG-30B, where the C_{org} and S_{AVS} distributions are poorly correlated and significant extraction of Hg by HF/HCl occurs *only* from sediments rich in monosulphides. Trends in $Hg_{HF/HCl}$:Hg_{sum} and S_{AVS} distribution similar to those in the Saguenay Fjord sediments are also observed in the Laurentian Channel (CL-1B), but here the variations in the $Hg_{HF/HCl}$:Hg_{sum} ratio are sufficiently small that definite conclusions are not justified.

There arises the question: how could Hg incorporated into AVS solids be extracted in the HF/HCl step of the protocol, rather than the 1N HCl step? In the presence of O_2,

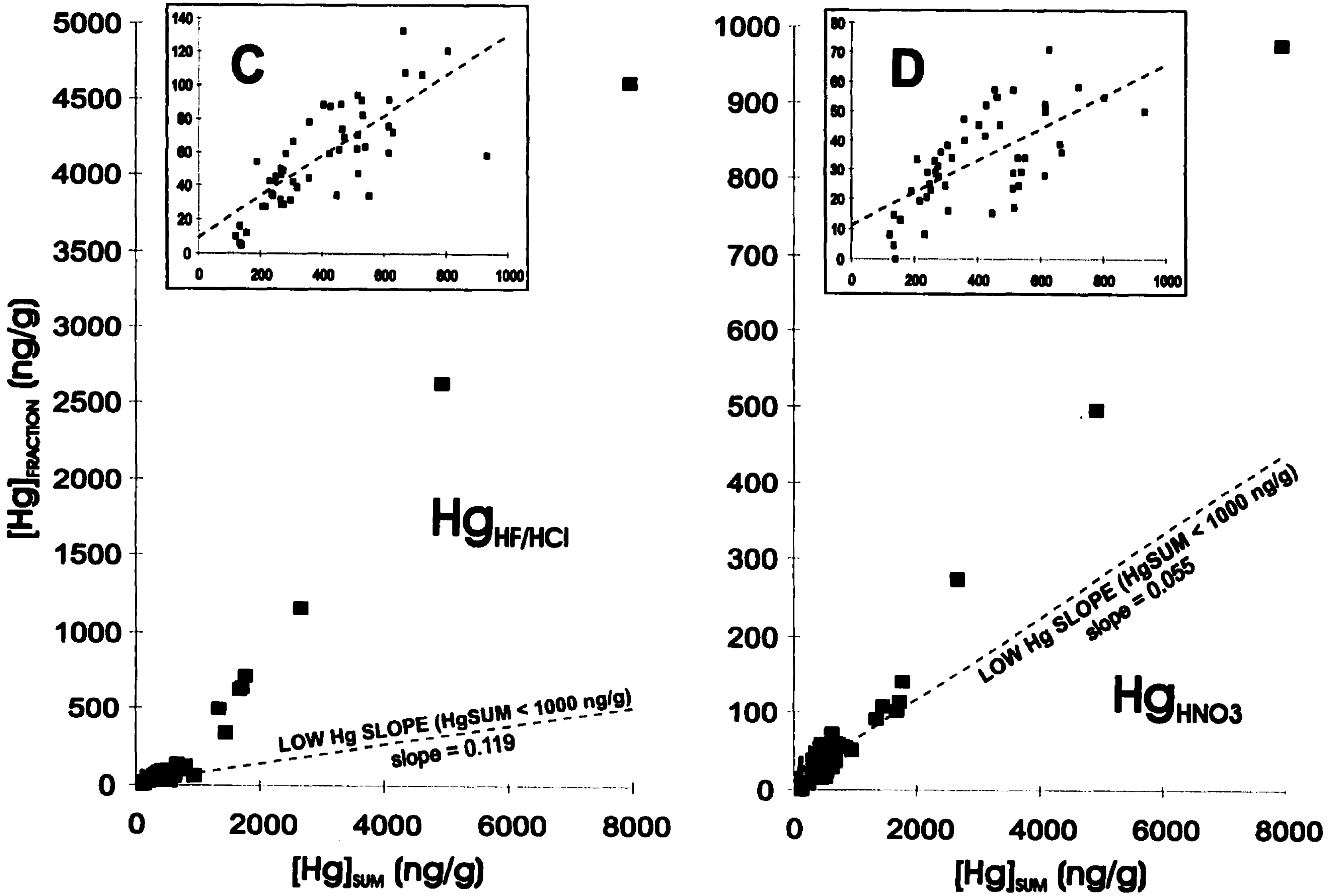

Figure 6.2 $[Hg_{FRACTION}]$ as a function of $[Hg_{SUM}]$; exploded views appear as shaded boxes. Dashed line represents the slope derived below $[Hg_{SUM}]$ = 1000 ng/g. A = Hg_{NaOH}; B = Hg_{HCl}; C = $Hg_{HF/HCl}$; D = Hg_{HNO3}.

monosulphides oxidize rapidly to solids (refractory iron oxides and elemental sulphur) which are resistant to dilute HCl (Raiswell *et al.*, 1994). The oxidation of AVS may have resulted in the transfer of Hg by co-precipitation with the oxidation products *in vitro*. It seems most likely that, as a result of the oxidation of AVS solids during freeze-drying, mercury was adsorbed or co-precipitated with refractory iron oxide and S(0) solids, which were then solubilized in the aggressive HF/HCl treatment.

HNO_3 Extractable Mercury

Profiles of the Hg_{HNO3}:Hg_{sum} ratio (**Figure 5.5**) appear relatively featureless and exhibit a slow increase with depth. This is consistent with the gradual accumulation of mercury by adsorption and co-precipitation over time to pyrite. The only other likely solid extracted by this reagent might be highly refractory organic matter such as lignins. This seems refuted, however, by preliminary results from samples taken from the Saguenay River. In these samples, both mercury and lignin concentrations in the sediments are much higher, but no significant correlation between mercury and lignins is in evidence (Louchouarn, 1996).

6.2.2 Factors Controlling Hg Distribution

In general, the partitioning of trace metals among various solid phase components may be limited by one or more factors:

- total trace metal concentration
- concentration of binding sites, both on solid surfaces and dissolved molecules
- comparative strengths of metal-ligand bonds
- competition for binding sites by other metals
- kinetics of metal-ligand bond formation

In the Saguenay Fjord, the predominant factor controlling partitioning of mercury among the solid components of sediments is the concentration of total Hg. Vertical distribution of Hg_{tot} principally reflects the anthropogenic input over time (Gobeil and Cossa, 1993). Consequently, diagenetic variables and mercury distribution are partially decoupled. Statistical correlations between geochemical parameters and either the absolute or relative concentrations of mercury are therefore difficult to extract, and the importance of the other factors is less easily discerned. Although the relative partitioning of mercury to a given phase may be *limited* by the availability of a sedimentary solid, Hg distribution seems otherwise fairly independent of substrate distribution. Generally, both relative and absolute mercury partitioning are governed primarily by the availability of the metal itself.

6.2.2a Distribution of total mercury

A plot of the concentration of each mercury fraction ($Hg_{NaOH,\ HCl,\ HF\ HCl,\ HNO_3}$) as a function of total extractable mercury (Hg_{sum}) reveals surprisingly linear relationships (**Figures 6.2a-d**). The resulting slopes (seen as dashed lines) represent the partition coefficients of mercury for each of the reactive pools, and are defined as the relative contributions of each phase to total extractable mercury (**Table 6.1**).

The relationships between $Hg_{fraction}$ and Hg_{sum} are generally linear at low (<1000 $ng{\cdot}g^{-1}$) and high (>1000 $ng{\cdot}g^{-1}$) concentrations of total extractable mercury, but characteristic non-linear features are apparent for each fraction. Specifically, the slopes of the curves at low Hg_{sum} are markedly different from those seen at elevated values. The curves for the NaOH extractable fraction decrease with increasing Hg_{sum} concentration, whereas the reverse is true for the HF/HCl and HNO_3 extractable pools of mercury. The HCl fraction is bifurcated and displays both characteristics. At low Hg concentration, least squares linear regressions for each fraction produce intercepts which pass through the origin within error tolerances (**Table 6.1; Figure 6.2, shaded box**).

Table 6.1 Least squares linear regression coefficients data of $Hg_{FRACTION}$ plotted against Hg_{SUM}; slopes describe partition coefficients of mercury among the extraction pools (Σ=1.000).

	Mercury Extraction Pool			
Low Hg_{SUM} (< 1000 ng·g^{-1} dry wgt)	Hg_{NaOH}	Hg_{HCl}	$Hg_{HF/HCl}$	Hg_{HNO_3}
Slope ($Hg_{FRACTION}$ / Hg_{SUM})	.69 ± 04	.14 ± .03	.12 ± .01	.065 ± .009
Intercept (pg·g^{-1} $Hg_{fraction}$)	-8 ± 54	-12 ± 44	+9 ± 19	11 ± 12
Linear Correlation Coefficient (r)	.856	.261	.579	.425
High Hg_{SUM} (> 1000 ng·g^{-1} dry wgt)	Hg_{NaOH}	Hg_{HCl}	$Hg_{HF/HCl}$	Hg_{HNO_3}
Slope ($Hg_{FRACTION}$ / Hg_{SUM})	.20 ± .02	.037 ± .009	.63 ± .01	.132 ± .005
Intercept (pg·g^{-1} $Hg_{fraction}$)	(intercepts deviate from origin due to non-linearity)			
Linear Correlation Coefficient (r)	.947	.747	.997	.992
All Points	Hg_{NaOH}	Hg_{HCl}	$Hg_{HF/HCl}$	Hg_{HNO_3}
Slope ($Hg_{FRACTION}$ / Hg_{SUM})	.26 ± .01	.051 ± .005	.57 ± 01	.114 ± .006

The non-linearities of the $Hg_{fraction}$:Hg_{sum} relationships suggest that, at greater Hg_{sum} concentrations, mercury is increasingly and disproportionately taken up by AVS and pyrite and lost by organic matter. The Hg_{HCl}:Hg_{sum} ratio, a special case, suggests both enrichment and depletion (positive and negative curves are bifurcated). The Hg_{HCl}:Hg_{sum} plot shows enrichment at SAG-30B, in samples where Fe_{HCl} concentrations are high, AVS is low, and Hg_{HCl} comprises a significant fraction of Hg_{sum}. The depletion (negative curvature) in Hg_{HCl} occurs in the deep, anoxic, highly contaminated layer in SAG-6B. Here, AVS predominates as the carrier phase for mercury, and the Fe_{HCl} solids are subject to gradual reductive dissolution and most likely lose mercury to other phases. These curvatures may reflect the redistribution of mercury to sedimentary solids on the basis of the availability of sites which can incorporate mercury. The number of accessible sites is dependent on the affinity of the solid as well as the concentration of mercury in that phase. It seems likely that the potential binding sites on organic solids (and possibly

Fe/Mn (hydr)oxides) which more readily adsorb mercury become saturated at elevated concentrations of Hg. Other solids would consequently become comparatively more competitive against the remaining lower-affinity sites which more weakly bind mercury. Additionally, mercury is more effectively taken up by co-precipitation rather than by surface adsorption, such that precipitating phases are more competitive sinks for the metal.

6.2.2b Distribution of sedimentary solids

The concentration and distribution of the solids which adsorb or co-precipitate mercury do not generally control the partitioning of mercury. Normalization of each plot of $Hg_{fraction}$ versus total extractable mercury for the distribution of C_{org}, S_{AVS}, and S_{CRS} generally increased scatter, and correction for substrate distribution did not linearize the partitioning curves. Although normalization for the distribution of C_{org} and S_{CRS} increased scatter somewhat, correction for the distribution of S_{AVS} reduced the correlation coefficient (r^2) to less than 0.10. A notable exception was the effect of Fe_{HCl} on the plot of Hg_{HCl} (**Figure 6.3**). Here, the partial bifurcation described previously was partly corrected, significantly *increasing* the correlation coefficient. The uncorrectable scatter and curvature of the $Hg_{fraction}$:Hg_{sum} plots confirms the primary dependence of mercury distribution on the solid phase affinity and concentration of Hg_{sum}.

6.2.2c Molar Affinities of Solid Phases

Although the majority of the extractable mercury in the Saguenay Fjord resides with organic matter, this occurs partly because the concentration of C_{org} is relatively large. When comparing the various solid-phase substrates on a molar basis, sulphides, which are present in micromolar quantities, have somewhat greater affinities for Hg than organic matter (**Table 6.2**). This suggests that in more intensely sulphidic systems, considerably greater proportions of Hg may be incorporated and sequestered by AVS and FeS_2,

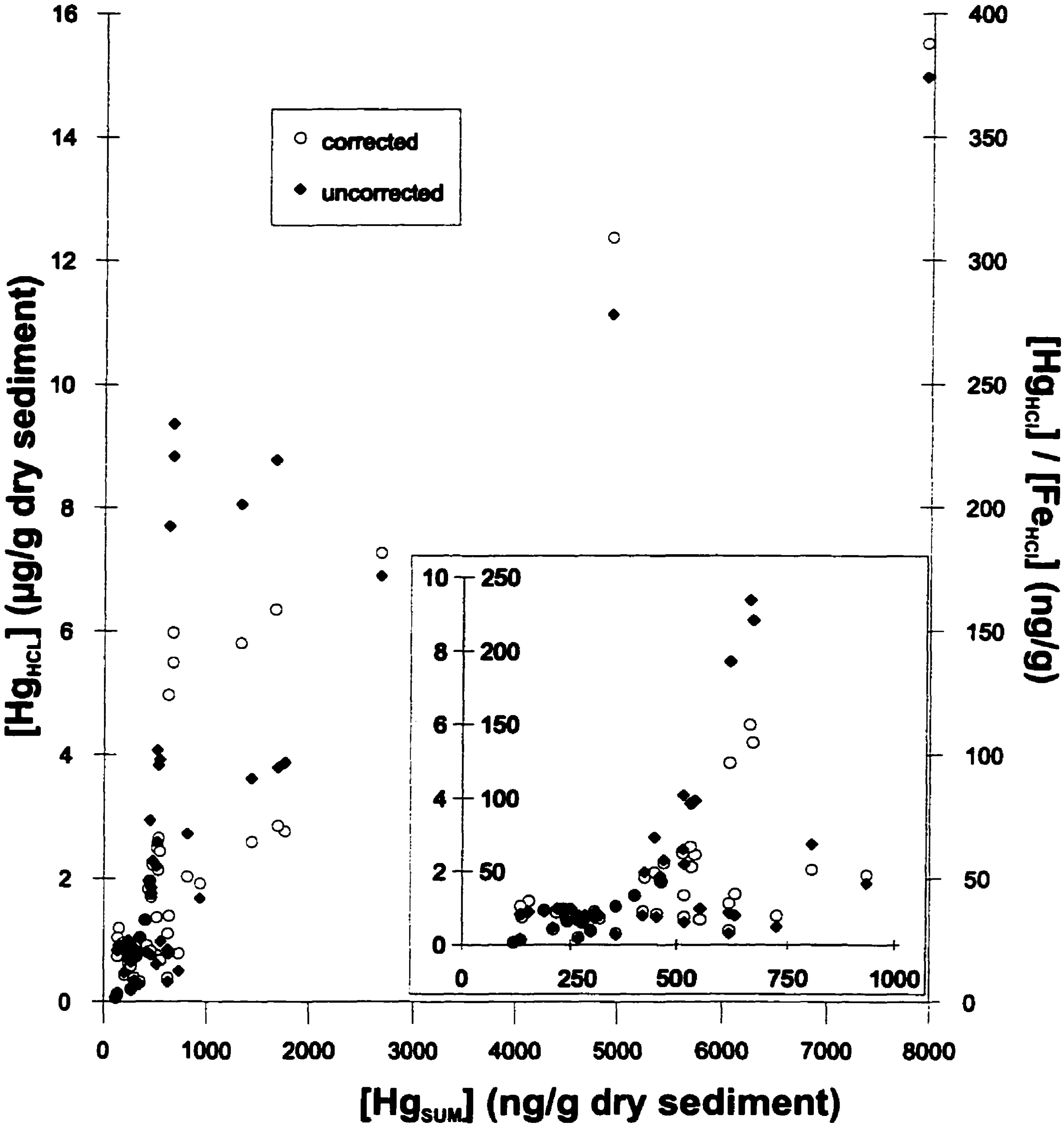

Figure 6.3 Comparison of [Hg$_{HCl}$] distribution as a function of [Hg$_{SUM}$] (see Figure 6.2b). with and without normalizing for Fe$_{HCl}$ distribution; shaded box depicts an exploded view.

Table 6.2 **Average molar affinities for mercury of targeted solids**

Mercury (μmol) per mole targeted solid substrate

	Hg_{NaOH}/C_{org}	Hg_{HCl}/Fe_{HCl}	$Hg_{HF/HCl}/S_{AVS}$	Hg_{HNO3}/S_{CRS}*
Average	1.0	0.6	66.3	54.4
±	0.7	0.8	86.6	73.0

*S_{CRS} produces the least scattered coefficient for pyrite; Fe_{pyr} gives 65 (± 135) μmol Hg_{HNO3} per mole pyrite)

conditional to the release of mercury to porewaters following the degradation of organic matter. In contrast, although present in comparatively high concentrations, HCl-soluble Fe and Mn solids generally incorporate only a small fraction of extractable mercury. Iron and manganese (hydr)oxides have the lowest affinity of any solid sedimentary substrate considered in this study.

6.3 Diagenetic Remobilization of Mercury

Remobilization of trace metals in sediments requires the release of the metal from the carrier phase, physicochemical conditions conducive to solubilization of the metal, and a mechanism to transport the dissolved metal within the sediments or to overlying waters.

Metals are scavenged in the water column and transported to the sediment/water interface by suspended particulates which are predominantly composed of biogenic organic matter (from primary production), but may also include flocculating organic and Fe/Mn (hydr)oxides colloids, clays, and, in euxinic waters, iron sulphides. Most of these substrates are sensitive to changes in Eh, pH, ionic strength, or to microbial degradation, and are solubilized during early diagenesis, releasing their associated metals.

Metals released from their transport medium will remain as free hydrolyzed metal, react with available ligands to form soluble complexes, absorb to existing solids, or precipitate as (or co-precipitate with) a solid phase. The remobilization of metals will therefore be dependent upon partitioning between dissolved organic and inorganic species, colloidal particulate matter, and mineralized solids — a particularly dynamic system in sediments undergoing early diagenesis. Metals may be recycled several times between the dissolved and solid phases following burial.

Metals and other species which accumulate in porewaters can diffuse along concentration gradients and thus be transported within a sediment. Compaction following burial results in the advection of porewaters toward the sediment/water interface and contributes to varying degrees to the transport of dissolved substances. Similarly, bioirrigation by benthic fauna increases advection within sediments.

Gagnon *et al.* (1997) observed small concentration gradients of dissolved Hg within the sediments of the Saguenay Fjord and St. Lawrence Trough and estimated that mercury transport through the sediment horizons to overlying waters is slow. The weak concentration gradients reflect the low concentrations of mercury in porewaters, despite high levels of mercury in the solid phases of some strata of the sediments. The large $Hg_{SOLID}:Hg_{DISSOLVED}$ ratio arises from the rapid uptake of mercury by solid components of the sediment via adsorption and co-precipitation compounded by the slow release of mercury as the organic matter which served as a vector to the sediments gradually decays. Additionally, Gagnon *et al.* (1997) reported the decoupling of solid-phase and aqueous mercury distributions in the Saguenay Fjord, and proposed that the solubility of mercury in these sediment porewaters is primarily dependent on the concentration of dissolved ligands.

In the Saguenay / St. Lawrence system, the transport of dissolved Hg complexes is primarily controlled by the rate of diffusion (LeClerc *et al.*, 1986) and greatly accelerated by bioturbation in surficial sediments (Gagnon *et al.*, 1997). Although some dissolved mercury is released to overlying waters, most is rapidly re-adsorbed and co-precipitated by settling particulate matter. In the Saguenay Fjord and Laurentian Channel, results reported by Mucci and Edenborn (1992) suggest the potential importance of monosulphides in sequestering mercury to the solid phase under anoxic conditions, while studies by Gobeil and Cossa (1993) and Gagnon *et al.* (1996b, 1997) suggest that oxic sediments serve as effective sinks for mercury. The diagenetic remobilization of mercury in this system is depicted in **Figure 6.4**.

6.3.1 Gulf of St. Lawrence - Laurentian Trough

Within the sediments of the Laurentian Trough (CL-1B), the majority of the mercury is retained by organic matter. Input of mercury to these sediments has been relatively low and is primarily of atmospheric origin (Gobeil and Cossa, 1993). Because the input of organic matter and sedimentation rate are comparatively low (Silverberg *et al.*, 1986), organic matter is rapidly remineralized in the water column or at the sediment-water interface. As a result, the remobilization of Fe and Mn (hydr)oxide solids is markedly less than at other sites studied, and iron monosulphides accumulate very gradually with depth. At this station, Hg remains predominantly associated with particulate organic matter. Mercury that is released is either taken up by inorganic solids, or readsorbed by remaining organic matter.

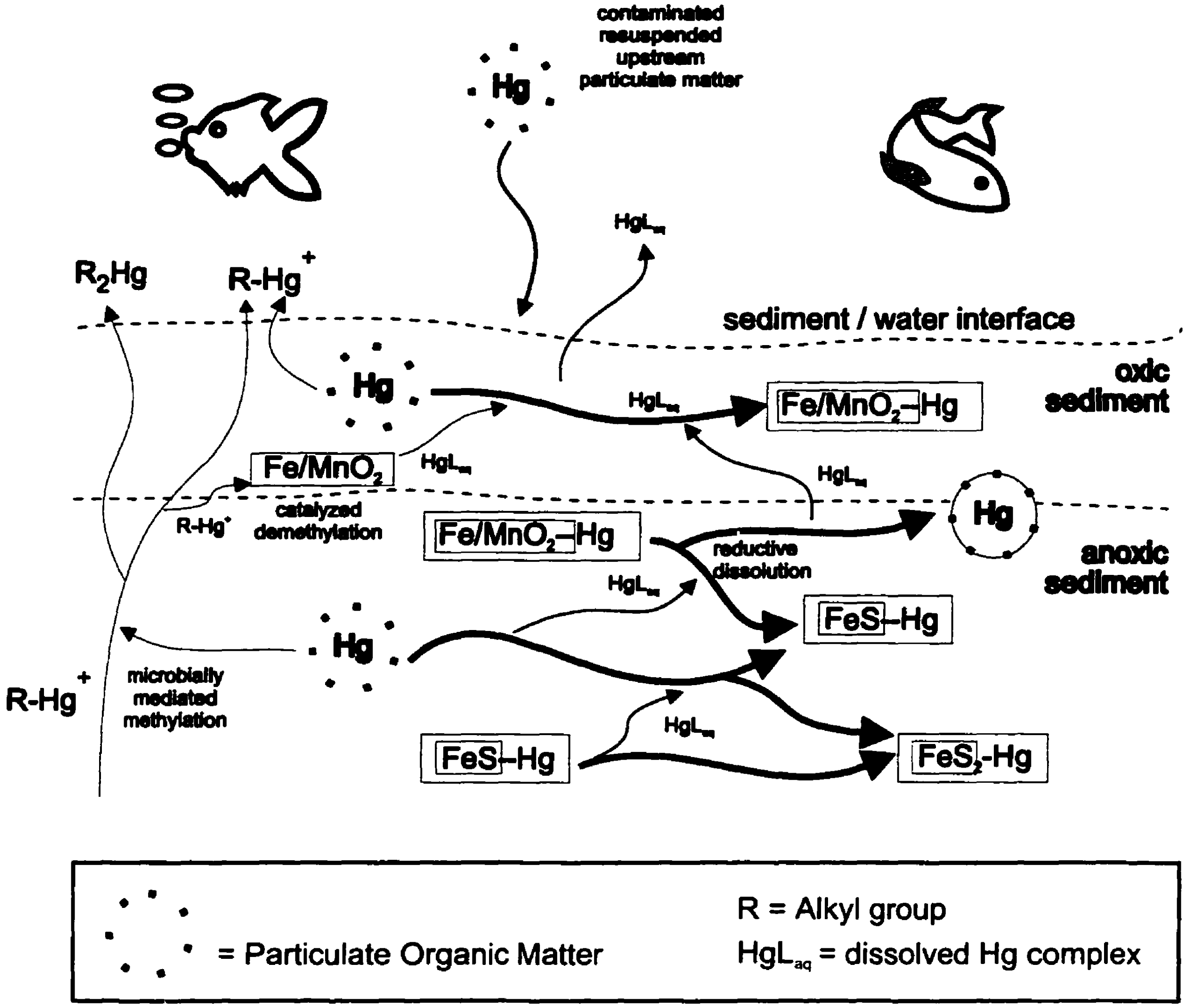

Figure 6.4 **Diagenetic redistribution and remobilization of mercury within Saguenay Fjord sediments.** Following scavenging by particulate organic matter in the water column, Hg was transported to the sediment/water interface and buried. Some organic carrier phase decayed, resulting in the redistribution of Hg to inorganic and remaining organic solids. Likewise, the reductive dissolution of inorganic substrates during early diagenesis caused further remobilization and redistribution of mercury. Although redistribution among the solid phases is considerable, the rapid uptake of Hg by particulate matter significantly retards the vertical transport of Hg to surficial sediments. High Hg concentrations in SPM in the waters of the Saguenay Fjord (Gagnon *et al.*, 1997) suggest that deposition of resuspended particulate matter from contaminated upstream sediments remains a significant input to these sediments.

6.3.2 Saguenay Fjord - Landward Basin Slope

Within sediments of the basin slope of the inner basin (SAG-6B), mercury distribution appears as two distinct maxima. Elevated concentrations of mercury are found near the sediment/water interface, but are far exceeded by mercury levels in sediments deposited between 1947 and 1971, the period of operation of the Arvida chlor-alkali plant.

The presence of allochthonous clay layers in the basin slope sediments complicates the physicochemical environment in which diagenetic processes take place. Because they are less porous, the clay landslide layers serve as partial physical barriers to the transport of dissolved species. Chemically, the clay layers are poorer in dissolved organic and polysulphide ligands which most effectively solubilize mercury and which would ordinarily contribute to mercury mobility and transport (Gagnon *et al.*, 1996a). Furthermore, sediments rich in labile organic matter were rapidly buried beneath the clay layers, resulting in high rates of sulphate reduction. The establishment of reducing conditions to the new sediment/water interface contributed to the reductive dissolution of iron and manganese (hydr)oxides within the clay layers (Mucci and Edenborn, 1992; Gagnon *et al*, 1995). The AVS solids which consequently precipitated both above and below the landslide layers are an immense sink for mercury and possibly serve as the most important barrier to the migration of Hg from this strata toward surficial sediments.

Whereas the transfer of mercury from the organic phase to FeS solids is most visible in **Figure 5.5**, the same diagram suggests that the accumulation of Hg by other phases (pyrite and Fe_{HCl}) is comparatively negligible. With the exception of surface enrichment and a small maximum in the buried 1971 landslide layer, the Hg_{HCl}:Hg_{sum} ratio presents a nearly featureless profile. Accumulation of mercury by pyrite is similarly featureless, displaying a surface minimum and what may indicate the gradual incorporation of Hg with very sparse authigenic FeS_2 production.

It is impossible to directly determine the source of recent mercury inputs to surficial sediments, which may be the result of resuspension of contaminated upstream sediments, diagenetic remobilization from deeper sediments, some as yet undetected source, or a combination of these. The predominance of organic substrates as chief adsorbing solid *above* the clay landslide layers does not lend support to any one mechanism or model. It may represent mercury diagenetically remobilized from the lower, highly contaminated layer, but re-adsorbed by humic material in organic-rich muds above the upper clay layer, or it could reflect the input of mercury to the sediment/water interface associated with particulate organic matter.

Gagnon *et al.*, (1997) calculated the flux of mercury from the surficial porewaters (0-0.5 cm) to overlying waters. They determined that the Hg flux out of the sediments is minor (3.8 to 36 $ng \cdot cm^{-2} \cdot a^{-1}$) and concluded that the vertical transport of mercury within the sediments following diagenetic remobilization could not account for the concentration of mercury in surficial sediments. Furthermore, they noted that ΣHg concentrations in SPM taken along the axis of the Saguenay Fjord (A. Mucci, pers. comm.) ranged from 0.25 $\mu g \cdot g^{-1}$ to 7 $\mu g \cdot g^{-1}$ and were independent both of sampling location and depth. From these data, they reasoned that the resuspension of contaminated sediments presently serves as the primary source of mercury to the sediment/water interface within the Saguenay Fjord.

Alternatively, the paucity of PAH in surface sediments contradicts the resuspension model (Pelletier *et al.*, 1989b). The distribution of PAH (polyaromatic hydrocarbon) compounds may serve as a crucial marker for mercury in the surficial sediments, since PAH contaminants in the Saguenay River and Fjord were released contemporaneously with mercury, before being substantially reduced in the mid 1970's (Pelletier *et al.*, 1989b). Because they are highly resistant to microbial degradation, PAH compounds are not subject to diagenetic remobilization. Resuspension of upstream sediments should result not only in the transport of mercury to the Saguenay Fjord, but also in an elevated PAH signature in the resettled contaminated sediments, yet this is *not* observed.

The input of mercury from SPM reported by Gagnon *et al.* (1997) could easily account for surface mercury concentrations in the Saguenay Fjord at the sites discussed in this study. In fact, input of mercury from resuspended sediments seems the most likely explanation for the shallower Hg_{sum} maxima at SAG-6B (5.5-11 cm, **Figure 5.4**), which coincides with a visible clay layer from a recent slumping event. Although there has been obvious redistribution of mercury to other sedimentary solids following the degradation of organic matter, diagenetic remobilization may, in fact, be minor if transport is negligible. Because mercury is rapidly readsorbed by particulate matter, the re-partitioning of mercury may occur without significant vertical transport within the sediments. Unfortunately, the concentrations of PAH compounds in the SPM samples cited by Gagnon *et al.* (1997) were not determined, so that the nature of the Hg - PAH decoupling in the Saguenay Fjord remains unclear.

6.3.3 Saguenay Fjord - Bottom of the Landward Basin

The thick clay layers which serve as a partial barrier to mercury transport in the basin slope sediments are absent from the basin bottom (SAG-30B). At this site, buried mercury is markedly redistributed throughout the profile (**Figure 5.5**). Concentrations of Hg_{sum} are higher overall than the other stations, but the sharply defined, highly contaminated ($Hg_{sum} > 5000$ ng·g^{-1}) strata present at SAG-6B appears as a broader, less intense maximum (**Figure 5.4**). As with landward basin slope, the source of the mercury to the surface sediments cannot readily be determined by direct evidence. Although high ΣHg concentrations in SPM suggests deposition and burial of resuspended contaminated sediments, a high degree of Hg partitioning, as well as inconsistencies between the Hg and PAH profiles (Pelletier *et al.*, 1989b) signal the potential importance of diagenetic remobilization of Hg throughout sediments at this site.

In the surficial sediments, where contamination is still significantly above pre-industrial levels, the majority of extractable mercury is found associated with organic matter. Overall, the profile of Hg_{NaOH} resembles that of Hg_{sum} at SAG-30B (**Figures 5.8 and 5.9**). Where total extractable mercury concentrations exceed 1000 $ng \cdot g^{-1}$, however, there is a large-scale transfer of Hg to inorganic solids (Figure 5.5).

A well-defined zone of Hg-enrichment in HCl-extractable solids runs from 5 to 15 cm depth, with a maximum at about 7 cm (Figure 5.8). The peak of Hg_{HCl} seems shifted toward the sediment/water interface relative to both Hg_{sum} and Hg_{NaOH}. The layers containing high Hg_{HCl} occur well above the depth where AVS accumulates (approximately 16 cm), and probably represent mercury associated with iron (hydr)oxides, which are present in much higher concentrations at this site. Mercury appears to be accumulating in reducible Fe solids (which persist to greater depth than Mn (hydr)oxides)) and possibly cycling diagenetically with iron at this depth.

The reapportioning of Hg to HF/HCl-extractable solids also seems to correspond to the distribution of Hg_{sum} (**Figures 5.4 and 5.5**). The maximum of $Hg_{HF/HCl}$, however, is vertically offset and distinct from both Hg_{NaOH} and Hg_{HCl}. The incorporation of Hg to HF/HCl-soluble solids takes place only upon the accumulation of AVS solids (**Figure 5.1**), as was observed at SAG-6B. The profile of $Hg_{HF/HCl}$ and its relationship to the distributions of AVS and other extractable Hg fractions (particularly Hg_{HCl}) reinforces the hypothesis that the $Hg_{HF/HCl}$ fraction in these sediments was initially associated with AVS (prior to sampling), and was solubilized with the oxidation products of iron monosulphides during the sequential extraction procedure. The marked turnover of mercury from the HCl-soluble fraction to $Hg_{HF/HCl}$ is consistent with the release of mercury following the reductive dissolution of Fe (hydr)oxides, continuing degradation of organic matter, and the subsequent scavenging of Hg by precipitating iron monosulphides.

Redistribution of mercury to pyrite (Hg_{HNO3}) is slight, and follows the distribution of Hg_{sum} (**Figure 5.8**). Unlike the other fractions, the Hg_{HNO3}:Hg_{sum} ratio remains nearly constant throughout the profile (**Figure 5.5**), and increases slightly with depth. The gradual accumulation of mercury in pyrite with depth is consistent with the slow formation of authigenic pyrite in the Saguenay Fjord. The paucity of mercury extractable by HNO_3, despite the high Hg-affinity of pyrite, reflects the very low concentration of pyrite in these sediments.

6.4 Diagenetic Chemistry of Solid-Phase Mercury in the Saguenay Fjord: Comparison to Previous Studies

Studies of mercury geochemistry, distribution, and partitioning in natural settings which appear in the literature (Eganhouse et al., 1978; Giordano et al., 1992; Huerta-Diaz and Morse, 1992; Gobeil and Cossa, 1993; Dmytriw *et al.*, 1994; Matty and Long, 1995; Gagnon *et al.*, 1996b; Gagnon *et al.*, 1997) present a detailed but varied body of research. The studies have been conducted in diverse environments (soils, lacustrine and marine sediments) or have focussed on the evaluation of Hg concentrations in only one or two extractable phases. As a result, there is no consensus on the general diagenetic behaviour of mercury in natural systems, and little basis for comparison.

Concentrations of mercury in the "exchangeable fraction" in this study were below detection limits, in agreement with the results reported by several others (Eganhouse, et al., 1978; Giordano et al., 1992, Huerta-Diaz and Morse, 1992; Dmytriw *et al.*, 1994;

Matty and Long, 1995). There seems, therefore, to be agreement that little or no mercury in natural systems is bound at ion-exchange sites on clays and other solids.

The affinity of mercury for organic matter, both *in vitro* and *in situ*, is well established (Section 2.2.4). Matty and Long (1995), working in a lacustrine system, reported temporary residence of mercury in the organic fraction near the sediment/water interface, prior to Hg release following burial and microbial degradation of the organic matter. In contrast, Giordano *et al.* (1992), who examined mercury partitioning in sediments off the coasts of Italy and Sicily, found little mercury associated with the organic fraction. Unfortunately, Giordano *et al.* (1992) regarded C_{org} as a refractory phase and isolated it very late in their extraction sequence. Given their protocol, it is likely that mercury associated with labile organic matter was solubilized in one or more of the initial extraction fractions. Loring (1975), on the basis of their vertical distribution in the bulk sediments of the Saguenay Fjord and Laurentian Trough, reported a strong statistical correlation between the organic carbon content and total mercury. In contrast, Eganhouse *et al* (1978), using a sequential extraction scheme, found that organically-associated Hg constituted only a small proportion of total extractable mercury in the Hg-contaminated, sulphidic Palos Verde sediments, despite concentrations of C_{org} (10% by weight) 2 to 5 times greater than in the Saguenay Fjord.

Surprisingly, results of this study agree with the seemingly incongruous results of both Loring (1975) and Eganhouse *et al* (1978). Although the marked statistical correlation between C_{org} and ΣHg reported by Loring (1975) which characterized the Saguenay Fjord and Laurentian Trough sediments was not evident in our analyses, the majority of the mercury at each of the sites investigated in this study reside with the organic carbon fraction. It may also be that, in the 20 years since the study by Loring, the effects of early diagenesis on the speciation and distribution of both organic carbon and mercury has scattered the relationship. It was also observed that, with increasing Hg_{sum}, the fraction of organically-associated mercury decreased, even though absolute concentrations increased. The sediments studied by Eganhouse *et al.* (1978) bore much greater concentrations of total mercury than most of those investigated in this study (typically 5 µg Hg per g dry sediment), so that only the layer of maximum mercury contamination at SAG-6B is comparable to those of Palos Verde. In fact, within the highly contaminated sediment strata at SAG-6B, the majority of extractable mercury resides in phases other than organic matter. Such results seem to indicate that the trend of decreased association of organic matter with elevated total mercury content is not limited to the Saguenay/St. Lawrence system.

Studies by both Gobeil and Cossa (1993 and Gagnon *et al.* (1996b, 1997) suggest that mercury adsorption by Fe/Mn (hydr)oxides in St. Lawrence Trough and Saguenay Fjord sediments is an important sink for mercury, particularly near the sediment/water interface. Gobeil and Cossa (1993) reported the simultaneous release of Fe, Mn, and Hg to the anoxic porewaters, and also noted the surface enrichment of hydroxylamine-soluble Fe, Mn, and Hg. Similarly, Gagnon *et al.* (1997) reported coincidental Fe, Mn, and Hg distributions using a 1N HCl extraction. Both research groups interpreted their data to suggest that the Fe/Mn (hydr)oxide-associated fraction of Hg serves as a potentially large reservoir of reactive mercury in these sediments, and may be released to porewaters following the reductive dissolution of the Fe/Mn solids following the onset of hypoxia. Gobeil and Cossa (1993) go on to note, however, that the amounts of Hg released to porewaters at the redoxcline, which they associated with degrading Fe/Mn (hydr)oxides, were minute relative to the bulk sediment content. Additionally, they did not examine the potential solubility of labile organic matter in their extraction scheme, which, in this environment, probably serves as an important source of contamination. Similarly, Gagnon *et al.*, 1997 performed a 1N HCl extraction without a prior C_{org} extraction step on the same sediment samples as those used in this study. We suspect that their method significantly overestimates the amount of mercury associated with Fe/Mn-(hydr)oxides. In contrast, neither Eganhouse *et al.* (1978), nor Giordano *et al.* (1992) observed detectable quantities of mercury associated with Fe/Mn-(hydr)oxides in marine sediments. These studies suffer from considerable methodological flaws as well, either resulting from incomplete dissolution of reactive Fe/Mn solids (Eganhouse *et al.*, 1978), or the late extraction of organic matter (Giordano et al., 1992). In the latter case, however, the absence of mercury in the reactive Fe/Mn pool possibly presents a true upper limit. Since potential contamination from organic matter would result in *over*-estimation of Hg, the measurement of negligible Hg levels suggests that, in fact, little Hg is associated with reactive Fe and Mn (hydr)oxides in their study.

Although the studies of Dmytriw *et al.* (1994) and Matty and Long (1995) were performed on different systems (soils and lacustrine sediments, respectively), the methodologies *did* provide for the extraction of organic matter prior to the solubilization of Fe/Mn (hydr)oxides. Matty and Long (1995) reported enrichment of mercury in Fe/Mn-(hydr)oxides following the degradation of labile organic matter, but prior to the reductive dissolution of reactive Fe and Mn at the redoxcline. They noted that a significant portion of mercury (as much as 50%) was released to porewaters at the redoxcline, migrated to surface sediments where it was scavenged by precipitating oxides. According to Dmytriw (1993), significant uptake of mercury by Fe/Mn (hydr)oxide phases was noted only in organic-poor, aerated soils, with a distinct (hydr)oxide-rich layer. Despite the biogeochemical differences between soils and estuarine sediments, results of the latter study are relevant in that they demonstrate the inability of Fe/Mn (hydr)oxide phases to effectively bind Hg in water-saturated, anoxic clay soils.

Again, the results of this study support many aspects of several of the other studies (Eganhouse, *et al.*, 1978; Giordano *et al.*, 1992; Dmitriw *et al.*, 1994; Matty and Long, 1995). Adsorption of Hg by iron and manganese (hydr)oxides *can* be important, *but only conditionally.* Significant adsorption of mercury occurs where high concentration of (hydr)oxides are precipitated and other ligands with a greater affinity for mercury are markedly depressed, or where mercury concentrations are high enough to allow (hydr)oxide solids to compete effectively with other solid phases. In cases where these conditions are not met, mercury associated with Fe/Mn (hydr)oxides may be undetectable.

Because of the paucity of AVS-monosulphides in most sediments, and due to the methodological difficulties of separating them from other reactive forms of iron, researchers have mainly speculated on, but have been unable to directly evaluate, the incorporation of mercury by monosulphides (Huerta-Diaz et al., 1993; Arakaki and Morse, 1994). Likewise, this study was unable to isolate monosulphides, or to prove statistical correlations between the distribution of AVS and a particular extractable fraction of mercury. Interestingly, however, coincidental extraction of high concentrations $Hg_{HF/HCl}$ and AVS were noted in the profiles of at least two of the stations studied here. Prior methodologies have utilized HF alone in the extraction of silicates. In this study, HCl (HF/HCl 10N/1N) was added to keep mercury in solution, and resulted in a dramatic increase in concentration compared to treatment with HF (10N) alone. Significant Hg concentrations were observed in phases more refractory than those dissolved in 1N HCl, but more reactive than those dissolved only in the hot HNO_3/HCl step. There are no comparable observations in the literature, since this protocol has not been utilized elsewhere. An alternative interpretation to the extraction of Hg associated with AVS oxidation products in the HF/HCl step is the dissolution of clay-metal-organic complexes, although there are few references to these in studies of trace metal partitioning. Since there is no way of separating the organic matter comprising CMO complexes from other refractory C_{org}, the establishment of distribution profiles comparable to those obtained for AVS are not possible at present. As a result, the relevance of CMO-associated Hg remains strictly speculative in this work.

Huerta-Diaz and Morse (1992), in contrast to previous studies, with the possible exception of Giordano *et al.* (1992), suggest that nearly all mercury in sulphidic environments is incorporated into pyrite. They reported DHgP values (see **Equation 2.2**) around 90%. Other studies (Eganhouse et al., 1978; Giordano et al., 1992; Matty and Long, 1995; Gagnon *et al.*, 1997), however, reported that a significant fraction of mercury was resident in what was merely termed a "refractory phase" (which in several cases nominatively included silicates and organic matter). No research group, including Huerta-Diaz and Morse (1992), was successful in ruling out overestimation of pyritized Hg concentrations due to mercury associated with refractory organic matter. Although it seems likely that pyritized mercury comprises the bulk of the "refractory" phase metal, caution must be exercised in the interpretation of these data. Methodological questions not withstanding, it is obvious that the DHgP of the Saguenay Fjord differs markedly from the high values obtained by Huerta-Diaz and Morse (1992). It is worth noting, however, that the DHgP values in *both* this study and that of Huerta-Diaz and Morse (1992) significantly exceed the DOP values. This reinforces the view that Hg uptake by FeS_2 in the Saguenay system is limited by the rate of pyrite formation. In addition, the molar concentration of pyritic Hg in the Saguenay Fjord and in the sulphidic marine sediments studied by Huerta-Diaz and Morse (1992) are remarkably close. Despite near total pyritization in some of the anoxic sulphidic marine sediments, the concentrations of pyritic mercury determined by Huerta-Diaz and Morse (1992) were typically between 9 and 31 μmol Hg per mole pyrite. The average value obtained from the wet sequential extraction analyses in this study (54 μmol Hg·$\mathrm{mol^{-1}}$ pyrite) is similar. Framboidal pyrite grains found in these sediments were analyzed by electron microprobe and revealed Hg concentrations below detection limits (100 μmol Hg · $\mathrm{mol^{-1}}$ pyrite), in agreement with the wet chemical analysis data. The authigenic nature of the framboidal pyrite grains was confirmed by their high (up to 1000 μg·$\mathrm{g^{-1}}$) As content (Mucci, pers. comm.). Although much has been made of the potential for organic contamination in the final extraction step, there is the possibility in this study of *under*-estimation. If a large portion of the pyrite in the Saguenay Fjord is detrital, DHgP values would also include comparatively Hg-poor allochthonous pyrite (Mucci and Edenborn, 1992).

7. CONCLUSIONS

7.1 A Customized Extraction Procedure

Evaluation of the present and future environmental risk posed by trace metal contamination in coastal sediments requires a clearer understanding of the chemical processes which determine the ultimate fate of a metal. Approaches to prevention, management, and possible remediation may be radically different depending on the pathways of the contaminants into the biosphere and, alternatively, into potentially permanent sinks. Developing a model of the diagenetic chemistry of a trace metal demands the elucidation of the metal contaminant partitioning among authigenic and autochthonous sedimentary solids, as well as the mechanisms of transfer between them.

Unfortunately, the most effective tool for quantifying the trace metal load of the various components of sediment and soil solid remains imperfect. Although extraction pools may be assigned to various target solid substrates, the fractions remain operationally defined in the absence of true specificity and complete extraction efficiency. Sequential extraction techniques require repeated fine-tuning, which is dependent on the nature of the metal as well as the chemistry of the samples to be handled. Failure to tailor methodology and reliance on unmodified, previously existing protocols for sedimentary solid and associated element extractions easily results in errors in the attribution of contaminants to different extraction pools. Even when protocols have been optimized, thorough and critical evaluation of the results is necessary to counter unresolved weaknesses inherent in the sequential extraction technique.

The sequential extraction protocol utilized here to chemically separate the solid components and their associated mercury was partially tailored for use with these sediments and for mercury. The protocol made use of various techniques which appear in the literature but added significant improvements over previously developed sequential extraction methods.

The first step applied in several protocols is the extraction of exchangeable metals which are bound by weak electrostatic forces to particulate surfaces. Initial findings confirmed the results of previous studies, all of which reported exchangeable mercury concentrations below detection limits (Eganhouse, et al., 1978; Giordano et al., 1992, Huerta-Diaz and Morse, 1992; Dmytriw, 1993; and Matty and Long, 1995). The $MgCl_2$ extraction step was excluded to reduce error from physical manipulation and streamline the extraction sequence.

The use of an alkali extraction step to separate reactive organic matter was successful in removing the majority of organic matter prior to the selective solubilization of other solids, most notably reactive iron and manganese solids. Although imperfect, the technique extracted as much as 76% of the organic matter from the sediments, while dissolving only minute quantities of iron and manganese.

Similarly, the subsequent dilute HCl step used to dissolve iron and manganese (hydr)oxides yielded positive but still mixed results. In contrast to both Kostka and Luther (1994) and Levanthal and Taylor (1990), we found that the 1N HCl (24 hr) extraction is *not* equivalent to the dithionite (Canfield, 1989; Raiswell *et al.*, 1993) benchmark. Nevertheless, the use of the HCl reagent minimized problems of contamination and the readsorption of dissolved metals, and did not result in the precipitation of mercury sulphides, nor in the reduction to Hg(0) and consequent loss.

The addition of HCl to the aggressive HF silicate extraction step corrects a potentially serious flaw in many previous protocols when applied to mercury by keeping Hg solubilized. In the absence of chloride or other suitable soluble ligand, mercury released from the target phase is rapidly (<24 hours) readsorbed on residual solids such as pyrite and refractory organic matter, so that measured dissolved Hg concentrations often drop below detection limits. Many of the trace metal extraction techniques derived from the modification of the method proposed by Lord (1982) for the chemical separation of sedimentary pyrite (Huerta-Diaz and Morse, 1990, 1992) are unsuitable for the determination of mercury because they utilize only HF and thereby potentially resulting in overestimation of pyritic mercury content. In the final step of the Lord (1982) method, a concentrated nitric acid digestion is used to solubilize pyrite. The addition of a small amount of HCl (Agemian and Chau, 1976, Dmytriw *et al.*, 1994) to this reagent also keeps mercury solubilized, thus minimizing loss of Hg(II).

7.2 Partitioning of Mercury in Contaminated Coastal Marine Sediments

Loring (1975) proposed that the scavenging by particulate organic matter serves as the main vector of mercury to the sediments of the Saguenay River system. Results of this study indicate that most of the mercury in the Saguenay Fjord resides in the alkali-soluble organic matter fraction and thus corroborate Loring's hypothesis. The presence of sediment strata where a significant fraction of the Hg is now associated with inorganic substrates, however, suggests that post-depositional diagenetic processes have altered the mercury distribution.

Following deposition and burial, the degradation of organic matter leads to the gradual release of Hg to surrounding porewaters. The predominant association of mercury with organic matter to depths exceeding 40 cm indicates that the reapportioning of Hg among the various sedimentary phases is probably limited by the rate of organic matter degradation as well as by readsorption to proximate particulate organic matter.

Some of the mercury which is released to porewaters is rapidly taken up by inorganic phases, including Fe/Mn (hydr)oxides, AVS, and pyrite. Sulphides (both AVS and pyrite) are present in comparatively minute concentrations, but significantly influence, and sometimes dominate, the partitioning of mercury in sediments. The relative affinity of sulphides for mercury is greater than for any other sedimentary phase, including organic matter.

Although previous authors (Gobeil and Cossa, 1993; Gagnon *et al.*, 1997) have proposed that Fe/Mn (hydr)oxides serve as a predominant geochemical trap for mercury, this study found, overall, that this was not the case in the Saguenay Fjord and Laurentian Trough. Strong evidence of an association between Hg and Fe/Mn(hydr)oxides has been presented here, but it was found that iron and manganese oxides, hydroxides, and oxyhydroxides bear a sizable fraction of total extractable mercury *only* when present in high concentrations where other fractions with a greater affinity for mercury (i.e. organic matter and reduced sulphur) are absent. Specifically, this was evident in the deep basin of the Saguenay Fjord (SAG-30B) where organic matter is the sparsest and least reactive. At this station, Fe_{HCl} concentrations exceed those found elsewhere in the Saguenay by nearly a factor of 2, and sulphate reduction becomes a dominant process deeper in these sediments than at any other site.

Although the mass distribution of mercury in the Saguenay Fjord appears as:

$$\mathbf{C_{org} > AVS \gg Fe/Mn\ (hydr)oxides \approx FeS_2,}$$

additional consideration of the distributions and concentrations of each substrate suggest that the *molar affinities* of the various substrates for mercury are altogether different:

$$\mathbf{AVS \approx FeS_2 > C_{org} > Fe/Mn\ (hydr)oxides.}$$

The difference between the mass distribution of mercury and the affinities of sedimentary solids for Hg arises from the relative concentrations of each sedimentary solid. For example, although C_{org} concentrations generally far exceed those of pyrite and AVS, sulphidic solids can dominate mercury distribution in some strata because of their markedly higher affinity. It should be cautioned that the relative affinities are actually more difficult to determine, since mercury arrived at the sediment/water interface strongly bound to organic matter -- in overlying waters and oxic surficial sediments, organic matter does not have to compete with the much more attractive sulphides which form below the sediment/water interface. Hg readsorbs rapidly to organic matter and to most other solids, and is readily co-precipitated in a variety of solids. As a result, in order to achieve significant redistribution of mercury to other geochemical phases, not only does Hg have to be released from organic matter during microbial degradation, but other substrates must be proximate and preferably simultaneously precipitating.

The redistribution of mercury among the sedimentary solids is dependent on the amount of total extractable mercury in a given sediment. The amount of mercury associated with AVS and FeS_2 increases with increasing total Hg, at the expense of organic matter and Fe/Mn (hydr)oxides. Such redistribution occurs because organic matter, which has a lower affinity than AVS and pyrite, is the primary medium of transport of Hg to the sediment/water interface. Where concentrations of mercury are greater, more mercury is released with the degradation of the same quantity of organic matter, and although some Hg may be readsorbed by remaining C_{org}, there will be an increased turnover to the phases with higher affinities. Moreover, mercury may be present in sufficient concentrations to saturate chelation sites on organic matter with high affinity for mercury. This results in greater partitioning to inorganic phases as they are more able to compete with remaining organic sites where mercury is held by weaker interactions.

The patterns of distribution of the mercury contamination in the Saguenay Fjord and Laurentian Channel vary by site. Although the contamination of the Laurentian Trough is less severe, Hg concentrations in surficial sediments remain elevated with respect to pre-industrial levels. Unlike the Saguenay Fjord, many of the anthropogenic Hg inputs to the St. Lawrence River and Gulf of St. Lawrence remain in place. The comparatively low concentrations of mercury and diagenetic activity, however, seem to have been insufficient to permit significant remobilization of mercury to other solids. Mercury in the Laurentian Channel remains buried predominantly with organic matter.

Mercury concentrations in the sediments of the landward basin slope (SAG-6B) contained the most contaminated stratum in the study. The marked decline in anthropogenic input of Hg to the Saguenay Fjord following implementation of government regulations on effluent discharge coincided with a massive landslide, resulting in the burial of the most contaminated sediments under several cm of organic-poor clay. Consequently, the clay layer has served as an effective physicochemical barrier, and relatively little of the mercury has been transported to overlying sediments. Beneath the clay barrier, HF/HCl-soluble solids (possibly AVS or clay-metal-organic complexes) have incorporated most of the mercury. A second, shallower zone of mercury contamination exists, associated almost exclusively with organic matter. It remains substantively impossible to directly determine the source of mercury in surficial sediments at SAG-6B. Although remobilization of Hg from deeper sediments is suggested by the marked redistribution of mercury to inorganic substrates and the absence of PAH compounds (Pelletier *et al.*, 1989b), the presence of high mercury concentrations in SPM and an extremely low Hg flux (Gagnon *et al.*, 1997) from sediments to overlying waters seem to indicate that part if not most of the mercury contamination in the uppermost strata arrived with resuspended contaminated upstream sediments. Redistribution may occur following burial and decay of particulate organic vectors without significant vertical transport as a result of the tendency of mercury to rapidly readsorb to solids.

The most contaminated sediments in the deep interior basin are not covered by a thick, distinct clay layer, since less of the landslide material was carried this far. Consequently, mercury was subjected to more extensive redistribution to other sedimentary solid phases. The partitioning appears to reflect the diffusion of mercury toward the sediment/water interface in zones of active precipitation of iron and manganese (hydr)oxides, iron monosulphides, and pyrite. Some mercury appears to be cycled at the redoxcline with Fe between Fe (hydr)oxide and AVS solids, before eventually being buried with AVS beneath the redoxcline. Although the majority of the mercury remains buried well below the sediment/water interface, surficial concentrations significantly exceed pre-industrial levels. As in the sediments of the basin slope, there is insufficient evidence to determine conclusively whether this mercury originates from re-suspended upstream sediments or remobilized Hg from deeper sediments. Although the flux of mercury from these sediments to overlying waters is weak and contaminated SPM transports mercury to this site, the rate of sedimentation is markedly lower relative to SAG-6B (Smith and Walton, 1980; Silverberg *et al.*, 1986; Gagnon *et al.*, 1997). Furthermore, the absence of PAH markers in surficial sediments at this site (Pelletier *et al.*, 1978) and the more pronounced redistribution of mercury within the sediment suggest that, although there remains an input of mercury to surficial sediments, diagenetic remobilization probably plays a comparatively stronger role at this site.

7.3 Future Work and Applications

Beyond the results of this study, there remain unresolved issues which merit further inquiry -- to correct for deficiencies in the sequential extraction protocol, as well as to clarify certain aspects of the diagenetic chemistry of mercury in the Saguenay Fjord.

The primary advantage of the sequential extraction procedure is that it permits the evaluation of the chemical behaviour of an element in more detail than is afforded by total element concentrations alone. By describing the partitioning of an element among different operationally-defined fractions of sediments and soils as well the vertical fractionated distributions, post-depositional pathways of an element become discernable.

In cases of environmentally sensitive systems, such studies permit action based on scientifically informed decisions. In order to improve the utility of such techniques, however, flaws inherent in the technique must be either corrected or minimized. Many of the possible sources of error discussed previously have solutions which have already been proposed in various forms. The most significant modification might be the cumbersome but potentially important pre-treatment and analysis of sediments under inert atmosphere (Rapin *et al.*, 1986). Frozen samples isolated from the atmosphere may be used, bearing in mind the difficulties of heterogeneity, lower reactive surface areas, protective coatings, and extended reaction times. Alternatively, whereas dehydration of sediments results in alterations in the sediments (some of which are irreversible), freeze-drying and grinding may both be performed under an inert atmosphere. This would resolve problems of oxidation without assuming the difficulties of using whole frozen sediments. Many of the methodologies which are currently employed to extract sedimentary solids lack defined specificity, and often ignore minerals which, although present in trace quantities in most environments, may have much great impact in a few unique environments. Specifically, the isolation of iron monosulphides from iron and manganese (hydr)oxides would provide an important new tool to document trace metal partitioning in a wide number of sedimentary environments. Similarly, most passive distillation protocols for the determination of AVS and FeS_2 ignore greigite, which may result in underestimation of AVS content, and overestimation of FeS_2 or elemental sulphur. Where methodologies cannot be devised to permit the solubilization of specific mineral phases, the effect of chemical treatment in a sequential extraction series (e.g. the effect of AVS mineral oxidation) must be precisely understood in order to differentiate between methodological artifact and the effect of natural processes. Finally, improvements must be sought in the quantification and characterization of both reactive and refractory organic matter. In particular, techniques which characterize and evaluate the distribution of clay-metal-organic complexes should be developed and incorporated into sequential extraction schemes.

In addition to methodology, other points were overlooked in this project which merit investigation. Solid-phase organosulphur compounds in the sediments of the Saguenay Fjord were not evaluated in either this or the accompanying studies of Gagnon *et al.* (1995, 1996a). The relationship between organosulphur functional groups and mercury distribution may provide considerable insight to the nature of the humate-mercury complexation, and therefore to the overall fate of mercury within sulphidic coastal sediments. Similarly, the characterization of iron-monosulphides in sediments of the Saguenay system, and the possible formation of significant quantities of greigite in this environment requires further assessment. Additionally, evaluation of the PAH load of SPM in the Saguenay Fjord may be instrumental in determining the cause of the decoupling of Hg and PAH in surficial sediments, and thereby help quantify the comparative contributions of diagenetic remobilization and the deposition of resuspended contaminated sediments to the sediment/water interface. Finally, during the process of the preparation of this manuscript, the Saguenay Fjord underwent catastrophic flooding in July, 1996. Despite the human cost, as with the massive 1971 St. Jean-Vianney landslide, this may provide an opportunity to evaluate the effect of massive, instant input of autochthonous terrigenous matter on early diagenetic chemistry.

Finally, the implications of results presented in this study, as well as that of Gagnon (1994) may find application in future management of the Saguenay system and its resources. Mercury appears to be transported within the Saguenay Fjord with suspended particulate matter, and this may represent the most significant input to surficial sediments (Gagnon *et al.*, 1997). The redistribution of mercury from organic matter to inorganic phases occurs to a marked degree in these sediments and may also contribute to the contamination of surficial sediments. The accumulation of mercury in AVS, which is metastable and rapidly degrades in the presence of oxygen, presents a serious threat to the biosphere of the Saguenay system and the Gulf of St. Lawrence. Should anoxic sediments become reworked, the oxidation of AVS would re-introduce mercury contamination to water, sediments, and biota of the Saguenay system, as well as the Gulf of St. Lawrence. In addition, much of the mercury remains associated with organic matter, even at depth, so mercury will continue to be released to porewaters and accumulated by inorganic substrates for some time. Because the formation of pyrite is slow, turnover from AVS and C_{org} to the comparatively more stable pyrite phase will be minor, and the potential hazard can be expected to persist well into the next century. Obviously, the association of mercury to redox metastable compounds strongly discourages the use of dredging techniques to clear shipping channels throughout the Saguenay system. In a more positive light, the retardation of vertical mercury transport in sites where heavily contaminated layers have been blanketed by a thick layer of organic-poor clay lends encouragement. In an area which receives uncontaminated detritus from slumping events, the transport of mercury to the water column and the food chain may be significantly attenuated, either naturally or through human efforts. Throughout the Saguenay system, continued observation of benthic fauna and surficial sediments in the future will be necessary in order to monitor the gradual progress of natural decontamination.

REFERENCES

Agemian, H. and Chau, A.S.Y. (1976) "An improved digestion method for the extraction of mercury from environmental samples" Analyst 101:91-95.

Aller, R. and Rude, P. (1988) "Complete oxidation of solid phase sulphides by manganese and bacteria in anoxic marine sediments" Geochim. Cosmochim. Acta 42:751-765.

Andersson, A., (1979) "Mercury in soils" The Biogeochemistry of Mercury in the Environment, O. Nriagu, (ed.), Elsevier, North-Holland Biomedical Press, pp. 79-112.

Arakaki, T. and Morse, J.W., (1993) "Coprecipitation and adsorption of Mn(II) with mackinawite (FeS) under conditions similar to those found in anoxic sediments". Geochim. Cosmochim., 57:9-14.

Bakir, F., Damluji, S.F., Amin-Zaki, A., Murtadha, M., Khalidi, A., Al-Rawi, N.Y., Tikriti, S., and Dhahir, H.I. (1973) "Methylmercury poisoning in Iraq" Science 181:230-241.

Balistrieri, L., Brewer, P.G., and Murray, J.W. (1981) "Scavenging residence times of trace metals and surface chemistry of sinking particles in the deep ocean" Deep-Sea Res. 28A:101-121.

Barbeau, C., Bourgie, R., and Côté, J.-E. (1981a) "Variations spatiales et temporelles du césium-137 et du carbone dans des sédiments du fjord du Saguenay" Can. J. Earth Sci. 18:1005-1011

Barbeau, C., Bougie, R., and Côté, J.-E. (1981b) "Temporal and spatial variations of mercury, lead, zinc, and copper in sediments of the Saguenay Fjord" Can J. Earth Sci. 18:1065-1074.

Barrow, N. and Cox, V. (1992) "The effects of pH and chloride concentration on mercury sorption. I. By goethite" J. Soil Sci. 43:293-304.

Beijer, K. and Jernelöv, A. (1979) "Methylation of mercury in aquatic environments" Topics in Environmental Health, Volume 3: Biogeochemistry of Mercury in the Environment, J.O., Nriagu, ed., Elsevier/North Holland Biomedical Press pp. 203-210.

Belzile, N. (1986) Etude Géochimique de l'Arsenic dans les Sédiments du Chenal Laurentien, Ph.D. Thesis, Université du Québec à Rimouski, 251 pp.

Belzile, N. and Lebel, J. (1986) "Capture of arsenic by pyrite in near-shore marine sediments" Chem. Geol. 54:279-281

Belzile, N., Lecomte, P., and Tessier, A. (1989) "Testing readsorption of trace elements during partial chemical extractions of bottom sediments" Environ. Sci. Tech. 23(8):1015-1020.

Benes, P. and Havlík, B. (1979) "Speciation of mercury in natural waters" Topics in Environmental Health, Volume 3: Biogeochemistry of Mercury in the Environment, J.O., Nriagu, ed., Elsevier/North Holland Biomedical Press pp. 175-201.

Berka, A., Vulterin, J., and Zyka, J. (1965) Newer Redox Titrants, H. Weisz, trans., Pergamon Press, New York, pp. 29-35.

Bermond, A.M. (1992) "Thermodynamics applied to the study of the limits of sequential extraction procedures used for the speciation of trace elements in sediments and soils" Environ. Tech. 13:1175-1179.

Berner, R.A. (1970) "Sedimentary pyrite formation" Amer. J. Sci. 268:1-23.

Berner R.A., Baldwin T., and Holdren G.R. Jr. (1979) "Authigenic iron sulfides as paleosalinity indicators", J. Sed. Petrol., 49(4):1345-1350.

Bloom, N. and Crecelius, E. (1983) "Determination of mercury in seawater at sub-nanogram per liter levels" Mar. Chem. 14:49-59.

Bloom, N. and Fitzgerald, W. (1988) "Determination of volatile mercury species at the picogram level by low-temperature gas chromatography with cold-vapour atomic fluorescence detection" Analytica Chimica Acta 208:151-161.

Boesen, C. and Postma, D. (1988) "Pyrite formation in anoxic environments of the Baltic" Am. J. Sci. 288:575-603.

Boyle, E., Collier, R., Dengler, A.T., Edmond, J.M., Ng, A.C., and Stallard, R.F. (1974) "On the chemical mass-balance in estuaries" Geochim. Cosmochim. Acta 38:1719-1728.

Boyle, E.A., Edmond, J.M., and Sholkovitz, E.R., (1977) "The mechanism of iron removal in estuaries", Geochim. Cosmochim. Acta 41:1313-1324.

Brady, N. (1974) The Nature and Property of Soils, 8th ed., McMillan, New York, NY.

Brosset, C. (1981) "The mercury cycle" Water Air Soil Poll. 16:253-255.

Brown, J.R., Bancroft, G.M., and Fyfe, W.S. (1979) "Mercury removal from water by iron sulphide minerals. An Electron Spectroscopy for Chemical Analysis (ESCA) study" Environ. Sci. Tech. 13(9):1142-1144.

Buckley, D.E. (1989) "Geochemical evidence of pore-water advection along a fault in plastic sediments from the Southern Nares Abyssal Plain (western North Atlantic)" Chem. Geol. 75:43-60.

Burdidge, D. (1993) "The biogeochemistry of manganese and iron reduction in marine sediments" Earth. Sci. Rev. 35:249-284.

Campbell, P.G.C. and Tessier, A. (1989) "Biological availability of metals in sediments: analytical approaches" Proceedings of the International Conference on Heavy Metals in the Environment, Geneva, Switzerland, pp. 516-525.

Canfield, D.E. (1989) "Reactive iron in marine sediments", Geochim. Cosmochim. Acta, 53:619-632.

Canfield, D., Raiswell, R., and Bottrell, S. (1992) "The reactivity of sedimentary iron minerals toward sulfide" Am. J. Sci. 292:659-683.

Chanton, J. and Martens, C. (1985) "The effects of heat and stannous chloride addition on the active distillation of acid volatile sulfide from pyrite-rich marine sediment samples " Biochem., 1:375-383.

Chen, K.Y. and Morris, J.C. (1972) "Kinetics of oxidation of aqueous sulfide by O_2" Environ. Sci. Tech. 6:529-537

Christian, G.D. (1977) Analytical Chemistry, John Wiley and Sons, New York. NY.. pp. 314-316.

Clevenger, T.E, (1990), "Use of sequential extraction to evaluate the heavy metal in mining wastes" Water Air Soil Poll. 50:251-254.

Cornwell, J.C. and Morse, J.W. (1987) "The characterization of iron sulfide minerals in marine sediments" Mar. Chem. 22:193-206.

Cossa, D. and Desjardins, C. (1984) "Evolution de la concentration en mercure dans les crevettes du fjord du Saguenay (Québec) au cours de la périod 1970-1983" Rapport Technique Canadien sur l'Hydrographie et les Sciences Océaniques No 32 8 pp.

Desjardins, C. (1989) Projet Saguenay 1989: Rapport Final, Pêches et Océans/Fisheries and Oceans Canada, Dossier #5516-11-1, 13 Septembre 1989.

Dmytriw, R., Mucci, A., Lucotte, M., and Pichet, P. (1994) "The partitioning of mercury in the solid components of pristine and flooded forest soils and sediments from a hydroelectric reservoir, Québec, (Canada)" Wat. Air Soil Poll. 80:1099-1103.

Drainville, G. (1968) "Le fjord du Saguenay; 1. Contribution à l'océanographie". Naturaliste Canadien, 95:809-855.

Dyrssen, D. and Kremling, K. (1989) "Increasing hydrogen sulfide concentration and trace metal behavior in the anoxic Baltic waters" Mar. Chem. 30:193-204.

Dyrssen, D. and Wedborg, M., (1991) "The sulphur-mercury (II) system in natural waters" Water Air Soil Poll., 56:507-519.

Edenborn, H., Mucci, A., Belzile, N., Lebel, J., Silverberg, N., and Sundby, B. (1986) "A glove box for the fine-scale subsampling of sediment box cores" Sedimentology 33:147-150.

Edenborn, H., Silverberg, N., Mucci, A., and Sundby, B. (1987) "Sulfate reduction in deep coastal marine sediments" Mar. Chem. 21:329-345.

Eganhouse, R.P., Young, D.R., and Johnson, J.N. (1978) "Geochemistry of mercury in Palos Verde Sediments" Env. Sci. Tech. 12(10) 1151-1157.

Emerson, S., Jacobs, L.J., and Tebo, B. (1983) "The behaviour of trace metals in marine anoxic waters: Solubility at the oxygen-hydrogen sulphide interface" Trace Metals in Sea Water, C.S. Wong *et al.*, ed., Plenum Press, New York, NY., pp. 579-608.

Environment Canada (1981), Status report on compliance with the chlor-alkali mercury regulations, Abatement and Compliance Branch, Water Pollution Control Directorate, Environmental Protection Service, Environment Canada.

Evans, L. (1989) "The chemistry of metal retention in soils" Environ Sci Tech. 23:1046-1056.

Evans, R. D. (1986) "Sources of mercury contamination in the sediments of small headwater lakes in South-Central Ontario, Canada" Arch. Environ. Contam. Toxicol. 15:505-512.

Fang, S. (1979) "Sorption and transformation of mercury vapor by dry soil" Env. Sci Tech. 12(3) 285-288

Farrah, H. and Pickering, W. (1977) "Influence of clay-solute interactions on aqueous heavy metal ion levels" Water, Air, and Soil Pollution 8:189-197.

Farrah, H. and Pickering, W. (1978) "The sorption of mercury species by clay minerals" Water, Air, and Soil Pollution 9:23-31

Fernex, F., Fevrier, G., Bénaïm, J., and Arnoux, A., (1992) "Copper, lead, and zinc trapping in Mediterranean deep-sea sediments: probable co-precipitation with Mn and Fe" Chem. Geol. 98:293-306.

Fields, M. and Claridge, G.G.C., (1975) "Allophane", Soil Components, vol II., Inorganic Components, ed., Gieseking, J.E., Springer Verlag, N.Y..

Flaig, W., Beutelspacher, H., and Rietz, E., (1975) "Chemical Composition and Physical Properties of Humic Substances", Soil Components, vol I., Organic Components, ed., Gieseking, J.E., Springer Verlag, N.Y.

Forbes, E.A., Posner, A.M., and Quirk, J.P. (1974) "The specific adsorption of inorganic Hg(II) species and Co(III) complex ions on goethite" J. Coll. Interface Sci. 49(3) 403-409.

Frimmel, F.H., Immerz, A., and Niedermann, H. (1984) "Complexation capacities of humic substances isolated from freshwater with respect to copper (II), mercury (II), and iron (II,III)" Complexation of Trace Metals in Natural Waters, Developments in Biogeochemistry, C.J.M. Kramer and J.C. Duinker (eds.), Martinus Nijhoff/Dr W. Junk Publishers, Boston, pp. 329-343.

Froelich, P.N., Klinkhammer, G.P., Bender, M.L., Luedtke, N., Heath, G.R., Cullen, D., Dauphin, P., Hammond, D., Hartman, B., and Maynard, V. (1979) "Early oxidation of organic matter in pelagic sediments of the eastern equatorial Atlantic suboxic diagenesis" Geochim. Cosmochim. Acta 43(7) 1075-1090.

Gagnon, C., (1994) Comportement géochimique du mercure anthropique et du soufre enfouis dans les sédiments du Fjord du Saguenay, Ph.D. Thesis, Université du Québec à Rimouski, 187 pp.

Gagnon, C., Arnac, M., and Brindle, J-R. (1992) "Sorption interactions between trace metals (Cd and Ni) and phenolic substances on suspended clay minerals" Wat. Res. 26(8):1067-107

Gagnon, C., Pelletier, E., Maheu, S., (1993) "Distribution of metals and some major constituents in sediments of the Saguenay Fjord", Mar. Pollut. Bull. 26(2) 107-110.

Gagnon, C., Mucci, A, and Pelletier, E. (1995) "Anomalous accumulation of acid-volatile sulphides (AVS) in a coastal marine sediment, Saguenay Fjord, Canada" Geochim. Cosmochim. Acta 59(13):2663-2675.

Gagnon, C., Mucci, A., and Pelletier, E. (1996a) "Vertical distribution of dissolved sulphur species in coastal marine sediments" Mar Chem., 59:2663-2675.

Gagnon, C., Pelletier, E., Mucci, A., and Fitzgerald, W.F. (1996b) "Diagenetic behaviour of methylmercury in organic-rich coastal sediments" Limnol. Oceanogr. 41(3):428-434.

Gagnon, C., Pelletier, E., and Mucci, A. (1997) "Behaviour of anthropogenic mercury in coastal marine sediments" Mar. Chem., submitted.

Gill, G.A. and Fitzgerald, W.F. (1985) "Mercury sampling of open ocean waters at the picomolar level" Deep-Sea Res. 32:287-297.

Giordano, R., Musmeci, L., Ciaralli, L., Vernillo, I., Chiraco, M., Piccioni, A., and Costantini, S. (1992) "Total contents and sequential extractions of mercury, cadmium, and lead in coastal sediments" Mar. Poll. Bull 24(7) 350-357.

Gobeil, C. and Cossa, D., (1993) "Mercury in the sediments and sediment pore water in the Laurentian Trough", Can J. Fish. Aquat. Sci. 50:1794:1800.

Gobeil, C., Silverberg, N., Sundby, B., and Cossa, D. (1987) "Cadmium diagenesis in Laurentian Trough sediments" Geochim Cosmochim Acta 51:589-596.

Goldberg, E.D., (1954) "Marine geochemistry 1. Chemical scavengers of the sea" J. Geol. 62:249-265.

Greenland, D. and Oades, J. (1975) "Saccharides" Soil Components, Volume I, J.E. Gieseking, Ed., Springer Verlag, New York, NY.

Greenwood, N. and Earnshaw, A. (1984) Chemistry of the Elements, Pergammon Press, Elmsford, N.Y. 1542 pp.

Guay, G. and Couillard, M. (1980) Projet mercure: Contamination de l'environnement par l'usine de chlor-alcali, Alcan, Arvida -- Dossier Synthese, Bureau d'Etude sure les Substances Toxiques, Environnement Québec.

Gunneriusson, L., Baxter, D., and Emteborg, H. (1995) "Complexation at low concentrations of methyl and inorganic mercury (II) to a hydrous goethite (a-FeOOH) surface" J. Colloid Interface Sci. 169:262-266.

Hatcher, P., Breger, I., Maciel, G., and Szeverenyi, N. (1985) "Geochemistry of Humin", Humic Substances in Soil, Sediment, & Water, Eds. Aiken, G., McKnight, D., and Wershaw, R., John Wiley & Sons.

Heimenz, P.C. (1986) Principles of Colloid and Surface Chemistry 2nd Ed. Marcel Dekker, New York, N.Y..

Holliday, L. and Liss, P.S. (1976) "The behaviour of dissolved iron, manganese, and zinc in the Beaulieu Estuary" Estuarine Coastal Mar. Sci. 4:349-353.

Hostettler, J. (1984) "Electrode electrons, aqueous electrons, and redox potentials in natural waters" Am. J. Sci 284:734-759.

Howarth, R. (1978) "Pyrite: Its rapid formation in a salt marsh and its importance in ecosystem metabolism" Science 203:49-51.

Howarth, R. (1984) "The ecological significance of sulfur in the energy dynamics of salt marsh and coastal marine sediments" Biogeochem. 1:5-27.

Howarth, R.W. and Jorgensen, B.B. (1984) "Formation of ^{35}S-labelled elemental sulphur and pyrite in coastal marine sediments (Limfjorden and Kysing Fjord, Denmark) during short-term $^{35}SO_4^{2-}$ reduction measurements" Geochim. Cosmochim. Acta 48:1807-1818.

Hsieh, Y.P. and Yang, C.H., (1989) "Diffusion methods for the determination of reduced inorganic sulfur species in sediments", Limnol. Oceanogr., 34:1126-1130.

Huerta-Diaz, M. (1989) "Geochemistry of trace metals associated with sedimentary pyrite from anoxic marine environments" Ph.D. dissertation, Texas A&M Univ..

Huerta-Diaz, M. and Morse, J.W., (1990) "A quantitative method for determination of trace metal concentrations in sedimentary pyrite" Mar. Chem., 19:119-144.

Huerta-Diaz, M. and Morse, J.W. (1992) "Pyritization of trace metals in anoxic marine sediments", Geochim. Cosmochim. Acta 56(7) 2681-2702.

Huerta-Diaz, M., Carignan, R., and Tessier, A., (1993) "Measurement of trace metals associated with iron monosulfides and pyrite in organic freshwater sediments" Environ. Sci. Tech. 27(12) 2367-2372.

Huerta-Diaz, M., Tessier, A., and Carignan, R. (1996) "Geochemistry of trace metals associated with reduced sulfur in freshwater sediments" submitted

Hunter, K.A. and Leonard, M.W. (1988) "Colloid stability and aggregation in estuaries: 1. Aggregation kinetics of riverine dissolved iron after mixing with seawater", Geochim. Cosmochim. Acta 52:1123-1130.

Hyland, M.M., Jean, G.E., and Bancroft, G.M. (1990) "XPS and AES studies of Hg(II) sorption and desorption reactions on sulphide minerals" Geochim Cosmochim Acta, 54:1957-1967.

Jean, G.E. and Bancroft, G.M. (1986) "Heavy metal adsorption by sulphide mineral surfaces" Geochim Cosmochim Acta 50:1455-1463.

Jenson, S. and Jernelöv, A. (1969) "Biological methylation of mercury in aquatic organisms" Nature 223:753-754.

Jordao, C.P. and Nickless, G. (1989) "Chemical association of Zn, Cd, Pb, and Cu in soils and sediments determined by the sequential extraction technique" Environ. Tech. Lett. 10:743-752.

Jorgensen, B.B. (1977) "The sulfur cycle of a coastal marine sediment (Limfjorden. Denmark)" Limnol. Oceanogr. 22(5) 814-832.

Jorgensen, B.B. (1982) "Mineralization of organic matter in the sea bed - the role of sulphate reduction" Nature 296:643-645.

Kerndorff H. and Schnitzer,M. (1980) "Sorption of metals on humic acid" Geochim Cosmochim Acta. 44:1701-1708.

Kheboian, C. and Bauer, C.F. (1987) "Accuracy of selective extraction procedures for metal speciation in model aquatic sediments" Anal. Chem. 59:1417-1423.

Killops, S. and Killops, V., (1993) An Introduction to Organic Geochemistry, Longman Scientific and Technical, London, UK.

Klein, C. and Hurlbut, C., (1985) Manual of Mineralogy, 20th ed., John Wiley and Sons, New York, N.Y., 596 pp.

Klinkhammer, G.P. and Palmer, M.R. (1991) "Uranium in the oceans: Where it goes and why" Geochim. Cosmochim. Acta 55:1799-1806.

Kolthoff, I.M. and Sandell, E.B. (1952) Textbook of Quantitative Inorganic Analysis, Third Ed., MacMillan, New York pp. 568-573

Kostka, J.E. and Luther, G.W. (1993) "Partitioning and speciation of solid phase iron in saltmarsh sediments" Geochim. Cosmochim. Acta 58:1701-1710.

Kostka, J.E. and Luther, G.W. (1995) "Seasonal cycling of Fe in saltmarsh sediments" Biogeochemistry 29:159-181.

Krabbenhoft, D.P. and Babiarz, C.L. (1988) "The role of groundwater transport in aquatic mercury cycling" Water Resources Research 28(12) 3119-3128.

La Rochelle, P., (1973) "Rapport de synthèse des études de la coulée d'argile de Saint-Jean-Vianney", Gouvernement du Québec, Ministère des Richesses Naturelles.

Lapp, B. and Balzer, W. (1993) "Early diagenesis of trace metals used as an indicator of past productivity changes in coastal sediments" Geochim. Cosmochim. Acta 57:4639-4652.

Laxen, D. (1979) "Trace metal adsorption/coprecipitation on hydrous ferric oxide under realistic conditions: the role of humic substances" Water Res. 19(10) 1229-1236.

Leclerc, A., Gagnon, M.J., Côté, R., and Rami, A. (1986) "Compaction and movement of interstitial water in bottom sediments of the Saguenay Fjord, Québec, Canada" Sed. Geol. 46:213-220.

Leventhal, J. and Taylor, C. (1990) "Comparison of methods to determine degree of pyritization", Geochim. Cosmochim. Acta, 54:2621-2625.

Lindberg, S.E. and Hariss, R.C. (1974) "Mercury-organic matter association in estuarine sediments and interstitial water" Env. Sci. Tech. 8(5) 459-462.

Lion, L., Altmann, R.S., and Leckle, J., (1982) "Trace-metal adsorption characteristics of estuarine particulate matter: Evaluation of contributions of Fe/Mn oxide and organic surface coating" Environ. Sci. Technol. 16(10) 660-666.

Locat, J. and Leroueil, S. (1988) "Physicochemical and geotechnical characteristics of recent Saguenay Fjord sediments" Can. Geotech. J. 25:382-388.

Lockwood, R.A. and Chen, K.Y. (1973) "Adsorption of Hg(II) by hydrous manganese oxides" Environ. Sci. Tech. 16(10):660-666.

Lord, C.J. III (1982) "A selective and precise method for pyrite determination in sedimentary materials" J. Sediment. Petrol. 52:664-666.

Loring, D.H. (1975) "Mercury in the sediments of the Gulf of St. Lawrence" Can. J. Earth Sci. 12:1219-1237

Loring, D.H. (1978) "Industrial and natural inputs, levels, behavior, and dynamics of biologically toxic heavy metals in the Saguenay Fjord, Gulf of St. Lawrence, Canada", Environmental Biogeochemistry and Geomicrobiology Vol. 3, Methods, metals and assessment. 1025-1040.

Loring, D.H. and Bewers, J.M. (1978) "Geochemical mass balances for mercury in a canadian fjord", Chem. Geol. 22(4) 309-330.

Louchouarn, P. (1996) Cycles Biogéochimiques de Composés Naturels et Anthropiques dans les Sédiments Récents d'un Environnement Côtier: Le système du Saguenay/St-Laurent, Canada, Ph.D. Thesis, Université du Québec à Montréal, 347 pp.

Louchouarn, P., Lucotte, M., Canuel, R., Farella, N., and Gagné, J-P. (1995) "Organic diagenesis in anoxic fjord and suboxic estuarine sediments of the St-Lawrence system: Canada" Quatriéme Symposium International sur les Estuaires Modeles: Résumés; Institut Français de Recherche pour l'Exploitation de la Mer / Institut de Biogéochimie Marine École Normale Supérieure, Nantes, France, 21-25 Mars 1995.

Lucotte, M. and d'Anglejan, B., (1985) "A comparison of several methods for the determination of iron hydroxides and associated orthophosphates in estuarine particulate matter", Chem. Geol., 48:257-264.

Luther, G.W. (1987) "Pyrite oxidation and reduction: Molecular orbital theory considerations" Geochim. Cosmochim. Acta 51:3193-3199.

Luther, G.W. (1991) "Pyrite synthesis via polysulphide compounds" Geochim. Cosmochim. Acta 55:2839-2849.

Luther, G.W. III and Church, T.M. (1992) "An overview of the environmental chemistry of sulphur in wetland systems" Proc. of SCOPE Meeting: Sulphur Cycling on the Continents, Chapter 6, pp 125-142.

Luther, G.W. III, Meyerson, A.L., Krajewski, J.J., and Hires, R., (1980) "Metal sulfides in estuarine sediments" J. Sed. Petrol., 50:1117-1120.

Luther, G.W., Kostka, J.E., Church, T.M., Sulzberger, B., and Stumm, W. (1992) "Seasonal iron cycling in the salt-marsh sedimentary environment: the importance of ligand complexes with Fe(II) and Fe(III) in the dissolution of Fe(III) minerals and pyrite, respectively" Mar. Chem. 40:81-103.

Macdonald, R.W., Macdonald, D.M., O'Brien, M.C., and Gobeil, C. (1991) "Accumulation of heavy metals (Pb, Zn, Cu, Cd) carbon and nitrogen in sediments from Strait of Georgia, B.C., Canada" Mar. Chem. 34:109-135.

MacNaughton, M.G. and James, R.O. (1973) "Adsorption of aqueous mercury (II) complexes at the oxide/water interface" J. Coll. Interface Sci., 47(2):431:440.

Mahan, K.I., Foderaro, T., Tressa, L., Garza, R., Martinez, R.M., Maroney, G., Trivisonno, M., and Willging, E. (1988) "Microwave digestion techniques in the sequential extraction of calcium, iron, chromium, manganese, lead, and zinc in sediments" Anal. Chem. 59(7) 938-949.

Martin, J.M., Nirel, P., and Thomas, A.J. (1987) "Sequential extraction techniques: Promises and problems" Mar. Chem. 22:313-341.

Matty, J.M. and Long, D.T. (1995) "Early diagenesis of mercury in the Laurentian Great Lakes" J. Great Lakes Res. 21(4) 574-586.

Mayer, L.M. (1982) "Aggregation of colloidal iron during estuarine mixing: Kinetics, mechanism, and seasonality", Geochim. Cosmochim. Acta 46:2527-2535.

Mayer, L.M. (1985) "Geochemistry of humic substances in estuaries" in Humic Substances in Soil, Sediment, and Water, G. Aiken, D. McKnight, R. Wershaw, and P. MacCarthy, eds. 211-23

Mayer, L.M. (1994) "Relationships between mineral surfaces and organic carbon concentrations in soils and sediments" Chem. Geol. 114:347-363.

Middelburg, J.J. (1991) "Organic carbon, sulphur, and iron in recent semi-euxinic sediments of Kau Bay, Indonesia" Geochim. Cosmochim. Acta 55:239-256.

Moore, R.M., Burton, J.D., Williams, P.J.L, and Young, M.L. (1979) "The behaviour of dissolved organic material, iron, and manganese in estuarine mixing", Geochim. Cosmochim. Acta 43:919-926.

Morel, F., McDuff, R.E., and Morgan, J.J. (1973) "Interaction and chemostasis in aquatic chemical systems:role of pH, pE, solubility and complexation" Trace Metals and Metal-Organic Interactions in Natural Waters, P.C. Singer (ed.), Ann Arbor Sci. Publ. Inc., Ann Arbor, Mich. pp. 157-200.

Morse, J.W., (1994) "Interactions of trace metals with authigenic sulfide minerals: implications for their bioavailability" Mar. Chem. 46:1-6.

Morse, J.W. and Arakaki, T. (1993) "Adsorption and co-precipitation of divalent metals with mackinawite (FeS)" Geochim Cosmochim 57:3635-3640.

Morse, J.W. and Cornwell, J.C. (1987) "Analysis and distribution of iron sulfide minerals in recent anoxic marine sediments", Mar. Chem. 22:55-69.

Mucci, A. (1988) "Manganese uptake during calcite precipitation from seawater: Conditions leading to the formation of a pseudokutnahorite" Geochim. Cosmochim. Acta 41:1859-1868.

Mucci, A. and Edenborn, H.M. (1992) "Influence of an organic-poor landslide deposit on the early diagenesis of iron and manganese in a coastal marine sediment" Geochim. Cosmochim. Acta 56:3909-3921.

Mucci, A., Lucotte, M., Montgomery, S., Plourde, Y., Pichet, P., and Tra, H-V. (1995) "Mercury remobilization from flooded soils in a hydroelectric reservoir of northern Québec, LG-2: results of a soil resuspension experiment", Can. J. Fish. Aquat. Sci. 52(11):2507-2517.

Nakahara, T., Tanaka, T., and Musha, S. (1978) "Flameless atomic fluorescence spectrometry by dispersive and nondispersive systems in combination with cold-vapor technique" Bul. Chem. Soc. Japan 51(7):2020-2024.

National Industrial Pollution Control Council (1970) Mercury: Staff Report, October, 1970, U.S. Govt. Print. Off.

Nriagu, J.O. and Pacyna, J.M. (1988) "Quantitative assessment of worldwide contamination of air, water, and soils by trace metals" Nature 333:134-139.

O'Brien, D.J. and Birkner, F.G. (1977) "Kinetics of oxydation of reduced sulphur species in aqueous solution" Environ. Sci. Tech. 11:1114-1120.

Ouellet, A. (1978) Géochimie du Soufre dans les Sédiments de l'Estuaire du St-Laurent et du Fjord du Saguenay M.Sc. Thesis, Université du Québec à Rimouski.

Pankow, J. and Morgan, J. (1979) "Dissolution of tetragonal ferrous sulfide (mackinawite) in anoxic aqueous systems. 1. Dissolution rate as a function of pH, temperature, and ionic strength", Environ. Sci. Tech. 13(10) 1248-1255.

Pearson, R.G. (1963) "Hard and soft acids and bases" J. Am. Chem. Soc. 85:3533.

Pelletier, E. and Canuel, G. (1988) "Trace metals in surface sediments of the Saguenay Fjord, Canada" Mar. Pollut. Bull. 19(7):336-338.

Pelletier, E., Rouleau, C., and Canuel, G. (1989a) "Niveau de contamination par le mercure des sédiments de surface et des crevettes du fjord du Saguenay" Revue des Sciences de l'Eau 2:13-27.

Pelletier, E., Ouellet, S., and Maheu, S., (1989b) "Etude comparative de la distribution du mercure total et des hydrocarbures polyaromatiques dans les sediments recents du fjord du Saguenay" Symposium sur le St. Laurent, Montréal, Québec 14 pp.

Petrovic, M., Kastelan-Macan, M., and Horvat, A.J.M (1994) "Sorption interactions between metals and humic substances on hydrous solid surfaces and their impact on heavy metal geochemistry", unpublished manuscript, 27 pp.

Pocklington, R. and Leonard, J.D. (1979) "Terrigenous organic matter in sediments of the Saguenay Fjord" J. Fish. Res. Bd. Can., 36, 1250-1255.

Porterfield, W.W. (1984) Inorganic Chemistry, Addison-Wesley Publishing, Reading, MA.

Postma, D. and Jakobsen, R. (1996) "Redox zonation: Equilibrium constraints on the Fe(III)/SO_4-reduction interface" Geochim Cosmochim Acta 60:3169-3175.

Presley, B., Kolodny, Y., Nissenbaum, A., and Kaplan, I. (1972) "Early diagenesis in a reducing fjord, Saanich Inlet, British Columbia: II. Trace element distribution in interstitial water and sediment" Geochim. Cosmochim. Acta 36:1073-1090.

Pruden, G. and Bloomfield, C. (1968) "The determination of ferrous sulfide in soil in the presence of ferric oxide" Analyst 93:532-534.

Pyzik, A.J. and Sommer, S.E. (1981) "Sedimentary iron monosulfides: kinetics and mechanism of formation" Geochim. Cosmochim Acta., 45:687-698.

Raiswell, R., Canfield, D., and Berner, R. (1993) "A comparison of iron extraction methods for the determination of degree of pyritisation and the recognition of iron-limited pyrite formation" Chemical Geology 111:101-110.

Raiswell, R. and Plant, J. (1980) "The incorporation of trace elements into pyrite during diagenesis of black shales, Yorkshire, England", Economic Geology 75:684-699.

Randle, K. and Hartmann, E.H. (1987) "Applications of the continuous flow stirred cell (CFSC) technique to adsorption of zinc, cadmium, and mercury on humic acids" Geoderma, 40:281-296.

Rapin, F., Tessier, A., Campbell, P.G.C., and Carignan, R. (1986) "Potential artifacts in the determination of metal partitioning in sediments by a sequential extraction procedure" Environ. Sci. Tech. 20(8) 836-840.

Rashid, M.A. (1985) The Geochemistry of Marine Humic Compounds, Springer Verlag, New York, N.Y.

Reeburgh, W.S. (1967) "An improve interstitial water sampler" Limnol. Oceanogr. 12:163-165.

Reimers, R.S. and Krenkel, P.A. (1974) "Kinetics of mercury adsorption and desorption in sediments" Water Poll. Con. Fed. Jour. 46:352-365.

Rendell, P.S., Batley, G.E., and Cameron, A.J. (1980) "Adsorption as a control of metal concentration in sediments extracts" Environ Sci. Tech. 14:314-318.

Rickard, D. (1975) "Kinetics and mechanism of pyrite formation at low temperatures" Amer. J. Sci 275:636-652.

Rickard, D. (1996) "Kinetics of pyrite formation by the H_2S oxidation of iron (II) monosulfide in aqueous solutions between 25°C and 125°C: the rate equation" Submitted to Geochim. Cosmochim. Acta.

Rickard, D., Schoonen, M.A.A., and Luther, G.W. III (1995) "Chemistry of iron sulphides in sedimentary environments" Geochemical Transformations of Sedimentary Sulphur, Murthy A. Vairavamurthy and Martin A.A. Schoonen (eds.), ACS Symposium Series, No. 612, 208th National Meeting of the American Chemical Society, Washington D.C. pp 168-193.

Rickard, D. and Luther, G.W. III (1996) "Kinetics of pyrite formation by the H_2S oxidation of iron (II) monosulfide in aqueous solutions between 25°C and 125°C: the mechanism" Submitted to Geochim. Cosmochim. Acta.

Robinson, G. (1984) "Sequential chemical extractions and metal partitioning in hydrous Mn-Fe-oxide coatings: Reagent choice and substrate composition" Chem. Geol. 47:97-112.

St. Louis, V.L., Rudd, J.W., Kelly, C., and Beaty, K.G. (1994) "Wetlands as sources of methyl mercury to boreal forest lakes in Northwestern Ontario" Can. J. Fish. Aquat. Sci. (submitted).

Sawlan, J.J. and Murray, J.W. (1983) "Trace metal remobilization in the interstitial waters of red clay and hemipelagic marine sediments" Earth Planet. Sci. Lett. 64:213-230.

Schafer, C., Smith, J.N., and Seibert, G. (1983) "Significance of natural and anthropogenic sediment inputs to the Saguenay Fjord, Quebec" Sediment. Geol. 36:177-194.

Schnitzer, M. and Kerndorff, H. (1981) "Reactions of fulvic acids with metal ions" Water, Air, and Soil Pollution 15:97-108.

Schnitzer, M. and Skinner, S.I.M. (1968) "Alkali versus acid extraction of soil organic matter" Soil Sci. 105(1) 392-396.

Schoonen, M.A.A. and Barnes, H.L., (1991) "Reactions forming pyrite and marcasite from solution: II. Via FeS Precursors below 100°C", Geochim. Cosmochim. Acta, 55:1505-1514.

Schroeder, W.H., Munthe, J., and Lindqvist, O. (1989) "Cycling of mercury between water, air, and soil compartments of the environment" Water, Air, and Soil Pollution, 48, 337-347.

Schuster, E. (1991) "The behavior of mercury in the soil with special emphasis on complexation and adsorption processes - a review of the literature" Water Air Soil Poll. 56:667-680.

Shaw, T.J., Gieskes, J.M., and Jahnke, R.A. (1990) "Early diagenesis in differing depositional environments: The response of transition metals in pore water" Geochim. Cosmochim. Acta 54:1233-1246.

Sholkovitz, E. (1976) "Flocculation of dissolved organic and inorganic matter during the mixing of river water and seawater" Geochim. Cosmochim. Acta, 40:831-845.

Sholkovitz, E.R. (1989) "Artifacts associated with the chemical leaching of sediments for rare-earth elements" Chem. Geol 77:47-51.

Sholkovitz, E.R., Boyle, E.A., and Price, N.B. (1978) "The removal of dissolved humic acids and iron during estuarine mixing", Earth and Planetary Science Letters 40:130-136.

Silverberg, N., Nguyen, H., Delibrias, G., Koide, M., Sundby, B., Yokoyama, Y., and Chesselet, R. (1986) "Radionuclide profiles, sedimentation rates, and bioturbation in modern sediments of the Laurentian Trough, Gulf of St. Lawrence" Oceanol. Acta 9:285-290.

Skei, J.M., Loring, D.H., and Rantala, R.T.T. (1988) "Partitioning and enrichment of trace metals in a sediment core from Framvaren, South Norway" Marine Chemistry 23:269-281.

Smith, J.N. and Loring, D.H., (1981) "Geochronology for mercury pollution in the sediments of the Saguenay Fjord, Québec", Environ. Sci. Tech. 15(8), 944-951.

Smith, J.N., Schafer, C.T., and Loring, D.H. (1983) "Depositional processes in an anoxic, high sedimentation regime in the Saguenay Fjord" Fjord Oceanography, H.

Freeland, D. Farmer, and C. Levings, editors (Plenum Press, New York, N.Y.). Volume 4, pp. 625-630.

Smith, J.N. and Walton, A., (1980) "Sediment accumulation rates and geochronologies measured in the Saguenay Fjord using Pb-210 dating method". Geochim. Cosmochim. Acta, 44:225-240.

Smith, R. and Martell, A. (1976) Critical Stability Constants, Vol. 4 Inorganic Complexes, Plenum Press, New York 257 pp.

Solomons, T.W. Graham (1988) Organic Chemistry, John Wiley & Sons, Toronto, Ontario.

Sorensen, J. and Jorgensen, B.B. (1987) "Early diagenesis in sediments from Danish coastal waters: Microbial activity and Mn-Fe-S geochemistry". Geochim. Cosmochim. Acta, 51:1583-1590.

Span, D. and Gaillard, J-F. (1986) "An investigation of a procedure for determining carbonate bound trace metals" Chem. Geol. 56:135-141.

Stevenson, F., (1985) "Geochemistry of Soil Humic Substances" Humic Substances in Soil, Sediment, and Waters, G. Aiken, D. McKnight, and R. Wershaw, eds., John Wiley & Sons, Toronto, Ontario.

Stevenson, F. (1994) Humus Chemistry: Genesis, Composition, Reactions; Wiley-Interscience, New York.

Stumm, W. and Morgan, J. (1972) Aquatic Chemistry, Wiley Interscience, New York.

Sundby, B. and Loring, D.H. (1977) "Geochemistry of suspended particulate matter in the Saguenay Fjord" Can. J. Earth Sci. 15:1002-1022.

Sundby, B. and Silverberg, N. (1985) "Manganese fluxes in the benthic boundary layer" Limnol. Oceanogr. 30:372-381.

Swift, R. (1985) "Fractionation of soil humic substances" in Humic Substances in Soil, Sediment, and Water, G. Aiken, D. McKnight, R. Wershaw, and P. MacCarthy, eds. 211-23

Szakácss, O., Lásztity, A., and Horváth, Zs. (1980) "Breakdown of organic mercury compounds by hydrochloric acid-permanganate or bromine monochloride solution for the determination of mercury by cold vapour atomic adsorption spectrometry" Anal. Chim. Acta 121:219-224.

Takizawa, Y. (1979) "Epidemiology of mercury poisoning" Topics in Environmental Health, Volume 3: Biogeochemistry of Mercury in the Environment, J.O., Nriagu, ed., Elsevier/North Holland Biomedical Press, pp. 325-365.

Tessier, A., Campbell, P.G.C., and Bisson, M. (1979) "Sequential extraction procedure for the speciation of particulate trace metals" Anal. Chem. 51(7) 844-851.

Thanabalasingam, P. and Pickering, W.F. (1985) "Sorption of mercury (II) by humic acids" Environmental Pollution (Series A) 9(4):267-279.

Thode-Anderson, S. and Jorgensen, B.B. (1989) "Sulfate reduction and the formation of ^{35}S-labelled FeS, FeS$_2$, and S° in coastal marine sediments" Limnol. Oceanogr. 34(5) 793-806.

Thomson, J., Higgs, N.C., Croudace, I W., Colley, S., and Hydes, D.J. (1993) "Redox zonation of elements at an oxic/post-oxic boundary in deep-sea sediments" Geochim. Cosmochim. Acta 57:579-595.

Tipping, E. (1981) "The adsorption of aqueous humic substances by iron oxides" Geochim. Cosmochim. Acta 45:191-199.

Tipping, E., Hetherington, N.B., and Hilton, J. (1985) "Artifacts in the use of selective chemical extraction to determine distributions of metals between oxides of manganese and iron" Anal Chem. 57:1944-1946.

Tremblay, A., Mucci, A., and Rheault, I. (1996) "Methyl mercury in a benthic food chain of two hydroelectric reservoirs and a natural lake of Northern Québec (Canada)" Water, Air, and Soil Poll. (submitted).

Van Delft, W. and Vos, G. (1988) "Comparison of digestion procedures for the determination of mercury in soils by cold-vapour atomic absorption spectrometry" Analytica Chimica Acta 209:147-156.

Wollast, R., Billen, G., Mackenzie, F.T. (1975) "Behavior of mercury in natural systems and its global cycles" Ecological Toxicology Research: Effects of Heavy Metal and Organohalogen Compounds: Proceedings of a NATO Science Conference, A.D. McIntyre and C.F. Mills, eds., Plenum Press, pp. 145-166.

Xiao, Z.F., Munthe, J., Schroeder, W.H., and Lindqvist, O. (1991) "Vertical fluxes of volatile mercury over forest soil and lake surfaces in Sweden" Tellus 43B:267-279.

Xu, H. and Allard, B. (1991) "Effects of a fulvic acid on the speciation and mobility of mercury in aqueous solutions" Water Air Soil Pollut. 56:709-717.

Yong, R.N., (1988) Contaminant - Soil Interaction Studies, Soil Mechanics Series No. 54, Geochemical Research Centre, Montréal, Canada.

Zhabina, N.N. and Volkov, I.I., (1978) "A method of determination of various sulfur compounds in sea sediments and rocks" Environmental Biogeochemistry and Geomicrobiology: Methods, Metals and Assessment, W. Krumbein, ed. pp. 725-746.

APPENDIX 1 Sample stations and depth intervals

Station CL-1B	Station SAG-6B	Station SAG-30B
3 June 1992	6 June 1992	6 June 1992
Laurentian Trough	Saguenay Fjord	Saguenay Fjord
48°37.22' N, 68°40.08' W	48°25.05' N, 70°47.20' W	48°21.30' N, 70°25.05' W
Water Depth = 310 m	Water Depth = 122 m	Water Depth = 274 m
Sampled Intervals (cm)	Sampled Intervals (cm)	Sampled Intervals (cm)
0 - 0.5	0 - 0.5	0 - 0.5
0.5 - 1	0.5 - 1	0.5 - 1
1 - 2	1 - 2	1 - 2
2 - 3	2 - 3	2 - 3
3 - 4	3 - 4	3 - 4
4 - 5	4 - 5	4 - 5
5 - 6	5 - 6	5 - 6
6 - 7	6 - 7	6 - 7
8 - 9	8 - 9	7 - 8
9 - 10	9 - 10	9 - 11
10 - 12	10 - 12	11 - 13
12 - 14	12 - 14	13 - 15
14 - 16	14 - 16	15 - 17
16 - 19	16 - 18	18 - 21
19 - 22	18 - 20	21 - 24
22 - 23.5	20 - 22	24 - 27
25 - 28	24 - 27	27 - 30
28 - 31	27 - 29	30 - 34
	29 - 33	
	33 - 36	
	36 - 40	

APPENDIX 2 Distribution and concentration of geochemically important elements with depth

Station CL-1B: Laurentian Channel

Depth (cm)	Fe-HCl (µmol/g)	Mn-HCl (µmol/g)	C-tot Wgt %	C-inorg Wgt %	C-org Wgt %	Ntot Wgt %	C/N Ratio	S-AVS (µmol/g)	S-CRS (µmol/g)	Fe-pyr (µmol/g)
0.25	501.1	37.26	1.90	0.202	1.70	0.14	13.6	1.32	9.75	6.96
0.75	513.9	29.49	1.82	0.197	1.62	0.13	14.0	1.31	7.33	6.63
1.5	523.1	12.26	1.93	0.196	1.73	0.14	13.8	1.42	9.66	8.34
2.5	460.6	15.44	1.93	0.189	1.74	0.14	13.8	2.39	8.36	8.50
3.5	452.0	12.77	1.88	0.200	1.68	0.13	14.5	6.23	17.61	10.65
4.5	468.4	11.14	1.88	0.218	1.66	0.13	14.5	11.51	14.62	9.88
5.5	463.6	11.20	1.75	0.203	1.55	0.10	17.5	26.59	9.06	10.72
6.5	434.4	11.18	1.87	0.202	1.67	0.12	15.6	26.95	13.11	9.20
8.5	446.9	11.81	1.78	0.199	1.58	0.12	14.8	10.92	25.35	10.06
9.5	448.9	13.09	1.74	0.204	1.54	0.11	15.8	16.54	15.33	11.71
11	461.5	12.77	1.78	0.205	1.58	0.11	16.2	23.42	8.16	3.45
13	462.9	8.77	1.76	0.204	1.56	0.11	16.0	22.96	10.44	3.75
15	458.1	15.44	1.74	0.202	1.54	0.11	15.8	25.49	8.72	3.54
17.5	477.3	13.35	1.64	0.209	1.43	0.11	14.9	26.66	8.37	3.60
20.5	480.7	12.73	1.61	0.183	1.43	0.10	16.1	34.06	11.53	3.59
22.75	477.1	11.85	1.45	0.172	1.28	0.09	16.1	24.15	9.73	3.32
25.75	458.5	13.59	1.49	0.172	1.32	0.10	14.9	31.34	8.40	3.31
27.25	488.9	12.90	1.45	0.169	1.28	0.09	16.1	31.34	8.40	3.20
28.75	488.9	13.75	1.48	0.169	1.31	0.10	14.8	34.93	6.77	3.17
30.25	499.3	12.85	1.38	0.169	1.21	0.09	15.3	34.93	6.77	2.50

Station SAG-6B: Upper Saguenay Fjord

Depth (cm)	Fe-HCl (µmol/g)	Mn-HCl (µmol/g)	C-tot Wgt %	C-inorg Wgt %	C-org Wgt %	Ntot Wgt %	C/N Ratio	S-AVS (µmol/g)	S-CRS (µmol/g)	Fe-HNO3 (µmol/g)
0.25	341.1	26.68	2.40	0.070	2.33	0.14	17.1	7.88	14.11	4.51
0.75	362.1	27.75	2.20	0.073	2.13	0.12	18.3	2.82	11.66	4.27
1.5	500.9	29.43	2.58	0.073	2.51	0.14	18.4	1.96	13.87	4.12
2.5	500.7	7.29	2.67	0.065	2.60	0.12	22.3	3.50	13.16	4.59
3.5	431.4	4.86	2.42	0.059	2.36	0.09	26.9	2.67	16.69	4.62
4.5	363.9	4.49	2.17	0.111	2.06	0.09	24.1	8.61	37.99	5.69
5.5	364.8	4.40	2.17	0.088	2.08	0.09	24.1	17.63	15.19	6.74
6.5	377.0	4.31	2.76	0.096	2.66	0.12	23.0	26.40	11.87	8.88
8.5	281.3	3.44	1.89	0.114	1.78	0.07	27.0	46.69	24.55	8.02
9.5	250.4	2.95	1.51	0.098	1.41	0.06	25.2	52.86	21.90	6.52
11	345.0	3.11	1.93	0.112	1.82	0.07	27.6	30.60	15.64	5.93
13	390.6	3.77	2.09	0.182	1.91	0.08	26.1	57.94	22.91	4.82
15	407.8	4.01	1.89	0.167	1.72	0.07	27.0	76.10	19.09	4.54
17	397.1	4.14	2.47	0.159	2.31	0.10	24.7	68.65	15.49	4.76
19	386.2	3.37	2.83	0.064	2.77	0.12	23.6	71.37	13.70	4.56
21	394.1	3.39	2.45	0.086	2.36	0.09	27.2	20.04	14.15	5.23
25.5	414.0	6.42	1.33	0.559	0.77	0.04	33.3	106.21	18.25	5.54
28	431.7	3.20	3.59	0.056	3.53	0.11	32.6	110.15	21.37	4.76
31	402.4	2.86	3.15	0.055	3.09	0.10	31.5	89.56	18.12	8.66
34.5	424.6	2.90	2.77	0.053	2.72	0.10	27.7	95.30	14.42	10.52
38	395.6	2.78	2.41	0.058	2.352	0.09	26.8	66.84	17.34	8.34

Station SAG-30B: Deep Saguenay Fjord

Depth (cm)	Fe-HCl (µmol/g)	Mn-HCl (µmol/g)	C-tot Wgt %	C-inorg Wgt %	C-org Wgt %	Ntot Wgt %	C/N Ratio	S-AVS (µmol/g)	S-CRS (µmol/g)	Fe-HNO3 (µmol/g)
0.25	669.1	29.95	2.75	0.083	2.67	0.13	21.2	1.31	6.53	3.95
0.75	722.7	33.59	2.77	0.086	2.68	0.12	23.1	0.97	5.90	3.94
1.5	806.2	36.25	2.58	0.080	2.50	0.11	23.5	1.23	5.37	3.59
2.5	732.7	10.50	2.73	0.083	2.65	0.12	22.8	1.06	6.23	3.89
3.5	718.2	9.71	2.76	0.080	2.68	0.13	21.2	1.97	7.24	3.89
4.5	644.5	8.55	2.81	0.087	2.72	0.13	21.6	6.12	7.34	4.21
5.5	694.2	9.16	2.86	0.086	2.77	0.12	23.8	2.79	7.04	3.61
6.5	719.2	8.92	2.80	0.087	2.71	0.12	23.3	4.75	8.13	3.90
7.5	700.8	8.67	2.77	0.089	2.68	0.11	25.2	6.53	6.94	3.50
10	619.6	7.30	2.54	0.081	2.46	0.11	23.1	9.45	6.91	3.44
12	619.4	7.18	2.61	0.082	2.53	0.11	23.7	22.08	7.72	3.26
14	629.5	8.69	2.57	0.082	2.49	0.11	23.4	11.51	7.29	5.20
16	596.0	10.17	2.55	0.082	2.47	0.11	23.2	40.11	8.79	4.36
19.5	626.1	9.28	2.57	0.082	2.49	0.11	23.4	40.26	8.64	4.49
22.5	600.9	9.23	2.40	0.075	2.32	0.10	24.0	37.03	8.28	4.54
25.5	638.2	9.21	2.31	0.078	2.23	0.10	23.1	40.14	8.78	4.48
28.5	549.0	9.09	2.16	0.078	2.08	0.10	21.6	34.79	8.28	3.83
32	559.8	8.50	2.01	0.079	1.93	0.07	28.7	48.10	8.76	3.65

APPENDIX 3 Distribution and concentration of total and partitioned mercury with depth

Station CL-18: Laurentian Channel

Depth	Hg-Total	Partitioned Hg (ng/g)				Hg-Sum
(cm)	ng/g	NaOH	HCl	HF	HNO3	ng/g
0.25	245	147.0	24.0	27.2	19.3	217
0.75	265	158.4	24.1	34.7	20.5	238
1.5	230	157.1	24.9	42.1	24.8	249
2.5	275	178.8	16.2	48.8	31.0	275
3.5	310	171.5	16.8	49.6	28.9	267
4.5	310	173.8	19.6	46.0	29.1	269
5.5	340	168.9	19.8	59.1	35.9	284
6.5	360	177.8	22.0	66.6	38.4	305
8.5	385	214.3	26.2	77.9	40.1	358
9.5	430	237.2	33.4	88.2	45.5	404
11	510	300.5	57.2	69.1	45.5	472
13	545	292.3	44.0	74.1	54.9	465
15	570	298.4	64.8	94.2	57.1	515
17.5	575	271.1	46.5	88.5	54.9	461
20.5	530	238.2	49.1	87.4	52.0	427
22.75	370	227.0	19.5	38.8	34.0	319
25.75	295	182.2	19.1	31.3	32.8	265
27.25	260	162.0	17.3	33.8	28.9	242
28.75	295	204.2	16.2	28.6	27.5	276
30.25	230	136.1	11.8	27.4	33.5	209

Station SAG-6B: Upper Saguenay Fjord

Depth	Hg-Tot	Partitioned Hg (ng/g)				Hg-Sum
(cm)	ng/g	NaOH	HCl	HF	HNO3	ng/g
0.25	145	107.4	22.7	12.0	13.0	155
0.75	145	102.4	21.0	6.0	4.6	134
1.5	175	112.8	20.7	5.0	0.0	138
2.5	255	159.2	24.0	45.0	23.1	251
3.5	310	158.3	23.1	42.2	8.3	232
4.5	440	230.8	18.3	41.8	16.1	307
5.5	740	401.3	15.3	70.3	28.7	516
6.5	865	482.4	8.0	75.6	49.9	616
8.5	810	546.3	12.4	106.3	58.3	723
9.5	1000	466.1	19.4	72.1	70.9	628
11	775	482.5	21.4	59.8	52.3	616
13	595	302.8	19.9	59.0	41.6	423
15	645	316.9	19.0	61.7	57.4	455
17	335	233.2	8.6	31.4	24.4	298
19	305	206.5	4.6	28.7	28.4	268
21	455	258.4	7.0	44.4	47.3	357
25.5	240	90.6	22.1	54.3	22.7	190
28	9500	1988.9	374.0	4606.0	976.2	7945
31	5850	1536.0	278.3	2622.4	495.4	4932
34.5	3150	1059.5	172.1	1159.6	274.5	2666
38	1150	782	42	58	50	932

Station SAG-30B: Deep Saguenay Fjord

Depth	Hg-tot	Partitioned Hg (ng/g)				Hg-Sum
(cm)	(ng/g)	NaOH	HCl	HF	HNO3	(ng/g)
0.25	455	324.7	73.3	34.1	15.4	447
0.75	520	398.3	54.9	47.2	17.2	518
1.5	520	329.6	95.8	82.2	24.4	532
2.5	525	326.2	101.9	62.1	23.5	514
3.5	570	349.1	98.1	63.3	29.0	540
4.5	700	307.3	96.0	90.8	34.1	528
5.5	665	304.3	192.8	91.1	28.0	616
6.5	760	304.0	220.7	107.4	35.8	668
7.5	855	256.6	234.0	132.7	38.8	662
10	1600	545.8	201.1	499.1	91.2	1337
12	1850	721.5	219.3	627.7	101.0	1670
14	2050	806.0	97.3	714.5	141.3	1759
16	1950	857.5	94.9	636.5	113.6	1702
19.5	1700	912.1	90.5	332.1	107.2	1442
22.5	1150	561.7	68.3	120.5	54.7	805
25.5	695	459.8	24.3	33.7	33.9	552
28.5	160	100.5	3.7	16.0	14.6	135
32	90	99.4	2.1	10.1	8.1	120

IMAGE EVALUATION
TEST TARGET (QA-3)

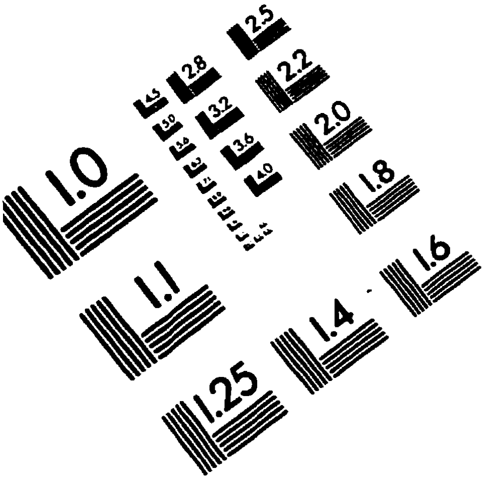

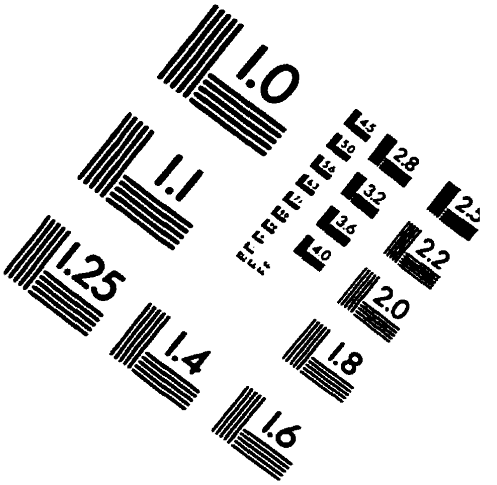

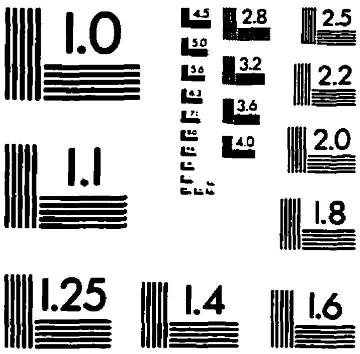

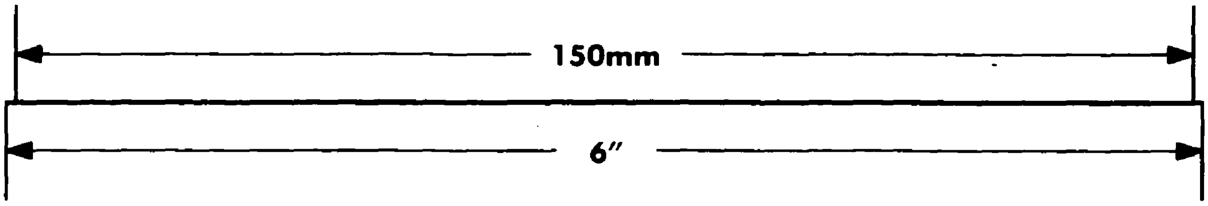

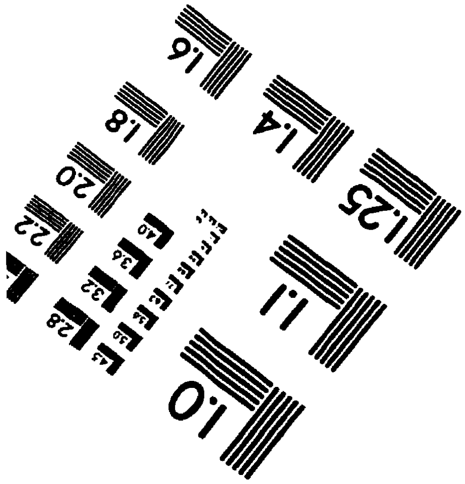

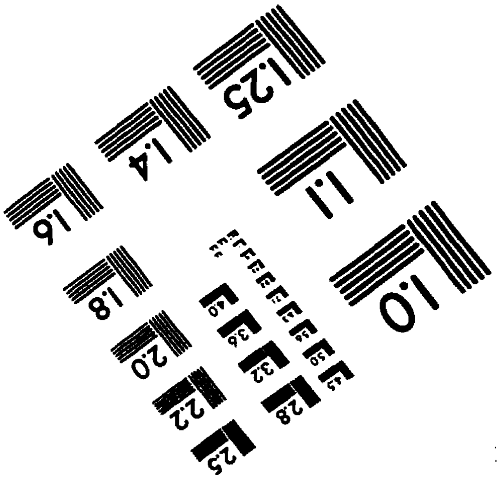

APPLIED IMAGE . Inc
1653 East Main Street
Rochester, NY 14609 USA
Phone: 716/482-0300
Fax: 716/288-5989